ANALYSIS OF HYDROCARBON RESOURCE POTENTIAL OF CHICHALI AND SAMANA SUK FORMATIONS, KOHAT SUB-BASIN, PAKISTAN

AHMAD KHAN

01-262192-012

Bahria University, Islamabad

ANALYSIS OF HYDROCARBON RESOURCE POTENTIAL OF CHICHALI AND SAMANA SUK FORMATIONS, KOHAT SUB-BASIN, PAKISTAN

AHMAD KHAN

01-262192-012

A thesis submitted in fulfilment of the
requirements for the award of the degree of
Master of Science (Geology)

Department of Earth and Environmental Sciences

Bahria University, Islamabad,

2021

APPROVAL FOR EXAMINATION

Scholar's Name: **Ahmad Khan** Registration No. **01-262192-012**

Programme of Study: **Master of Science in Geology**

Thesis Title: **Analysis of Hydrocarbon Resource Potential of Chihcali and Samana Suk Formations, Kohat Sub-Basin, Pakistan.**

It is to certify that the above scholar's thesis has been completed to my satisfaction and, to my belief, its standard is appropriate for submission for examination. I have also conducted a plagiarism test of this thesis using HEC prescribed software and found similarity index _____% that is within the permissible limit set by the HEC for the MS degree thesis. I have also found the thesis in a format recognized by the BU for the MS thesis.

Principal Supervisor's Signature_____

Date: _____

Name:_____

AUTHOR'S DECLARATION

I, **Ahmad Khan** hereby state that my MS thesis titled "**Analysis of Hydrocarbon Resource Potential of Chihcali and Samana Suk Formations, Kohat Sub-Basin, Pakistan.**" is my work and has not been submitted previously by me for taking any degree from this Bahria University, Islamabad or anywhere else in the country/world.

At any time if my statement is found to be incorrect even after my graduation, the University has the right to withdraw/cancel my MS degree.

Name of scholar: _____

Scholar's Signature: _____

Date: _____

PLAGIARISM UNDERTAKING

I, solemnly declare that the research work presented in the thesis titled "**Analysis of Hydrocarbon Resource Potential of Chihcali and Samana Suk Formations, Kohat Sub-Basin, Pakistan.**" is solely my research work with no significant contribution from any other person. Small contribution/help wherever taken has been duly acknowledged and that complete thesis has been written by me.

I understand the zero-tolerance policy of the HEC and Bahria University towards plagiarism. Therefore I as an Author of the above-titled thesis declare that no portion of my thesis has been plagiarized and any material used as reference is properly referred/cited.

I undertake that if I am found guilty of any formal plagiarism in the above-titled thesis even after awarding of PhD degree, the university reserves the right to withdraw/revoke my PhD degree and that HEC and the University have the right to publish my name on the HEC / University website on which names of scholars are placed who submitted plagiarized thesis.

Scholar / Author's Sign: _____

Name of the Scholar: _____

ACKNOWLEDGEMENTS

First of all, I am thankful to Almighty Allah for bestowing me the intellect and resources to carry out my thesis.

I am extremely grateful to my Supervisor Mr Muhammad Raiees Amjad and Co-Supervisor Mr Shoaib Amir Fahim for their sincere supervision and guidance throughout my whole research to complete my thesis.

Besides faculty, I am extremely thankful to my parents who have enabled, supported and encouraged me to pursue my Master of Science degree. Without their support, it would not have been possible to pursue my degree.

Moreover, I am extremely obliged and indebted to Landmark Resources (LMKR), Pakistan for their support by delivering me a free licence of Geographix software to carry out my research analysis efficiently and accurately.

ABSTRACT

The present study is focused on the analysis of hydrocarbon resource potential of Chichali Shale and Samana Suk Limestone in Kohat Sub-basin, Pakistan based on open-hole wireline log qualitative and quantitative analysis in well of Makori-01, Manzalai-02 and Maramzai-02. The analysis reveals Chichali Formation comprises two main Shale units with the non-Shale unit in between. The first zone of Shale demonstrates good outcomes regarding unconventional reservoir properties with TOC of 1.3 to 1.91% and Shale porosity of 5.1% to 9.6%. While the second zone shows TOC of 0.52 to 0.73% and Shale porosity of 6.4% to 8.71%. The mineralogical assessment shows Chichali Formation mainly bears Mixed layer clays, Illite, Glauconite and Mica bearing Shale. Mechanical properties assessment through compressional and Shear Sonic log favours Chichali Formation as good brittleness possessing Shale making it an optimistic target for hydraulic fracturing. The Samana Suk Limestone shows good hydrocarbon Saturation with poor porosity and permeability. The Porosity ranges from 1.54% to 3.58% with average permeability of less than 1 mD. The permeability categorises the Samana Suk Formation as a tight reservoir. The analysis shows Samana Suk Limestone bears 23.02% of Sw in Manzalai-02, 27.6% in Makori-01 and 44.06% in Maramzai-02 well. Mapping reveals the source rock potential of the Chichali Formation in terms of organic richness increases from E to W in zone-1, and from SE to NW in zone-2. While Shale porosity increase from NE to SW. Moreover, Samana Suk Limestone illustrates enhancement in reservoir attributes like Sw, PHIA and PHIE while traversing from NE to SW and degradation in hydrocarbon saturation from NE to SW.

TABLE OF CONTENTS

CHAPTER	TITLE	PAGE
	APPROVAL FOR EXAMINATION	ii
	AUTHOR'S DECLARATION	iii
	PLAGIARISM UNDERTAKING	iv
	ACKNOWLEDGEMENTS	**v**
	ABSTRACT	vi
	TABLE OF CONTENTS	vii
	LIST OF TABLES	xii
	LIST OF FIGURES	xiii
	LIST OF ABBREVATIONS	xii
1	**INTRODUCTION**	1
	1.1 Study Area	3
	1.2 Problem Statement	4
	1.3 Objectives of research	5
	1.4 Scope of research	6
2	**TECTONICS AND STRATIGRAPHY OF THE STUDY AREA**	**7**
	2.1 Regional Geology	7
	2.1.1 Tectonic division of NW Pakistan	9
	2.1.2 Karakoram Block	10
	2.1.3 Kohistan Island Arc	10
	2.1.4 Northern deformed fold and thrust belt	10
	2.1.5 Southern deformed fold and thrust belt and Indo Gangetic Foredeep	11
	2.2 Local tectonics of study area	11
	2.3 Stratigraphy of study area	13
	2.3.1 Samana Suk Formation	18
	2.3.2 Chichali Formation	18

3 LITERATURE REVIEW 19

4 METHODOLOGIES 23

4.1 Data Collection 23

4.2 Data Processing 23

4.2.1 Data Check 24

4.2.2 Removal of End effect 24

4.2.3 SP Baseline Shift 24

4.2.4 Rescaling 24

4.2.5 Splicing 24

4.2.6 Software utilization 25

4.2.6.1 Geographix software 25

4.2.6.2 Graphics software 25

4.3 Data Interpretation 25

4.4 Petrophysical attributes calculations 26

4.4.1 Caliper log 26

4.4.1.1 Borehole Rugosity 26

4.4.2 Spontaneous potential Log 27

4.4.3 Gamma Ray Log 27

4.4.3.1 Natural Gamma Ray (NGR) 27

4.4.3.1.1. Volume of Shale 27

4.4.3.2 Spectral Gamma Ray (SGR) 28

4.4.3.2.1. Shale Mineralogy assessment 28

4.4.4 Resistivity Log 29

4.4.5 Sonic Log 30

4.4.5.1 Sonic Porosity 30

4.4.6 Neutron Log 30

4.4.7 Density Log 30

4.4.7.1 Density Porosity 31

4.4.8 Average porosity 31

4.4.9 Effective Porosity 32

4.4.10 Shale Porosity 32
4.4.11 Water and Hydrocarbon saturation 33
4.4.11.1 Calculation of Rw 34
4.4.12 TOC calculation-Passey Δlog R Method 34
4.4.13 Permeability 36
4.4.14 Brittleness Index 36

5 UNCONVENTIONAL PETROPHYSICAL CHARACTERIZATION OF CHICHALI SHALE 41
5.1 Makori-01 well 43
5.1.1 Well Description 43
5.1.2 Qualitative Interpretation 43
5.1.3 Quantitative analysis 44
5.1.3.1 Zone-1 (3209 to 3235 meters) 44
5.1.3.2 Zone-2 (3245 to 3287 meters) 48
5.2 Manzalai-02 well 50
5.2.1 Well Description 50
5.2.2 Qualitative Interpretation 51
5.2.3 Quantitative analysis 52
5.2.3.1 Zone-1 (3688 to 3730 meters) 52
5.2.3.2 Zone-2 (3748 to 3762 meters) 55
5.3 Maramzai-02 well 58
5.3.1 Well Description 58
5.3.2 Qualitative Interpretation 58
5.3.3 Quantitative analysis 59
5.3.3.1 Zone-1 (2918 to 2977 meters) 59
5.3.3.2 Zone-2 (2982 to 3008 meters) 62

6 PETROPHYSICAL CHARACTERIZATION OF SAMANA SUK LIMESTONE 65
6.1 Makori-01 well 66
6.1.1 Well 66
6.1.2 Qualitative Interpretation 67

6.1.3 Quantitative analysis 68
6.2 Manzalai-02 well 72
6.2.1 Well Description 72
6.2.2 Qualitative Interpretation 73
6.2.3 Quantitative analysis 74
6.3 Maramzai-02 well 75
6.3.1 Well Description 75
6.3.2 Qualitative Interpretation 76
6.3.3 Quantitative analysis 77

7 STRATIGRAPHIC CORRELATION AND ATTRIBUTE MAPPING 81
7.1 Stratigraphic Correlation 81
7.2 Mapping of Petrophysical Attribute 83
7.2.1 Chichali Formation 83
7.2.1.1Zone-1 83
7.2.1.2 Zone-2 88
7.2.2 Samana Suk Formation 92

8 RESULTS 96
8.1. Conclusions 98
8.2 Recommendations 98

REFERENCES 100

LIST OF TABLES

TABLE NO.	TITLE	PAGE NO.
Table 8.1	Summarised computed petrophysical attributes of Chichali and Samana Suk Formations in Makori-01, Manzalai-02 and Maramzai-02 wells.	98

LIST OF FIGURES

FIGURE NO.	TITLE	PAGE NO.
Figure 1.1	Map showing the location of Wells in Kohat Sub-basin.	4
Figure 2.1	Tectonic Map elaborating the Regional Geological environment of the study area.	9
Figure 2.2	Generalized local tectonic map of Indus Basin, showing Kohat Sub-basin and Potwar Sub-basin.	13
Figure 2.3	Generalize Exposed Stratigraphic column of Kohat Sub-Basin.	17
Figure 4.1	Chart of the methodology adopted in the present study.	26
Figure 4.2	Potassium-Thorium crossplot to assess Shale mineralogy	29
Figure 4.3	Image shows Shale porosity components model	33
Figure 4.4	Graph use for calculation of LOM from vitrinite reflectance.	36
Figure 4.5	Crossplot of Young Modulus and Poisson ratio use for indication of Brittle and Ductile zone.	39
Figure 4.6	Brittleness Index vs Gamma-ray indicating level of Brittleness	40
Figure 5.1	Open hole wireline logs for Chichali Shale in Makori-01 well.	43
Figure 5.2	Calculated petrophysical attributes of Chichali Formation' zone-1 drilled in Makori-01 well.	44
Figure 5.3	Potassium-Thorium cross plot depicting the Shale mineralogy of Chichali Formation's zone-1 penetrated in Makori-01 well	45
Figure 5.4	Young's Modulus (YM) - Poisson's Ratio (PR) Crossplot depicting Brittleness qualitatively of zone-1 drilled in	

Makori-01 well. 46

Figure 5.5 Brittleness index (%) vs Gamma-ray (API) Crossplot depicting Brittleness qualitatively of Chichali Formation's Zone-1 drilled in Makori-01 well. 47

Figure 5.6 Calculated petrophysical attributes of Chichali Formation' zone-2 drilled in Makori-01 well. 48

Figure 5.7 Potassium-Thorium Crossplot depicting Shale mineralogy for zone-2 of Chichali Formation penetrated in Makori-01 well 49

Figure 5.8 Young's Modulus (YM) - Poisson's Ratio (PR) Crossplot depicting Brittleness qualitatively of Chichali Formation's zone-2 drilled in Makori-01 well. 49

Figure 5.9 Brittleness index (%) vs Gamma-ray (API) Crossplot depicting Brittleness qualitatively of Chichali Formation's zone-2 drilled in Makori-01 well. 50

Figure 5.10 Image showing all available log run in Chichali Formation penetrated in Manzalai-02 well. 51

Figure 5.11 Calculated petrophysical attributes of Chichali Formation's zone-1 penetrated in Manzalai-02 well. 52

Figure 5.12 Potassium-Thorium crossplot depicting the Shale mineralogy of Chichali Formation's zone-1 penetrated in Manzalai-02 well. 53

Figure 5.13 Young's Modulus (YM) - Poisson's Ratio (PR) Crossplot depicting Brittleness qualitatively of Chichali Formation's zone-1 drilled in Manzlai-02 well. 53

Figure 5.14 Brittleness Index vs Gamma Ray (GR) Crossplot depicting Brittleness qualitatively of Chichali Formation's zone-1 drilled in Manzlai-02 well. 54

Figure 5.15 Calculated petrophysical attributes of zone-2 penetrated in Manzalai-02 well. 55

Figure 5.16 Potassium-Thorium crossplot depicting the Shale mineralogy of Chichali Formation’s zone2 penetrated in Manzalai-02 well. 56

Figure 5.17 Young's Modulus (YM) - Poisson's Ratio (PR) Crossplot depicting Brittleness qualitatively of Chichali Formation’zone-2 drilled in Manzalai-02 well. 56

Figure 5.18 Brittleness index (%) vs Gamma ray (API) Crossplot depicting Brittleness qualitatively of Chichali Formation’s zone-2 drilled in Manzalai-02 well. 57

Figure 5.19 Image showing available open hole wireline logs in LAS file of Maramzai-02 well for Chichai Formation. 58

Figure 5.20 Calculaed petrophysical attributess for Chichali Formation’s zone-1 in Maramzai-02 well. 59

Figure 5.21 Potassium-Thorium crossplot depicting the Shale mineralogy of Chichali Formation’s zone-1 penetrated in Maramzai-02 well 60

Figure 5.22 Young's Modulus (YM) - Poisson's Ratio (PR) Crossplot depicting Brittleness qualitatively of Chichali Formation’s zone-1 drilled in Maramzai-02 well . 60

Figure 5.23 Brittleness Index vs Gamma Ray (GR) Crossplot depicting Brittleness qualitatively of Chichali Formation’s zone-1 drilled in Maramzai-02 well. 61

Figure 5.24 Calcualted petrophysical attributess for Chichali Formation’s zone-2 in Maramzai-02 well. 62

Figure 5.25 Potassium-Thorium crossplot depicting the Shale mineralogy of Chichali Formation’s zone-2 penetrated in Maramzai-02 well. 63

Figure 5.26	Young's Modulus (YM) - Poisson's Ratio (PR) Crossplot of zone-2.	63
Figure 5.27	Brittleness index (%) vs Gamma ray (API) Crossplot of zone-2 .	64
Figure 6.1	Image showing complete log suits available for Samana Suk Formation drilled in Makori-01 well.	67
Figure 6.2	Image shows the interpreted logs and calculated petrophysical attributes in Samana Suk Formation drilled in Makori-01 well.	68
Figure 6.3	DT-PHIN crossplot showing the porosity ranges and matrix mineralogy of Samana Suk Formation.	69
Figure 6.4	RHOB-DT crossplot showing the porosity ranges and matrix mineralogy of Samana Suk Formation.	70
Figure 6.5	RHOB-PHIN crossplot showing the porosity ranges and matrix mineralogy of Samana Suk Formation.	70
Figure 6.6	M-N Crossplot showing matrix lithology of Samana Suk Formation drilled in Makori-01 well.	71
Figure 6.7	Uma-Rhoma Crossplot drawn for assessing matrix lithology of Samana Suk Formation drilled in Makori-01 well.	72
Figure 6.8	Image showing all available logs run in Samana Suk Formation drilled in Manzalai-02 well.	73
Figure 6.9	Image shows the interpreted logs and calculated petrophysical attributes of Samana Suk Formation drilled in Manzalai-02 well.	74
Figure 6.10	DT-PHIN crossplot furnished for Samana Suk Formation drilled in Manzalai-02 well.	75
Figure 6.11	logs available for analysis of Samana Suk Formation drilled in Maramzai-02 well.	76
Figure 6.12	Image showing the interpreted logs and calculated petrophysical	

attributes for Samana Suk Formation drilled in Maramzai-02 well. 77

Figure 6.13 DT-PHIN crossplot furnished for Samana Suk Formation drilled in Maramzai-02 well. 78

Figure 6.14 RHOB-DT crossplot furnished for Samana Suk Formation drilled in Maramzai-02 well. 79

Figure 6.15 RHOB-PHIN crossplot furnished for Samana Suk Formation drilled in Maramzai-02 well. 79

Figure 6.16 Uma-Rhoma crossplot drawn for assessing matrix lithology of Samana Suk Formation drilled in Maramzai-02 well. 80

Figure 6.17 Uma-Rhoma Crossplot drawn for assessing matrix lithology of Samana Suk Formation drilled in Maramzai-02 well. 80

Figure 7.1 Base map showing the location of of wells. 81

Figure 7.2 Stratigraphic correlation constructed among wells of Manzalai-02, Maramzai-02 and Makori-01 well. 82

Figure 7.3 Volume of Shale map constructed for zone-1. 84

Figure 7.4 Average porosity map constructed for zone-1. 85

Figure 7.5 Shale porosity map constructed for zone-1 86

Figure 7.6 Total organic carbon richness map constructed for zone-1. 87

Figure 7.7 Volume of Shale map constructed for zone-2. 88

Figure 7.8 Average porosity map constructed for zone-2.. 89

Figure 7.9 Shale porosity map constructed for zone-2. 90

Figure 7.10 Total organic carbon richness map constructed for zone-2. 91

Figure 7.11 Volume of Shale map constructed for Samana Suk Formation. 92

Figure 7.12 Average porosity map constructed for Samana Suk Formation. 93

Figure 7.13 Effective porosity map constructed for Samana Suk Formation. 94

Figure 7.14 Saturation of water map constructed for Samana Suk Formation. 95

LIST OF ABBREVATIONS

API	-	Unit of GR log (American Petroleum Institute)
B.I	-	Brittleness Index
B.H.F	-	Bad Hole Flag
CGR	-	Computed Gamma Ray
DGPC	-	Director General of Petroleum Concession
DT	-	Sonic log representation (ΔT)
DT_{ma}	-	DT matrix
E	-	Young Modulus
EIA	-	Energy information administration
Et al.	-	Et alia (Latin phrase meaning; and others)
GR	-	Gamma Ray
IGF	-	Indo Gangetic Foredeep
KIA	-	Kohistan Island Arc
LAS	-	Log ASCII Standard
LOM	-	Level of Maturity
mD	-	Milli Darcy
MBT	-	Main Boundary Thrust
MKT	-	Main Karakoram Thrust

MMT	-	Main Mantle Thrust
NPhi	-	Neutron Porosity
PhiA	-	Average Porosity
PhiS	-	Sonic Porosity
PR	-	Poisson's Ratio
ResD	-	Deep Resistivity
ResM	-	Medium Resistivity
ResS	-	Shallow Resistivity
RhoB	-	Bulk Density
R_{mf}	-	Resistivity of Mud Filtrate
R_W	-	Resistivity of Water
SGR	-	Spectral Gamma Ray
SRT	-	Salt Range Thrust
SP	-	Spontaneous Potential
S_W	-	Saturation of Water
TOC	-	Total Organic Content
UIB	-	Upper Indus Basin
V_{SH}	-	Volume of Shale

CHAPTER 1

INTRODUCTION

From a few decades, due to the increase in oil prices and depletion of conventional reservoirs, interest in low permeability tight reservoirs and unconventional reservoirs has been increased. The definition for unconventional reservoir includes all reservoirs which cannot produce on conventional methods and needs extra treatment of reservoir like hydraulic fracking to be productive (Jurčić et al., 2012; Orlandi et al., 2011; Rezaee, 2015; Zou, 2017). Shale having organic richness (>2%), maturity (R_o>1.1%), with abundant brittle minerals is commonly considered as a potential unconventional reservoir (Slatt, 2011). Shale can act as a conventional source, as well as an unconventional reservoir. While tight reservoirs refer to strata with permeability below 1 mD (Ministry of Petroleum and natural resources, Pakistan 2011).

Both unconventional and tight reservoirs are characterized by low permeability (Kumar et al., 2013), and complex reservoir heterogeneity, which leads to the most important issue of their economic production. To curb these issues, hydrocarbons industries have delineated strategies to better understand and characterize tight and unconventional reservoirs from wireline log responses.

Characterizing a tight reservoir is different from conventional reservoirs because of the complex pore network. To characterize the tight reservoir, Petrophysical analysis is of high significance to understand and delineated the zone with better petrophysical parameters in terms of porosity and permeability. These zones are known as “Sweet Spots”. Which must be properly characterized for a successful production.

However, due to certain criticalities associated with tight reservoir characterization, log data must be integrated with core data. Similarly, To assess Shale for the unconventional reservoir potential, Brittleness, Volume of Clays, Total organic carbon, Organic matter type, and its maturity is crucial in the evaluation of Shale rock. The logging method to evaluate source rocks potential in the exploratory stage is devised by (Passey et al., 1990), which utilizes the Gamma Ray log, and Sonic log, Resistivity logs, and Density log. This method includes the calculation of TOC based on log

responses assuming that mature source rock has high resistivity, low density, and high sonic transit time.

In recent years, Technologies innovation has made it possible to cause production from the non-reservoir interval of wells through geo-steering and hydraulic fracturing in Shale intervals of wells (Kumar et al., 2013; Slatt, 2011). Although there are various pre-requisite for Shale interval to be the potential candidate for unconventional production (Slatt, 2011). While, Tight reservoirs exploitation needs acidizing, slickwater fracturing, and stimulation to produce from it (Hyne, 2012; Kumar et al., 2013). Hence, at present, the target for hydrocarbon production in Pakitan is almost conventional resources. However, due to the swift depletion of conventional reservoirs, the importance of Shale as unconventional reservoirs and tight reservoirs has been increasing.

In Pakistan, Several rock successions deposited in basins can be considered as a potential tight reservoirs and unconventional reservoirs for significant hydrocarbon production. The potential target for unconventional reservoirs in the Indus basin are; Paleocene Ranikot and Patala Shales, Cretaceous Sembar and Chichali Shales, and Jurassic Shinawri and Datta Formations (EIA, 2013). Besides Shale as unconventional reservoirs, Jurassic Datta Sandstone and Samana Suk Limestone are the renowned tight reservoirs of Indus basins hosting significant hydrocarbon potential.

The successful exploration and production of Shale-gas resources in the United States and Canada set a new possible solution towards the energy crisis presently affecting most countries of Asia including Pakistan. Although, a lot of studies have been carriedout in Pakistan to assess the conventional reservoirs but inadequate research has been carried out to assess the unconventional and tight reservoirs. Like other basins of Pakistan, the Kohat sub-basin is also vastly targeted by explorers in term of its structural evolution, stratigraphy, Depositional environment, Reservoir characterization, and source rocks evaluation, But it still lacks the understanding of the Potential of the Kohat sub-basin for its hydrocarbon production from unconventional and tight reservoirs through evaluating the wireline logging responses.

The present study is focused on the petrophysical analysis of unconventional and tight reservoirs of Cretaceous Chichali Formation in the upper Indus basin (analogous to

Sembar Formation of Lower Indus Basin) and Jurassic Samana Suk respectively, deposited in Kohat sub-basin through wireline logging responses for hydrocarbon potential.

1.1 Study Area

The wells studied are Makori-01 (71°13’ 26.730” **E**, 33°17’ 38.619” **N**), Maramzai-02 (70°59’ 17.00” **E**, 33°16’ 29.87” **N**), and Manzalai-02 bearing coordinates 71°06’ 56.42” E, 33°25’ 58.61” N belongs to Kohat Sub-basin, Pakistan. The Kohat Sub-basin is part of a complex Himalayan foreland belt constrained by Main Boundary Thrust, in the north and by the Surghar range in the South.

The upper Indus basin of Pakistan is delineated into two Sub-basin by the Indus river. One lying towards the eastern side is Potwar Sub-basin, While on the western side is Kohat Sub-basin. The Kohat-Potwar Sub-basin is characterized by the deposition of rocks from Pre-Cambrian to Quarternary.

The rock units in the present investigation are deposited in both Potwar and Kohat Sub-basin. But present study targets the characterization of Chichali and Samana Suk Formations from wells penetrated in the Kohat Sub-basin.

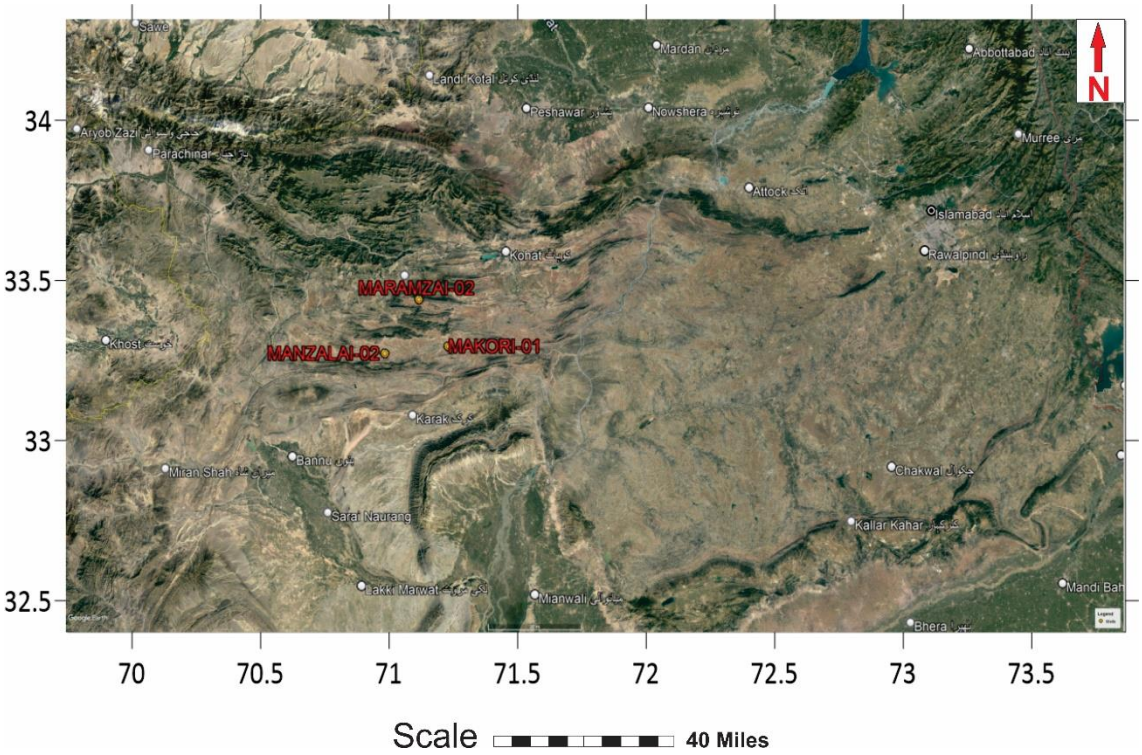

Figure 1.1 Location map of the wells studied in Kohat Sub-basin .

1.2 Problem Statement

The Energy Information Administration (EIA, 2013) has made their investigation to assess the technical recoverable Shale Oil/Gas of Pakistan in the Lower Indus Basin. They have calculated TOC for Paleocene Ranikot and Cretaceous Sembar Formation as 2.0% and categorize Ranikot and Sembar formation best for Unconventional Hydrocarbons production (EIA, 2013).

Likewise, the Lower Indus Basin, Kohat sub-basin the sub-basin of Upper Indus Basin, is characterized by deposition of reservoirs and source rock units. The main reservoirs of Kohat-Potwar are Chorgali and Sakesar (Eocene), Lockhart (Paleocene), Hangu Wargal (Permian), Datta and Lumshiwal (Cretaceous) while the Potential source rocks are; Grey Shales of Mianwali Formation (Triassic), Datta Shales (Jurassic), Chichali Formation (Cretaceous), and Patala of Paleocene age (Jamil et al., 2012; Kadri, 1995; Khan et al., 1986; Wandrey et al., 2004).

The Cretaceous Chichali Shales of the Upper Indus basin is considered Analogous to Cretaceous Sembar Shales of Lower Indus Basin in Lithology, Age and Fossils

contents are considered a potential source rock of Kohat sub-basin(Amjad et al., 2017; Wandrey et al., 2004). Keeping its resemblance to Sembar, the Chichali formation potential to act as an unconventional reservoir needs to be investigated.

Moreover, Samana Suk Formation has been reported as a tight reservoir because, it is characterized by the permeability of less than 1 mD (Ahmad et al., 2020). So, to extensively characterize the reservoir potential of Samana Suk, its detailed study through wireline logs needs to be investigated.

A lot of studies have been published probing depositional, lithological facies, and source rock potential over surface samples. Although, a detailed investigation to portray the unconventional potential of the Chichali and Samana Suk Formation as a tight reservoir is still lacking. Further study needs to assess the porosities and permeability, Detailed TOC calculation, and fluid saturation with help of wireline logs of these formations.

Therefore, the current study is focused on the evaluation of petrophysical parameters of unconventional and tight reservoirs of Chichali Formation and Samana Suk Formation respectively penetrated in three wells of Makori-1, Manzalai-2, and Maramzai-2. Hence, will give us more reliable and detailed characteristics of these two targetted formations.

1.3 Objectives of the research

The main objectives of the research are:

i. Analysis of Cretaceous Chichali Shales to delineate its potential for unconventional reservoir using wireline logs.
ii. Reservoir evaluation of Jurassic Samana Suk Formation as a tight reservoir.

1.4 Scope of research

This research will portray the reservoir characteristics and behaviour of tight Samana Suk Limestone and the Unconventional reservoir potential of Chichali Shales. The research will help understand the economic significance of both rock units from a hydrocarbon point of view and will lead a step for the upcoming researchers to further evaluate these units by a different methodology.

CHAPTER 2
TECTONICS AND STRATIGRAPHY OF AREA

2.1 Regional Geology

Pakistan preserves the northwestern edge of the Indian lithospheric plate. The Indian plate remained part of southern Gondwana from Permian to Jurassic Period (Wandrey et al., 2004).

The tectonic evolution of the Indian plate was initiated in the Late Jurassic around 167 Mya with the breakup of Gondwana. This includes the rifting of the Indian plate from Gondwana, its subsequent northward migration, its collision with Kohistan Island Arc at Main Mantle Thrust (MMT) and with the Eurasian Plate at Main Karakoram Thrust (MKT) (**Fig.** 2.1). This tectonic evolution resulted in the tectonic setup of northern Pakistan characterized with exceptionally diverse and intense tectonic features majorly comprising of major faults, Metamorphism, Island Arc and converging boundaries. This compressional tectonics is also responsible for generating compressional thin-skinned tectonic features since Eocene time on the northern and northwestern borders of the Indo-Pakistani Plate (Shah, 2003).

The continuous subduction of the Indo-Pakistan Plate since Cretaceous produced the remarkable foreland basins, mountain ranges of the Himalaya and a chain of foreland fold-and-thrust belts as thick sheets of sediments thrusted over the Indian Craton (Kemal, 1991). The Himalayan range is E-W trending of 2500 km long and 250 km wide (N-S).

The formation of all these features in the Northern edge of the Indian Plate is endorsed by the global tectonics when the Indo-Pakistan continent was parted from the

Gondwana in South about 130 Mya and started its journey northward (Johnson et al., 1976). The consequences of this drift appeared in form of the shrinking of Neo-Tethys present between the Indian and Asian continents. The continental drift and shrinkage were aided by the consumption of Neo-Tethys and the opening of the Indian Ocean behind the transform motion beside the Owen fracture zone situated towards SE of the Indo-Pakistani continent (McKenzi et al., 1973). The closure of Neo-Tethys was

characterized by intra-oceanic subduction, which has given rise to a series of arcs (Searle, 1991; Treloar & Izatt, 1993).

The Kohistan Island Arc (KIA) is one of those arcs, which had occurred magmatism for 40 million years after which closure of the back-arc basin occurred and KIA was thrusted on a Eurasian plate(Petterson & Windley, 1985; Searle, 1991; Treloar & Izatt, 1993). After the KIA collided with the Eurasian plate in the north about 50-55 Mya (Searle et al., 1999; Treloar et al., 1989), the subduction of Neo-Tethys was continued beneath the KIA. As a consequence, the foremost edge of the Indian Plate completely got consumed and collided with KIA along with MMT in the middle Eocene (Arif et al., 1999; Coward et al., 1986; Joseph, DiPietro & Pogue, 2004; P. Treloar et al., 1989). The collisional boundary between KIA and Indian plate is referred to as Main Mantle Thrust (MMT), while that between KIA and the Eurasian plate is known as Main Karakoram Thrust (MKT). The MMT is extended in the east to Afghanistan and in the west, it passes through Swat, Babusar, Nanga Parbat-Haramosh massif to Ladakh Arc Complex.

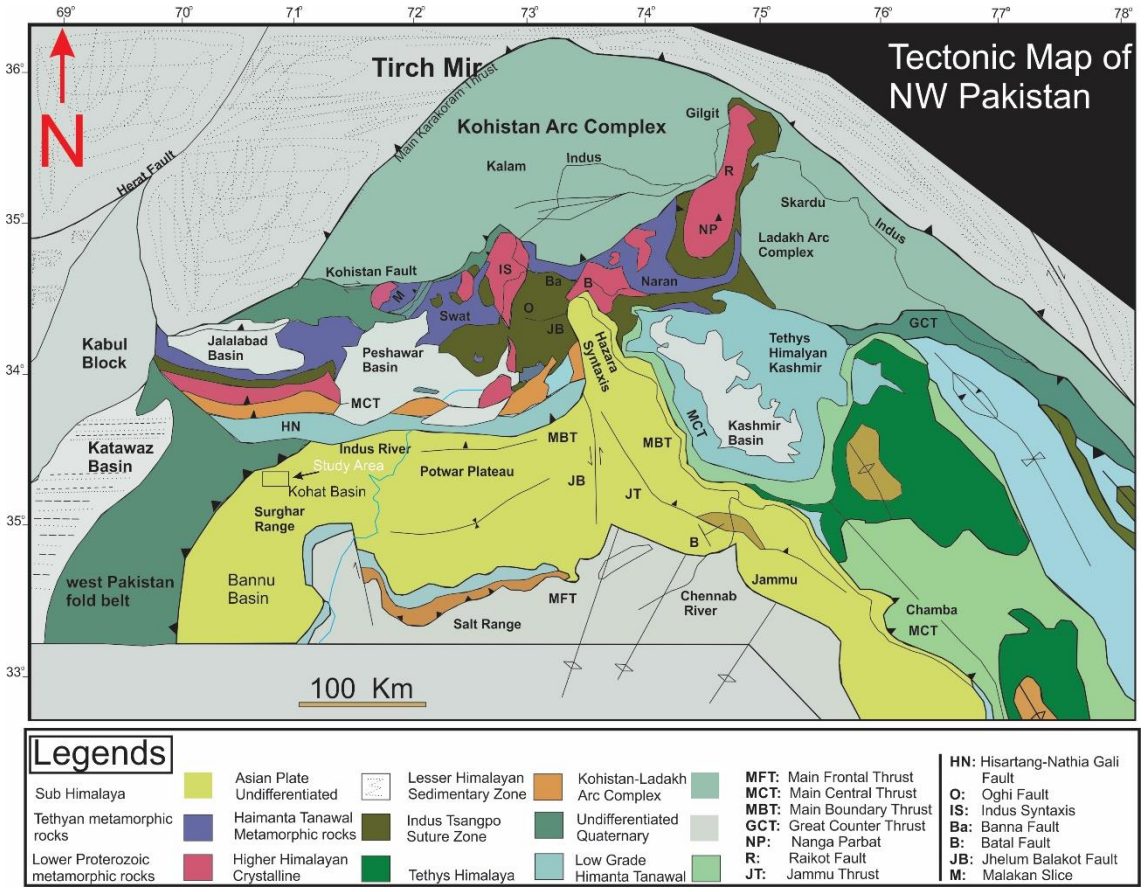

Figure 2.1 Tectonic Map elaborating the Regional Geological environment of the study area. Sources: Redrawn after (DiPietro and Pogue, 2004)

The southward migration of deformation from MMT is represented by MBT, which demarcates the boundary between the northern deformed fold and thrust belt and molasse sediments of Upper Indus Basin (UIB).

Along the western margin, the collisional tectonics of Indian craton is controversial (Shah, 2003). However, Chaman Fault is commonly taken as the western limit of the Indo-Pakistan plate. However, several plate margin indicators and cratonic blocks have been documented about 100-300 km SE of the Chaman Fault. Kabul Block is one of these cratonic blocks. Chaman Fault joins the Makran's subduction zone in the south with the Himalayan zone in the North.

2.1.1 Tectonic division of NW Pakistan

North-western Pakistan is mainly divided into five tectonic units bifurcated by major faults. From South to North is comprises of Ido-Gangetic Foredeep, Southern

deformed fold and thrust belt, Northern deformed fold and thrust belt, Kohistan Island Arc and Karakoram Block.

Salt Range Thrust (SRT) marks the boundary between Indo-Gangetic Foredeep and Southern deformed fold and thrust belt, MBT demarcates the boundary between Southern deformed fold and thrust belt and Northern deformed fold and thrust belt, MMT marks between Northern deformed fold and thrust belt and KIA, while MKT splits KIA from Karakoram Block.

2.1.2 Karakoram Block

Karakoram Block the northernmost tectonic unit, on the virtue of its proximity to the deformed zone, it mainly comprises deformed sedimentary, meta-sedimentary and igneous rocks. The southern limit of the block is characterized by MKT, which is marked by bifurcation of Palaeozoic metasediments of Karakoram Block from Cretaceous-Tertiary KIA.

2.1.3 Kohistan Island Arc

The subduction of Neo-Tethys under Asia has developed KIA during Jurassic-Cretaceous (Searle, 1991). The Arc comprises a variety of volcanic and plutonic rocks subjected to a varying degree of metamorphism and deformation. KIA is delimited by NS trending Nanga Parbat Haramosh massif (NPHM) into KIA and Ladakh Arc. The KIA is lined by MKT and MMT in North and South respectively.

2.1.4 Northern deformed fold and thrust belt

To the south of MMT, the tectonic unit lying is termed as Northen deformed fold and thrust belt. Characterized by intensely deformed sedimentary, metasedimentary and igneous rocks. The unit stretches from the Kashmir basin in the east toward the Kurram area in the West near the Afghan border. The northern border of this unit MMT is tilted in a trend called Nanga Parbat Haramosh Massif. The correlation of MMT to the Indus Suture Zone has been documented. The southward boundary of Northern Deformed Fold And Thrust Belt is marked by MBT, which separates it from the Southern Deformed Fold and Thrust Belt.

2.1.5 Southern Deformed Fold and Thrust Belt and Indo Gangetic Foredeep

This tectonic unit is the main depocenter for the influx of molasse whose deposition commenced in the early Miocene. This tectonic unit is separated from the northern deformed fold and thrust belt by MBT in the north. While SRT in the south separates it from the Indo-Gangetic foredeep. The active deformational front is represented by SRT and Trans Indus Ranges, where the Cambrian-Paleocene strata have been thrusted on Indo Gangetic Foredeep (IGF). The IGF is overlain by Quaternary sediments, eroded and transported from the deformational zone of Himalayan orogeny.

2.2 Local Tectonics of Study Area

The present area of study lies in the Southern Deformed Fold and Thrust Belt, which was far away from the northern margin at the time of the collision. The southward deformation evolution in the late Miocene has affected this area harshly.

Kohat-Potwar Sub-basins of the Indus basin lies in the south of Himalaya and Karakoram rock units resulted from the compressional tectonics of Indo-Eurasian collision (Paracha, 2004). The collisional tectonics between the Indian and Eurasian plates has severely affected the tectonics and structural evolution of Pakistan. This tectonic resulted in the formation of the Himalayan orogenic belt with foreland basins (Wandrey et al., 2004). Kohat basin is also one of the compressional basins of the Himalayan foreland belt.

The zone, west to the Indus river comprises Kohat sub-basin. Also known as Kohat plateau because of the development of low hills and dissected valleys has formed it as a composite Plateau.

The Kohat sub-basin comprises the Southern depression known as Bannu depression and northern uplift known as Kohat Salt Zone. Fluvial sedimentation mostly covers the flat area of the salt zone. The salt base is neither uplifted to the surface nor has been discovered through drilling. Bannu depression is alluvial plain and is completely covered by alluvials.

The Kohat sub-basin is bounded in the north by Kala Chitta Range and MBT. Along with MBT, the highly deformed rocks of Mesozoic are brought over the Eocene-Miocene Sediments of Kohat Basin (Yeats & Hussain, 1987). While in the south, Kohat sub-basin is restricted by Salt Range Thrust and Western extension of Salt range thrust i.e Trans Indus ranges and Surghar ranges. Similarly, the eastern and western side is bounded by the Indus river and Kurram Fault respectively. The Kurram Fault, a left-lateral transform fault is marked by the juxtaposing of highly deformed Mesozoic rocks of, Darsmand, Waziristan and Samana with Eocene-Miocene strata of Kohat basins. The Indus River in the east separates the Potwar Sub-basin from Kohat Sub-basin. Kalabagh fault the dextral fault lies towards the SE of Potwar Sub-basin marked between the Trans Indus Range and Salt range Thrust (**Fig.** 2.2)

Surghar range is marked by the overthrust of Mesozoic sediments over the alluvium of the Punjab platform (Zeb et al., 2020). These Mesozoic sediments are then juxtaposed by the kurram fault with Eocene-Miocene sediments. The salt range thrust lies towards SE of Kohat Sub-basin and is separated from the Surghar range by the Dextral Kalabagh fault.

The tectonic environment of the Kohat sub-basin is responsible for the trap mechanism of the petroleum system. Both structural and stratigraphic trap has been noticed including, flower structures, antiformal stack, fault propagating folds and thrusted anticlines (Hussain & Zhang, 2018). The other possible target of potential trap could be truncations between Jurassic strata and Cretaceous strata, thrusted anticlines and gentle folds (Wadood, Awais, & Sheikh, 2018).

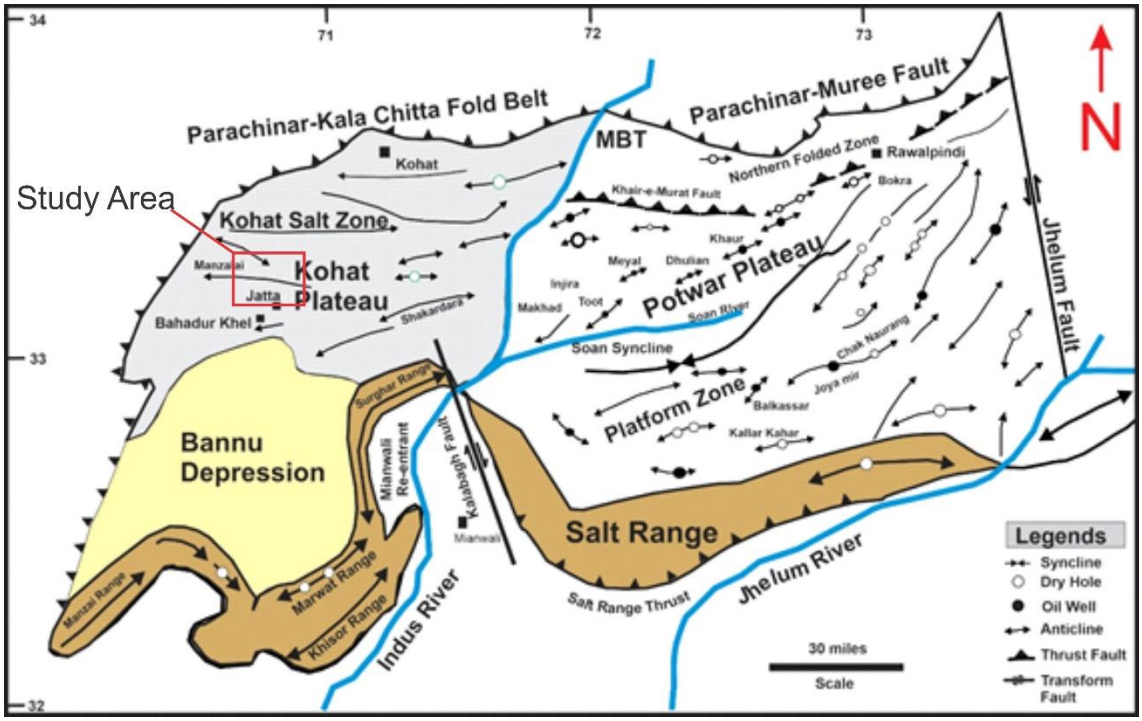

Figure 2.2 Generalized local tectonic map of Indus Basin, showing Kohat Sub-basin and Potwar Sub-basin. Sources: (Khan et al., 1986; Shami and Baig, 2002; Zahid et al., 2014)

2.3 Stratigraphy of Study Area

The EW trending Kohat Sub-Basins, located on the northwestern margin of the Indian Plate, are structurally defined petrolific regions with an area of approximately 4000 square kilometres in the north of Pakistan. This basin is a commercially very significant sub-basin of the Indus basin for the production of hydrocarbons (Khan et al., 1986; Charles et al., 1974).

The basin is characterized by a relatively complete depositional record with a stratigraphic thickness of 25000+ feet. Sedimentation ranges in age from Late Proterozoic to Holocene, while rocks from Jurassic to Quaternary are exposed only (Charles et al., 1974; Wandrey et al., 2004; Zeb et al., 2020). Basement Metamorphic rocks are overlain by the oil-impregnated Shales, evaporites and interbedded carbonates of Salt Formation. Thick Carbonates overlain by Evaporites marks the upper part of the Salt Range Formation.

Over the Salt Range Formation, the stratigraphic sequence records the deposition of Khewra Sandstone; A massive Sandstone and Marine Shales of Braided stream. The Khewra Sandstone is producing reservoir in Adhi, Rajian, and Chak Naurang (Petroconsultants, 1996). The Khewra Formation is overlain by the Glauconitic shoreface Sandstone and Siltstone of Kussak Formation, which gave us production in Missa Keswal (Petroconsultants, 1996). The Kussak Formation is overlain by Dolomite and nearshore Sandstone of Jutana Formation.

The top of the Cambrian stratigraphic sequence is marked by the deposition of Shales with interbedded Sandstones of Baghanwala Formation in the Potwar region, while Salts of Khisor Formation in Kohat region. Over a sequence of the Baghanwala Formation, the depositional record of the Kohat Sub-basin shows the hiatus in deposition, which remain until the Jurassic.

The hiatus in depositional record is broken by the deposition of the Jurassic Datta Formation comprising variegated siliciclastics with non-marine Sandstones (Khan et al., 1986). Datta Formation has been produced in Dhulian Oil Field. The Datta Formation is overlaid by platform Carbonates of Samana Suk Formation. Basinal Shales of early Cretaceous Chichali Formation, Sandstone of middle Cretaceous Lumshiwal, and Limestone of Late Cretaceous Kawagarh Formation are deposited over the Samana Suk Formation depicting the low-stand events in Kohat Sub-basin.

The commencement of Cenozoic sedimentation is marked by the deposition of the Paleocene Makarwal Group. The Makarwal group is represented by the Hangu, Lockhart and Patala formations. Siliciclastics of Hangu Formation deposited over the erosional surface of Kawagarh Formation delineating the top of Kawagarh Formation. A transitional contact lies between the Hangu and overlying Carbonate Shelf of Lockhart Formation and in between Lockhart Formation and overlying shallow marine Shale and Subordinate Carbonates of Patala Formation (Iqbal & Shah, 1980; Shah, 1977). Lockhart and Patala formations both have been recorded for its Hydrocarbon production. During Paleocene, sedimentation on the passive margin of the Eastern Tethys was taken up with the deposition of the clastics of shallow marine/lagoonal deposition of the Lower to Middle Eocene, which provided an excellent platform for the accumulation of hydrocarbons (Wadood et al., 2018).

The Eocene successions are recorded by deposition of Panoba Shale, Bahadur Khel Salt, Sheikhan Formation, Jatta Gypsum, Mamikhel Clay, and Kohat Formation. Panoba Formation is characterized by deposition of Marine to Logoonal Shales with interbedded Limestone. Deposition of Lower Eocene Bahadur Khel Salt over Panoba Shale has been reported only in Kohat Sub-basin. The Bahadur Khel Salt is overlain by Shale of Sheikhan Formation. Formation mainly composed of Carbonates and Gypsiferous Shales.

Cherat group of Eocene includes the Jatta, Mamikhel and Kohat Formations. The Jatta Gypsum is reported as a lateral face of the Sheikhan Formation in Kohat Sub-basin (Sameeni, Haneef, Rehman, & Lipps, 2009). Jatta Gypsum is overlain by the deposition of Mami khel Clay. The Jatta Gypsum is considered as lateral facie of Kuldana Formation and comprises of brownish red to red Shale, which is reported as calcareous and silty within Sandstone beds (Sameeni et al., 2009). The late Eocene Kohat Formation is characterized by lithology of mainly Carbonate with interbedded Shale deposited over the Mamikhel Clay.

Kohat-Potwar fold-and-thrust belt is a constantly explored prolific hydrocarbon province having many proven petroleum systems with considerable values of organic content. Mainly the potential reservoirs range from Mesozoic to Tertiary with anomalous oil and gas potential in Paleocene mixed clastics and carbonates of the Kohat-Potwar Sub-Basins (Bilal. Wadood et al., 2018). Major hydrocarbon discoveries in the basin are from Makori, Mela, Chanda, Nashpa and Manzalai fields (Zeb et al., 2020). Kohat Formation has sharp and distinct contact with lower-lying Mamikhel Clay (Shah, 1977).

The Miocene succession in Kohat Sub-basin is characterized by deposition of Molasses. Molasse sedimentation in Kohat Sub-basin commenced in the early Miocene with deposition of the Muree Formation. The Miocene successions were mainly composed of the Rawalpindi group and Siwalik Group. Rawalpindi group includes the Formations of Muree and Kamlial, while the Siwalik group includes the sedimentation of Chinji, Nagri, and Dhok Pathan Formations.

The Early-Miocene Muree formation comprises dark red, Purple to greenish-grey Sandstone depicting deposition in highly oxic conditions. It is well exposed in the

northern region of the Kohat Sub-basin. Muree Formation is unconformably deposited over the Kohat Formation while its upper contact with Kamlial Formation is transitional**.** Muree formation is the youngest producing reservoir in Kohat Sub-basin.

Kamlial Formation is composed of grey to greenish-grey colour Sandstone with thinly interbedded Shales. The upper contact of Kamlial Formation with Chinji Formation is conformable. Chinji Formation of Late-Miocene is comprised of red Clay with subordinate Sandstone. It is conformably overlain by Nagri Formation. Nagri Formation deposited during Late-Miocene over Chinji Formation and is comprised of mainly Sandstone with minor Clay and interbeds of Conglomerates. The Formation has conformable lower and upper contact with Chinji and Dhok Pathan formations respectively.

A lot of studies have been carried out highlighting the potential source and reservoir rocks. The main source rocks of the basin include the Chichali Formation of Cretaceous age, Mianwali formation of lower Triassic, and Sardhai formation of Early Permian age. While main producing reservoirs are the Warcha Formation of Early Permian, Wargal formation of Permian, Samana Suk Formation of Jurassic, Lockhart Formation of Paleocene, Chorgali Formation of Eocene and Muree Formation of Miocene age (Kadri, 1995). The petroleum rocks geometry is mainly structurally trapped with Fault bounded pop up the structure are common in Kohat sub-basin.

The basin has proven source rocks, with TOC ranging from poor to good. As from (fig 2.3) it is clear that the basin is characterized by several units of Shale, so, a potential for unconventional production might exist in these units. Several studies have been performed targetting these Shale lithologies in terms of their depositional environment and microfacies analysis while a few papers are published in journals targetting for unconventional potential using wireline logging. The current study will delineate the unconventional potential of Chicali Shale and Sama Suk Limestone from the wireline logging response experienced over various wells.

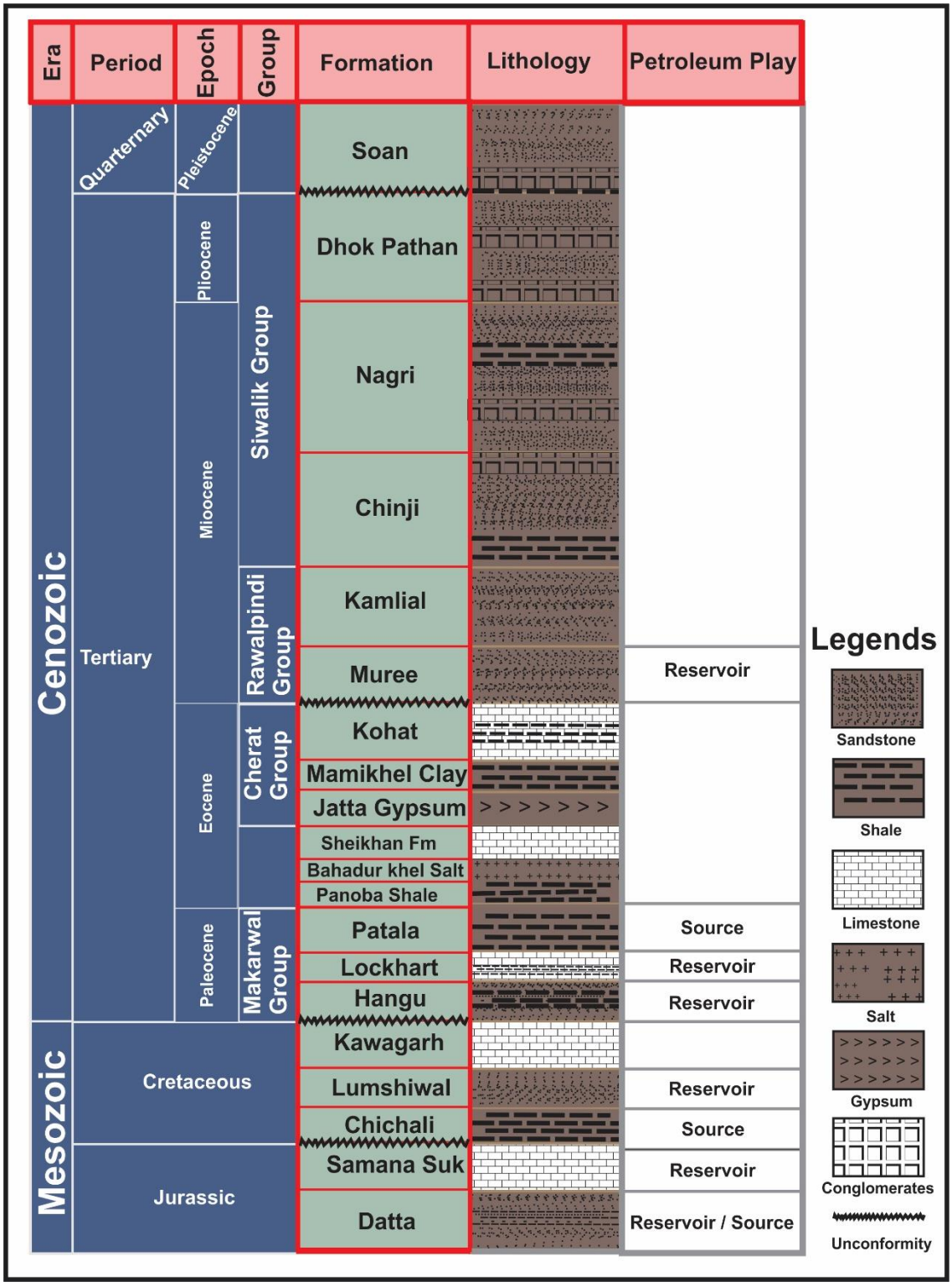

Figure 2.3 Generalize Exposed Stratigraphic column of Kohat Sub-Basin. Sources: after (Kadri, 1995; Zeb et al., 2020)

2.3.1 Samana Suk Formation

The rocks from Samana Range near Hangu for the first time were named Samana Suk by Davies in 1930 formerly named as “Kioto Limestone” by Middle miss (1896). The term Samana Suk is derivative of the peak’s name in Samana Range.

It is dark grey to Brownish grey, dense to very fine-grained crystalline beds of Limestone (Meissner et al., 1974). The age of the Samana Suk Formation is Jurassic (Hussain et al., 2012). At the type locality, the Samana Suk comprises grey, medium to thick-bedded Limestone with subordinate marls and clays. The Formation is oolitic in Kala Chitta and Hazara and it includes some dolomitic and ferruginous sandy, oolitic beds but these are absent here in the Nammal area. The formation is widely distributed in the western Salt Range, Kohat, Trans Indus ranges, Hazara and Kala Chitta.

2.3.2 Chichali Formation

This formation was termed by (Danilchik, 1961) for rocks earlier described as the “Belemnite beds” in the salt and Trans Indus ranges. The Cretaceous age’s Chichali formation is mainly comprised of Shale with Sandstone in the upper parts. The formation has good exposure at the Mizari tang section. The formation contains Belemnites and the Sandstone portion is comprised of Glauconites (Meissner Jr et al., 1974).

The type section is Chichali pass in the Surgar range. At the type locality, the formation contains weathered rusty brown glauconitic sandstone with dark grey sandy, silty glauconitic Shale in the lower part. In the western salt range, it has three members. Lower member with glauconitic Shale with some phosphatic nodules passing upward into dark green Glauconitic.

CHAPTER 3
LITERATURE REVIEW

The Cretaceous Chichali Formation was formerly named as Belemnites beds (Oldham, 1892). After that, it was named Belemnite Shales (Danilchik, 1961). A lot of studies have been published regarding the petrophysical analysis and field analysis of various reservoirs units of the Kohat basin. Many foreign and indigenous researchers have targeted the Kohat basin for its potential to be a productive basin. The main rocks units targetted in the current proposal is Chichali Shales and Samana Suk Limestone. The Chichali Shale will be evaluated in terms of its potential as an unconventional reservoir while Samana Suk for its reservoir characteristics as tight Limestone.

The well-detailed portrayal of the hydrocarbon potential of the Kohat-Potwar basin is performed by Khan et al. (1986), Meissner et al. (1974). The work is a pioneer in term investigating the petroleum play of the upper Indus basin of Pakistan. The study investigated the structural, Stratigraphical and Tectonic aspects of the Upper indus basin and identified the potential reservoirs and source rocks of the basin.

The recently renowned works reported targetting the Chichali Formation are of: Zeb et al. (2020), Natasha (2019), Hashmi et al. (2018), Amjad et al. (2017) and Siyar et al. (2018).

Zeb et al. (2020) has studied the environment of deposition, hydrocarbon potentiality, thermal maturity, and source of organic matter of Chichali Formation in the Kohat sub-basin through field and lab analysis. They categorised Chichali Formation as Poor to good petroleum source potential with type-II kerogen and deposition under anoxic conditions.

Natasha (2019) evaluated Datta formation penetrated in Chanda-01 and Chanda Deep-01 wells. The study involves petrophysical analysis combined with fluid substitution modelling of the Datta reservoir. Datta formation came up with a bearing of good hydrocarbon-bearing zones in both wells with one zone in Chanda-01 and four zones in Chanda Deep-01 wells. Fluid substitution models show formation has affected

Compressional Velocity (V_p), Density (RHOB) while Shear wave velocity (V_s) remain unaffected with fluid substitution of Hydrocarbons by brine fluids.

Hashmi et al. (2018) studied the Reservoir quality, Diagenetic modifications, and sequence stratigraphy of the Chichali Formation in the Nizampur basin and declared the middle to outer ramp depositional environment of formation. The study also noticed laterite, glauconitic bearing sandstone and carbonaceous green Shale of the Chichali Formation.

Siyar et al. (2018) has calculated the TOC of the Chichali Formation through wireline logs of Chanda-01 wells between 0 to 1.38%.

Husssain and Zhang (2018) mapped the structural features of the Kohat Sub-basin resulted due to collisional tectonics through integrating 2D seismic data with field observations. He recorded the tight anticlines and broad synclines as structural evolution indications of the basin. The study also suggested the deformation in three episodes with detachments folds development on Eocene evaporites in the first episode, followed up by truncation by thrust faults in the second phase and third phase involved rotation of early formed folds and faults through the influence of Kalabagh dextral fault.

Amjad et al. 2017 integrated well logs analysis of Chichali Formation penetrated in Chanda-01 well, Kohat Sub-basin with lab analysis undergone on the rock cutting samples. Properties like TOC and vitrinite reflectance were measured and evaluated. Results showed good correlation and categorised Chichali Formation as fair source rock with TOC greater than 1%.

Saddique et al. (2016) characterized the properties of the reservoir of Lockhart, Hangu and Lumshiwal formations penetrated in Kahi-01 well near Kahi village, Kohat sub-basin. The wireline logs were evaluated in the investigation of the reservoir potential of these formations. Three prospective zones with comparatively high hydrocarbon saturation in Hangu formation, while Lockhart and Lumshiwal formation show no promising intervals because of inadequate porosity.

Qureshi et al. (2007) Investigated the microfacies analysis of Chicali formation from the Kala Chitta Range and has revealed four microfacies having deposition in from

shallow to anoxic environment. The shallow environment is supported by the presence of Glauconites, Ammonites and Belemnites while the presence of black Shale confirms the deposition in an anoxic environment (Qureshi et al., 2007).

Similarly, vast research has been published regarding Samana Suk Formation's microfacies analysis, reservoir potential and sequence stratigraphy while no detailed research focusing on evaluating reservoir characteristics of Samana Suk Formation on logs based is published. The renowned works published on Samana Suk Formation are of (Ahmad et al., 2020), (Wadood et al., 2020), (Rahim et al., 2020), (Hayat et al., 2019), (Nizami, 2019), (Rehman et al., 2018), (Hussain et al., 2012) and (Cheema, 2010).

The Samana Suk Formation has been reported as tight limestone possessing permeability ranging from 0.04 to 0.5 mD (Ahmad et al., 2020). A detailed integrated study has been performed on surface sampling from the Kala Chitta range in the context of Petrography, Palynology, SEM and XRD by (Ahmad et al., 2020) proving Samana Suk Formation as a potential hydrocarbon reservoir.

Wadood et al. (2020) probed in the sequence stratigraphic framework of the Samana Suk Formation from the Kala Chitta Range. The study reported one local cycle and three regressive system tracts and two transgressive system tracts in the rock unit (Wadood et al., 2020).

Rahim et al. (2020) probed in the diagenetic evolution and associated dolomitization of the Samana Suk Formation in lesser Himalaya. The study revealed six phases of Dolomitization. From the study of isotopes, the source of dolomitization is declared to be from evaporative processes, hydrothermal fluid sources and meteoric fluids (Rahim et al., 2020).

Hayat et al. (2019) studied Samana Suk Formation from Nammal Gorge and investigated sequence stratigraphy and reservoir characterization. The study revealed Samana Suk Formation comprises of one 2^{nd} order cycle and three 3^{rd} order cycles. Based on the petrographic analysis the rock unit was declared as a good reservoir with porosity ranging from 6% to 18% (Hayat et al., 2019).

Nizami (2019) focused on Faunal Assemblages of the Middle Jurassic Samana Suk Formation, Chichali Gorge Section, Surghar Range. They reported the presence of foraminifers, gastropods, pelecypods, bryozoans, echinoids, sponges, brachiopods, and corals in rock units (Nizami, 2019).

Rehman et al. (2018) studied the geotechnical aspects of Samana Suk from the Marwat Range and investigated the aggregate suitability of rock units. The results were compared with standards of ASTM and AASHTO and recommended to be suitable for the aggregate purpose (Rehman et al., 2018).

Hussain et al. (2012) studied the Samana Suk Formation from the Harnoi section and delineated the diagenetic fabrics of the Samana Suk Formation and reported various diagenetic events present are; stylolites, veins, fractures, and dolomitization (Hussain et al., 2012).

Cheema (2010) studied the Depositional environment, microfacies and Diagenesis of Samana Suk Formation in south-east Hazara and Saman Range. The investigation revealed shallow to very shallow marine depositional environment typical of slightly dipping shelf/ramp. The study suggested diagenetic sequences ranges from marine phreatic to deep burial (Cheema, 2010).

In the light of the above literature it is clear that a lot of studies have been published focusing on Facie analysis, Reservoir characterization based on petrography, Sequence stratigraphy, and diagenetic study, but it still lacks the characterization of Samana Suk in the Kohat sub-basin with the help of logs responses to identify the fluid type, porosity and permeability and saturation of both Cihchali and Samana Suk Formation. Hence, the present study will endeavour to cover these gaps in understanding the unconventional potential of Chichaliand Reservoir characteristics of Samana Suk Formations based on wireline logs responses

The data provided was adequate to compute the lacking parameters of Chichali and Samana Suk Formation through open hole wireline logs that has been pointed out in literature review Although a high accurate analysis could have been made if drill cuttings, NMR log and Pulsed Neutron Mineralogy logs were provided.

CHAPTER 4

METHODOLOGIES

This chapter is mainly focused on demonstrating the methods and theoretical background which is applied in conducting the present study. The methodology followed in the present study to analyze and interpret the wireline logs responses can be categorised into three major phases.

i. Data collection
ii. Data processing phase.
iii. Interpretation and petrophysical attributes calculations.

4.1 Data collection

The present study has utilized the open-hole wireline logs responses from three wells; Manzalai-02, Maramzai-02 and Makori-01 to analyze the potential of the source rock of Chichali, and the tight limestone of Samana Suk Formation. The well logs data was acquired from Director General Petroleum Concessions (DGPC) in digital LAS format. Logs suites included Spectral Gamma Ray log (GR), Resistivity log (Deep, Medium, Shallow), Spontaneous Potential Log (SP), Neutron log, Density log, PEF log and Sonic log. The data was then loaded to Geographix software for analysis and calculation of petrophysical attributes.

4.2 Data processing

The data processing involves the extensive quality checking of data to assess its reliability and accuracy and the availability of all necessary logs.

There are many steps in data processing depending on the quality of data, but the following are the few data processing steps that were required and applied in the present study:

4.2.1 Data check

The first phase of data processing involved the ensuring availability of complete log suits needed in the analysis. The digital LAS files of wells were scrutinized for the availability of complete log suits required in both conventional reservoir analysis and Shale analysis. Spectral Gamma Ray logs were missing initially the data provided by the Directorate General of Petroleum Concession (DGPC), which were then provided upon request.

4.2.2 Removal of end effect

Eliminating the erroneous response of the tool just at the start or end of the log run. The log gives us static reading right at the start or end of the reading, which must be removed to give us reliable and accurate analysis. In the present study, in Makori-01 well, the end effect of few logs of SGR, CGR, K-U-THOR curves and Resistivity logs were removed using the Gverse petrophysics curve editing tools. The rest of the logs in the remaining wells had not any erroneous value due to the end effect.

4.2.3 SP baseline shift

In the unprocessed SP log, the SP log against the Shale lithology gives us drift in the Shale baseline. This shift in SP log against Shale lithology requires to be taken to the proper baseline to identify our negative and positive deflection to make our interpretation accurate. In the present study, SP log from all three wells was corrected for the Shale baseline.

4.2.4 Rescaling

It involved the definition of a standard scale for each log. Upon loading the LAS file, few logs were found to have been assigned with improper scale, which was then edited and proper scale were defined.

4.2.5 Splicing:

Splicing is the process of Joining the individual log that runs into a single composite log. LAS file included two or more than two individual log runs in a single

composite log. In the present study, all three wells contained different log runs that were spliced into a single composite curve using Gverse Petrophysics' curve editing tools.

4.2.6 Software utilization

4.2.6.1 Geographix Software

The software used for analysis is Geverse Petrophysics of Landmark Resources (LMKR). Complete Geographix suite software's licence was provided upon request from the competent authority of LMKR.

4.2.6.2 Graphics Software

The Corel Draw X6 portable graphic software was utilized for the creation of stratigraphic columns, Geological and Tectonic maps, and editing photographs.

4.3 Data Interpretation

Interpretation and petrophysical attributes calculations involve the loading of processed data in software and its subsequent analysis by computing default and user-defined equations. Both the qualitative and quantitative approaches were taken to interpret the logs response. The data was interpreted for conventional and unconventional hydrocarbon resource potential of Samana Suk Limestone, and Chichali Shale respectively.

The conventional Petrophysical attributes for Samana Suk Limestone computed in the present study includes Volume of Shale, Porosity Calculation, Hydrocarbon Saturation, Permeability analysis, and Net pay summations.

Whereas, Unconventional petrophysical attribute for Chichali Formation comprises, Volume of Shale, Shale mineralogy, Porosity calculation, Shale porosity, Total organic carbon, water saturation, and Petroelastic properties of the formation.

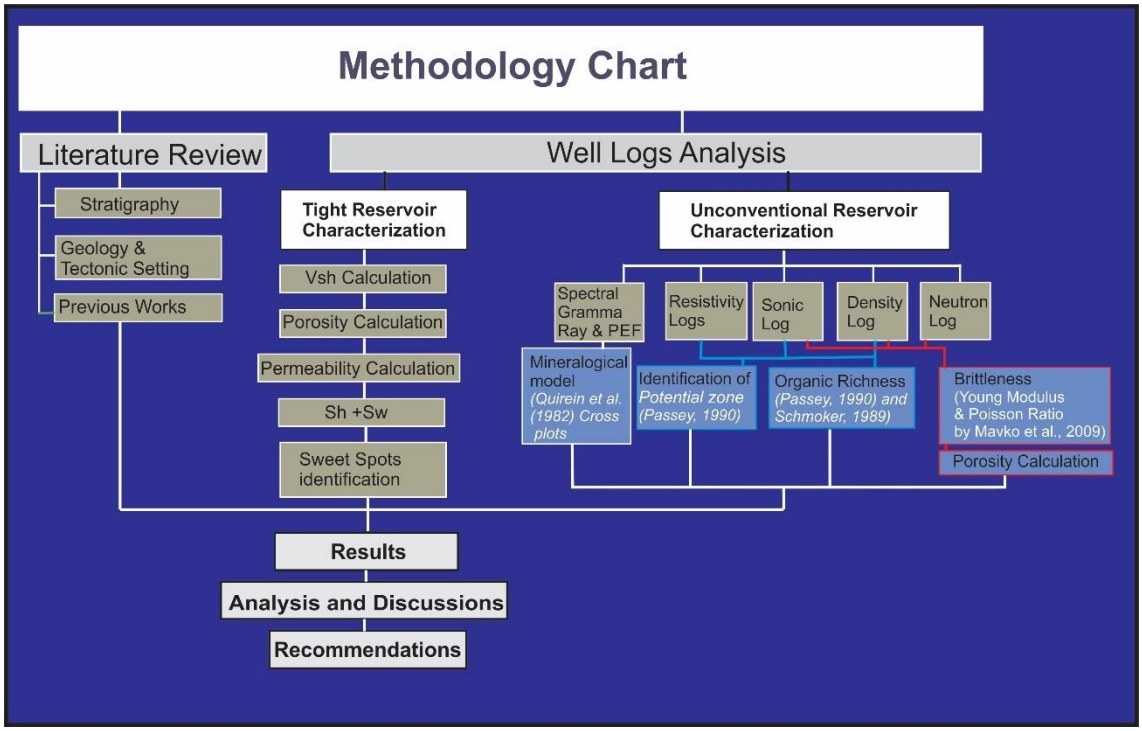

Figure 4.1 Chart of methodology adopted in the current study.

4.4 Petrophysical Attributes Calculation

Each log tool measures a particular property of rock, which is then analyzed qualitatively and quantitatively. The principal tool's measurements and how they are used in reservoir and source rock petrophysical attributes computations and their interpretation in the present study are discussed as follow:

4.4.1 Caliper Log

Calliper log is run into the well to measure the size and shape of the well. This is a simple mechanical caliper that records the vertical profile of the wellbore. The tool can be used to point out the bad hole flag in the borehole, against which data recorded of certain logs should be checked with extra consideration for its reliability.

4.4.1.1 Borehole Rugosity

The algorithm to calculate the hole rugosity is given as (Rider, 1986);

Borehole Rugosity = Caliper size – Bit Size

If Borehole rugosity > 2, then it gives us a bad hole flag.

4.4.2 SP Log

Spontaneous potential log (SP) measures the potential variance between the reference electrode at the surface and the electrode in the borehole. The principal use of the Sp log is the measurement of formation water resistivity.

4.4.3 Gamma Ray log

The gamma-ray log is used to count the formation of natural radioactivity. As Shale has high radiation value, so in Shale reservoir, GR log is used to qualitatively demarcate the zone of Shaly formation, Source rock and clean reservoir zone. The tool can be divided into two categories;

4.4.3.1 Natural Gamma Ray tool (NGR):

it gives the composite radioactivity from Uranium, Potassium, and Thorium in combined form as a single log value. Help in quantitative interpretation of Shale volume calculations.

4.4.3.1.1 Volume of Shale

The algorithm for the volume of shale is (Asquith, Krygowski, & Gibson, 2004; Rider, 1986);

$$\mathbf{Vshl} = \frac{(\mathrm{GRlog} - \mathrm{Grmin})}{(\mathrm{GRmax} - \mathrm{GRmin}}$$

Where **GRlog** = Gamma-ray value from log.

GRmax = GR log's Maximum value.

GRmin = GR log's Minimum value of.

The best method to calculate the volume of Shale can be from computed Gamma-ray log (CGR) if available. As Uranium could be associated with sediments due to adsorption by organic matter, thus the Uranium radioactivity needs to be subtracted from Natural Gamma Ray to rectify the effect of radioactivity given by adsorbed Uranium in organic

matter. The high Natural Gamma Ray readings due to adsorbed Uranium by organic matter can give us the erroneous volume of Shale content (Greater than actual Shale content). In Makori-01, and Manzalai-02 well volume of Shale has been calculated from CGR log using algorithm;

$$\mathbf{Vshl} = \frac{\text{CGRlog} - \text{CGrmin})}{(\text{CGRmax} - \text{CGRmin}}$$

4.4.3.2 Spectral Gamma Ray tool (SGR):

it discriminates between the individual radioactivity of Uranium, Potassium, and Thorium and gives three logs, one for each radioactive element. It is used for assessing the mineralogical composition of Shale using (Quirein, Gardner, & Watson, 1982) and (Schlumberger log interpretation charts, 1997) cross plots.

4.4.3.2.1 Shale Mineralogy Assessment

Among the sedimentary rocks, Shale lithology has comparatively high gamma-ray values. This fact compels the Gamma-ray log to be used for the calculation of the volume of Shale. The radioactivity of Shale is mainly due to Uranium, Potassium, and Thorium. The abundance of each radioactive element varies reasonably with clay type. Illite bears a high value of Potassium, while the richness of Potassium decreases with the presence of Kaolinite and Smectite (Rezaee, 2015). The Uranium content in Shale rock plays a vital role in the qualitative analysis of TOC. Under the Marine depositional environment, TOC has a positive relationship with the richness of Uranium (Bohacs & Miskell-Gerhardt, 1998).

The spectral gamma-ray log is utilized for the inferring of the Shale mineralogy of the Chichali Formation. The cross plot (Quirein et al., 1982;) are used to plot the values of Potassium and Thorium over it which then indicates the mineralogy of Shale. The Plot portrays Potassium on a Scale of 0-5% on X-axis and Thorium on the scale of 0-25 ppm on Y-axis.

The Thorium the stable radioactive element of Shale along with Potassium is used to plot on cross plot and infer the mineralogy type (Quirein et al., 1982).

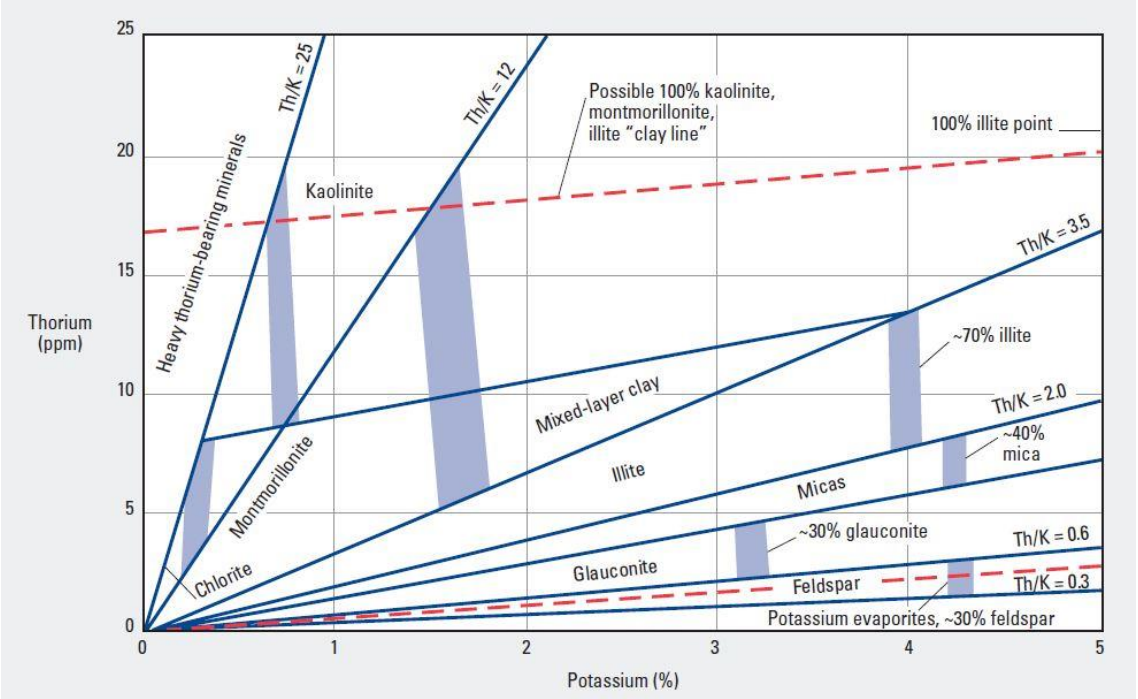

Figure 4.2 Potassium-Thorium crossplot to assess Shale mineralogy (Quirein et al., 1982).

4.4.4 Resistivity Log

The resistivity log measures the resistivity of the formation's fluid. It plays a vital role in measuring water and hydrocarbon saturation. Resistivity log helps in qualitative and quantitative interpretation of hydrocarbons because source rock and reservoirs rich in hydrocarbon possess high resistivity because of the presence of organic matter (Rider, 1986). This is valid only if the source rocks has gained enough maturity to generate hydrocarbons.

The resistivity logs can be divided into three types based on the depth of investigation of the good bore; Shallow resistivity, medium resistivity, and deep resistivity. Shallow measure resistivity of the flushed zone, medium measures resistivity of the transition zone, and deep resistivity measure the resistivity of the uninvaded formation. Deep resistivity is used in the calculation of water saturation of formation, and qualitative and quantitative assessment of source rock organic richness.

4.4.5 Sonic Log

Sonic log measures the formation capacity to transmit the sound waves. The log gives us response in a unit of microsecond/ft. The principal use of the sonic log in the present study is estimating the porosity of formation, lithology identifications, Brittleness estimation and TOC calculation of source rock. In unconventional reservoir analysis, the sonic log can be used on the same track with deep resistivity to estimate the TOC of formation (Passey et al., 1990).

4.4.5.1 Sonic Porosity

The algorithm to calculate porosity from the sonic log is given by Wyllie as (Rider, 1986);

$$\textbf{PHIS} = \frac{(\mathrm{DTlog} - \mathrm{Dtma})}{(\mathrm{DTfld} - \mathrm{Dtma})}$$

Where**;** DTlog = interval transit time from Sonic log.

DTma = Transit time of matrix.

DTfld = Transit time of fluid.

4.4.6 Neutron Log

Neutron log measures formation hydrogen index, and gives us response in neutron porosity units. The tool continously bombards neutron against the formation and records the number of nuetrons that bounces back without aborption by formation. The prinicpal use of neutron log is in calculation of porosity, lithology descrimination, and discrimination between gas bearing and oil-bearing reservoirs. The porosity can be read directly from the tool's response and requires no algorithm to be applied. Neutron log is utilized in the computation of average Neutron-Density porosity.

4.4.7 Density Log

The density log measures the density of formation and is an important log in describing the lithology and porosity of the rock under investigation (Rider, 1986). The

density log can also be used to calculate the TOC in source rock through the method devised by (Schmoker & Hester, 1989).

4.4.7.1 Density Porosity

The algorithm for computation of density porosity from density log is given as (Rider, 1986);

$$\mathbf{PHID} = \frac{(\mathrm{RhoM} - \mathrm{RHOB})}{(\mathrm{RhoM} - \mathrm{RhoF})}$$

Where; PhiD = Density porosity.
RhoM = matrix's density.
RHOB = density value from log.
RhoF = Density of fluid.

Density porosity is also used for the computation of average porosity in combination with Neutron Porosity.

4.4.8 Average porosity

It is the average porosity calculated from the density and neutron porosity. This is calculated to avoid any uncertainties to interpret the data calculated from individual logs (Rider, 1986). The algorithm to calculate the average porosity from neutron and density log is given as (Rider, 1986);

$$\mathbf{PHIA} = \frac{(\mathrm{PHID} + \mathrm{PHIN})}{2}$$

Whereas; PHIA = Average Porosity
PHID = Density Porosity
PHIN = Neutron Porosity

If the Density log is not reliable, then average porosity can be assumed from Sonic porosity. In the present study, all three wells have shown non-reliable density readings, hence the average porosity is assumed from the Sonic porosity calculation.

Average porosity in combination with the volume of Shale can be used to assess the effective porosity.

4.4.9 Effective Porosity

The ratio of interconnected pores to that of the volume of rock, or it is the porosity of rocks with interconnected pores. This parameter gives us how effectively the reservoir will be producing and transmitting fluid across it. In petrophysical analysis, this parameter of rock is crucial to be calculated to assess the permeability of the rock. If we have no core data then well logs can be used to calculate the effective porosity. It is also used in calculating the reservoir interval out of gross interval. In the reservoir, where Shale is dominating most of the porosity will be occupied by clay particles that may not be producible and have no economic importance in the petroleum industry. To avoid these kinds of uncertainties, the effective porosity is calculated to assess the quality of the reservoir. The algorithm to calculate the effective porosity is given as (Rider, 1986);

$$\textbf{PHIE} = PHIA * (1-Vshl)$$

Whereas; PHIE = Effective porosity
PHIA = Average porosity
Vshl = Volume of Shale.

4.4.10 Shale Porosity

The porosity of Shale after applying TOC correction and effective porosity correction. The model for Shale porosity is given as;

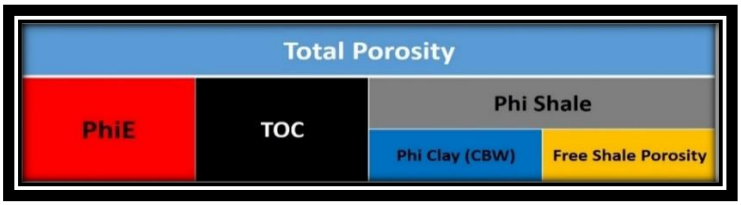

Figure 4.3 Image shows Shale porosity components model. (Michael et al., 2012).

Figure 4.3 shows porosity in Shale is comprised of effective porosity, TOC content, and porosity of Shale content (Clay bound water, and Free Shale porosity). To calculate the porosity that is exclusive of effective porosity and TOC content, we applied the TOC correction on average porosity within Shale, and then effective porosity was subtracted from average porosity after TOC correction. The algorithm for TOC correction on average porosity is given as (Rezaee, (2015);

$$\textbf{TOC corrected porosity} = \frac{(\mathrm{DTlog} - \mathrm{DTma}) + (\mathrm{TOC} / \mathrm{RhoK}) * \mathrm{RHOB}) * (\mathrm{DTma} - \mathrm{DTtoc})}{DTfld - DTma}$$

Where; RHOK = Kerogen density (1.2 gm/cm^3)

DTtoc = Sonic transit time for kerogen (120 usec/ft)

After TOC correction on average porosity, the effective porosity must be subtracted from it to give us Shale porosity. This Shale porosity is the sum of Clay bound water and free shale porosity. Clay bound water is water present in the chemical structure of clays, while free Shale porosity is pores spaces present in between grains of Shale.

Shale porosity = TOC corrected porosity – Effective porosity

The Shale porosity is the amount of porosity that is comprised of porosity due to clay bound water in Shale and free shale porosity.

4.4.11 Water and Hydrocarbon saturation

The water saturation and hydrocarbon saturation is the proportion of rock that is invaded with water and hydrocarbon respectively. The Archie equation is use for the calculation of water saturation in the clean zone. The equation of Archie water equation is (Rider, 1986);

$$S_w^n = \frac{a.R_w}{\emptyset^m.R_t}$$

Where a, m and n are constant with value of 1, 2 and 2 respectively.

Rw = Resistivity of water

Φ = Average porosity

Rt = True Resistivity

4.4.11.1 Calculation of Rw

The resistivity of the formation's water can be calculated through four different methods. These methods are;

i. Dissolved solid method; i.e. Sampling formation water and measuring resistivity in the laboratory.
ii. From SP log through Schlumberger charts.
iii. Apparent water resistivity method; through formula i.e Rw = Rt * $PHIA^m$
iv. Pickett Plot method.

In the present study, the Pickett plot method has been utilized to calculate the formation's water resistivity. The method involves plotting the deep resistivity on X-axis through a logarithmic scale from 0.1 to 1000 ohm-m, and average porosity on the y-axis on a logarithmic scale from 0.01 to 1.

4.4.12 TOC calculation- Passey Δlog R Method

The total organic carbon has been calculated from open hole wireline logs by a method devised by Passey et al. (1990). The method involves the utilization of deep resistivity and sonic log to characterize the organic richness of formation. The method is based on the assumption that the source rock rich in organic matter will have a characteristic sonic and deep resistivity log response, with an increase in organic richness the formation will cause high sonic transit time and high deep resistivity information characterized by high organic richness. This both highness of sonic transit and resistivity in organic-rich formation is because the organic matter being less dense causes high sonic

travel time compared to adjacent non-rich source rock, and high resistivity due to maturation of organic matter and its transformation into hydrocarbons.

The methodology involves the plotting of deep resistivity and sonic logs over the same track. The scale is assigned in a way that, one logarithmic scale of deep resistivity will indicate 50 µsec/feet of sonic transit time. Overlaying of Sonic and deep resistivity logs in mature and organic enriched source rock will cause negative separation between these two logs i.e., Δ log R. The algorithm for calculation of TOC from Δ log R Method is;

$$\mathbf{TOC} = (\Delta \log R)10^{2.297-0.1688*LOM}$$

Where; $\Delta \log R = \log(ResD/ResD_{baseline}) + 0.02 \times (\Delta t - \Delta t_{baseline})$

LOM = Level of Maturity (Calculated from chart)

ResD = Deep resistivity from log

ResD = Deep resistivity from overlain of Sonic and resistivity.

$\Delta t =$ Sonic transit time from log

$\Delta t_{baseline} =$ Sonic transit time from overlain of Sonic and resistivity

For the calculation of LOM, we need the vitrinite reflectance of the sample. In the present study, we had no well cuttings or outcrop sample to measure its vitrinite reflectance. To calculate LOM we referred to the vitrinite reflectance from the investigations of Zeb et al. (2020), the paper has calculated the vitrinite reflectance of Chihcali Formation in Kohat sub-basin from well cuttings sample. The average vitrinite reflectance calculated by Zeb et al. (2020) is 0.7%, after plotting it on the graph (Fig. 10) it gives us a LOM of 10, which is further used in the calculation of TOC in the present study.

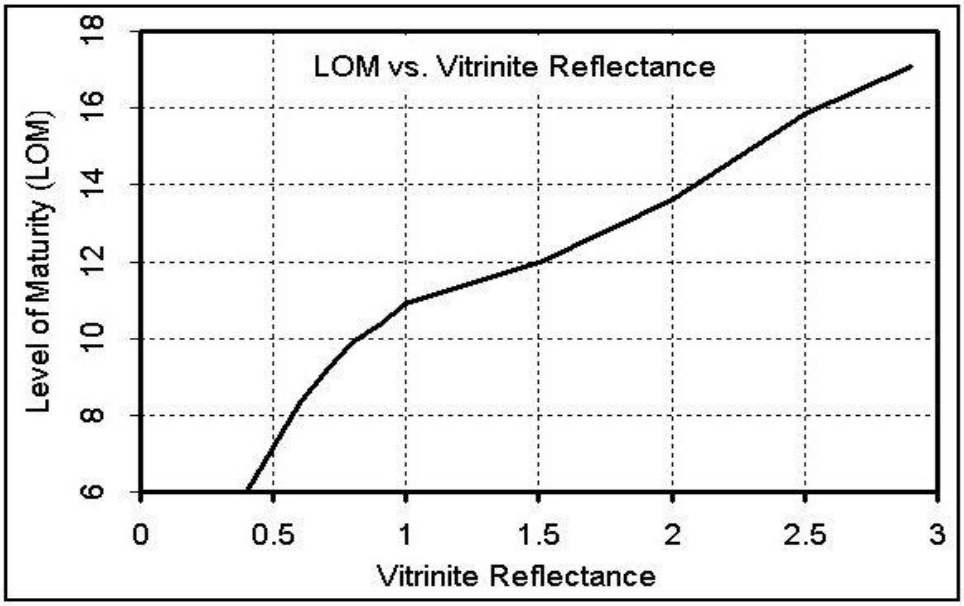

Figure 4.4 Graph use for calculation of LOM from vitrinite reflectance. (Crain, 1986)

4.4.13 Permeability

Permeability is the ability of the rock unit to transmit the fluid through it. It is a crucial property of reservoir and is vital to be analyzed to assess the reservoir characteristics. The Permeability of rock can be measured both in the laboratory and through good logs. To calculate the permeability of reservoir rock units through well logs, Tixier (1949) equation is used. The Tixier equation is given below;

$$\mathbf{K} = (250 * PHIE^3/Swirr)^2$$

Where K = permeability

PHIE = Effective porosity

Swirr = Irriducible water saturation

4.4.14 Brittleness Index

The petrophysical and petrophysical property of rock like brittleness is an important property of rocks, which play important role in marking the zone for hydraulic fracturing, and well drilling design. Compressional and Shear Sonic logs can be used to estimate the brittleness of rocks. The two parameters that are crucial to finding out the brittleness index are the Poisson's ratio and Young modulus.

Young modulus is the ratio between uniaxial extensional stress and uniaxial extensional strain (Mukerji & Dvorkin, 2009). It indicates the resistance of rock to deformation, while Poisson's ratio indicates the tendency of rock to fail under stress. The equations to calculate the Young modulus and Poisson ratio from well logs are given as (Lobo et al., 2017);

$$\mathbf{E} = RHOB * \left(\frac{4 - \left(3 * \frac{\mathrm{DTs2}}{\mathrm{DTc2}}\right)}{\mathrm{DTs2} * \left(1 - \left(\frac{\mathrm{DTs2}}{\mathrm{DTc2}}\right) * 13474\right.}\right)$$

Where; **E** = Young Modulus

RHOB = Density from Density log. Gm/cc

DTs = Shear sonic transit time from log (µs/ft)

DTc = Compressional sonic transit time (µs/ft)

And, $\mathbf{PR} = \frac{2-\left(\frac{DTS2}{DTC2}\right)}{2*\left(1-\frac{DTS2}{DTC2}\right)}$

Where; **PR** = Poisson Ratio.

Brittleness is the amount of energy that can be store by a rock before its failure. The lithology is a key parameter to control the brittleness of rock. An increase in clay content increases the ductility of lithology, while the increase in Limestone, Dolomite and Quartz content can increase the brittleness. Besides, laboratory measurements the Brittleness index can be calculated from the Poisson ratio and Young Modulus as(Rickman et al., 2008);

$$\textbf{Brittleness index} = \frac{(\mathrm{BE} + \mathrm{BV})}{2}$$

Where; $\mathbf{B_E} = \frac{\mathrm{Elog} - \mathrm{Emin}}{\mathrm{Emax} - \mathrm{Emin}}$

Elog = Young Modulus from log (Calculated at each depth)

Emin = Minimum Young Modulus

Emax = Maximum Young Modulus.

$$\mathbf{B_v} = \frac{\text{PRlog} - \text{PRmin}}{\text{PRmax} - \text{PRmin}}$$

Where; PRlog = Poisson ratio from log (calculated at each depth)

PRmax = Maximum Poisson ratio

PRmin = Minimum Poisson ration

The objective for calculating the brittleness index is to identify the Brittle zone and ductile zone, as brittle shale is a more optimistic target for Shale reservoir development. Consequently, in tight formations and unconventional reservoirs, optimal hydraulic fracturing design must be selected in intervals of high brittleness index i.e high Young modulus and low Poisson ratio.

Additionally, to analyze the brittleness or ductility of the zone, the crossplot portraying the Young Modulus on Y-axis and Poisson ratio on X-axis devised by Grieser and Bray, 2007 has been used.

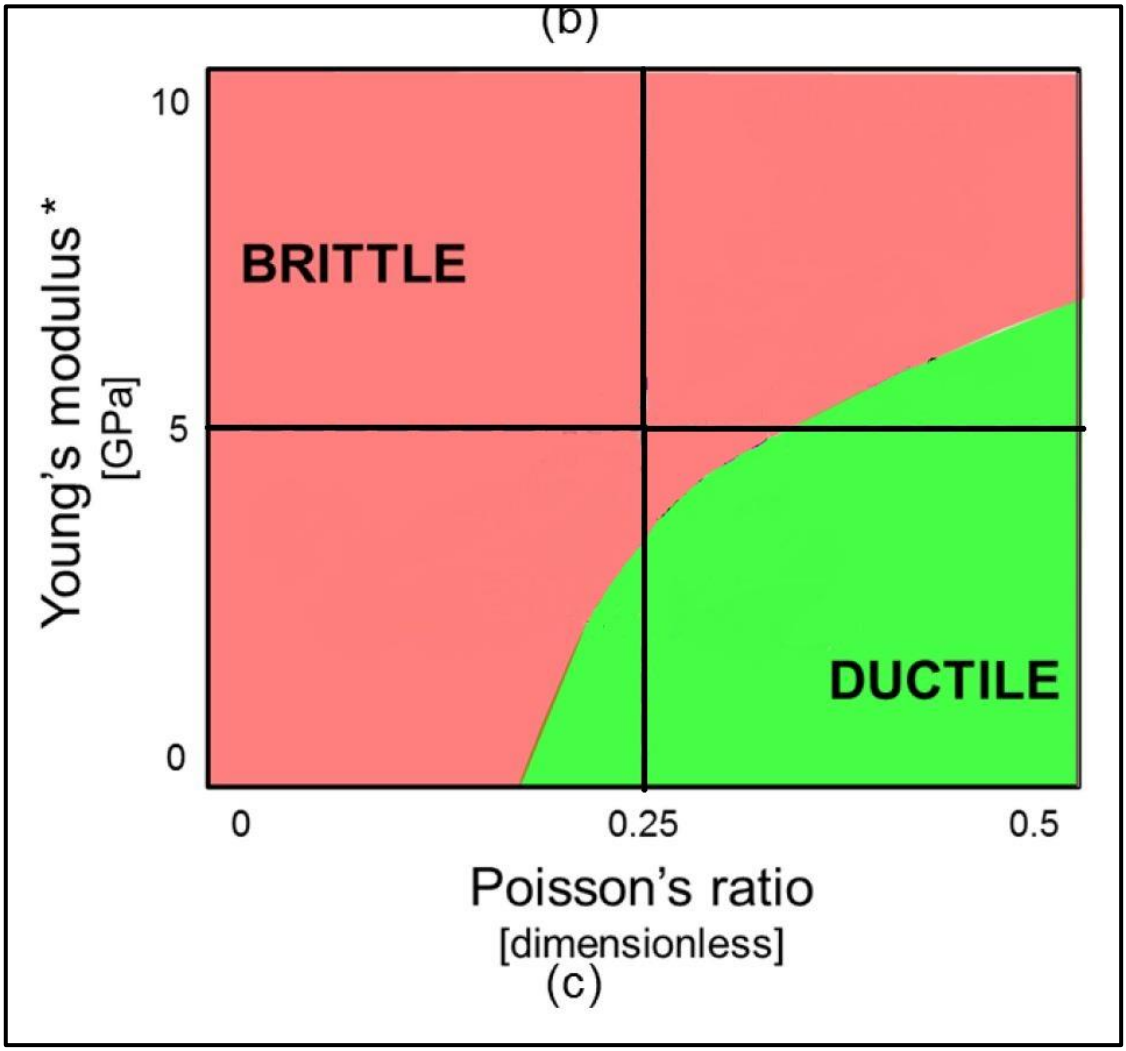

Figure 4.5 Crossplot of Young Modulus and Poisson ratio use for indication of Brittle and Ductile zone (Grieser and Bray, 2007).

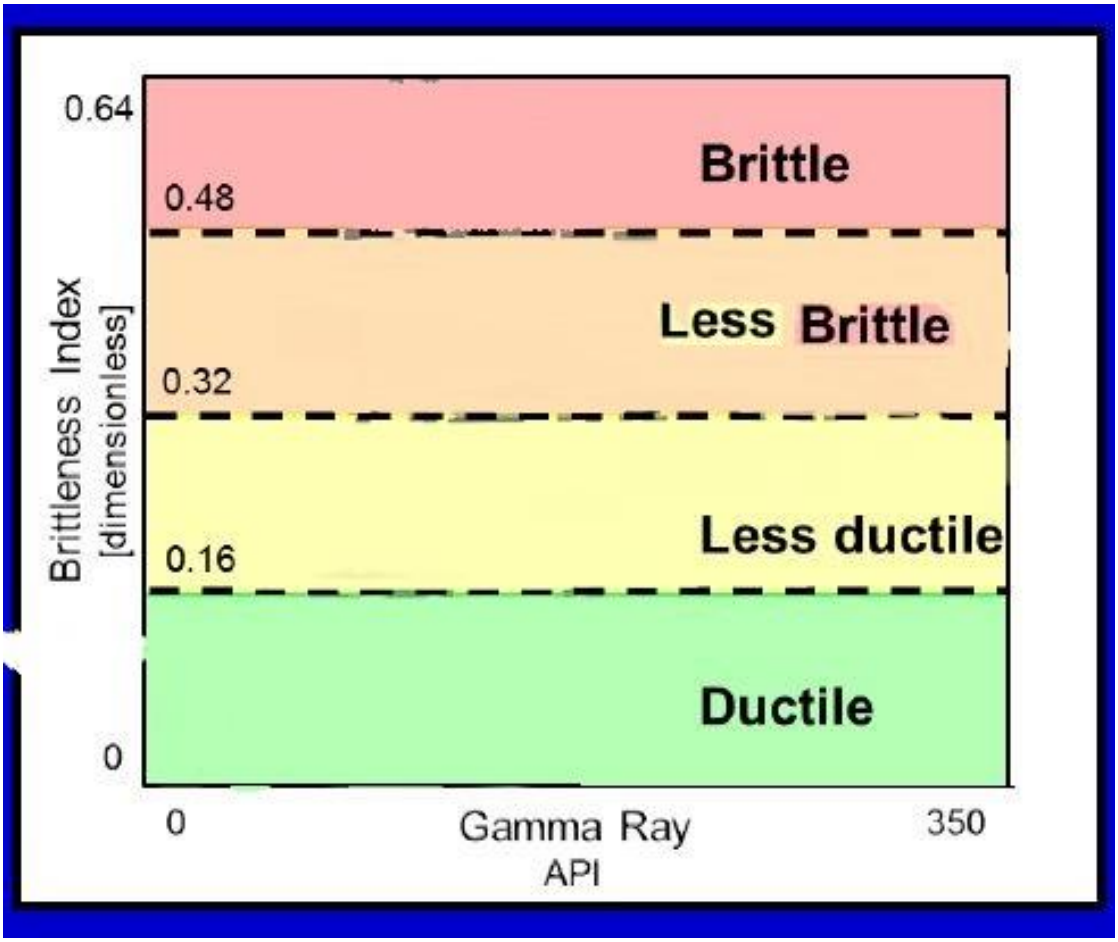

Figure 4.6 Brittleness Index vs Gamma ray indicating level of Brittleness. (Perez., (2013).

CHAPTER 5

UNCONVENTIONAL PETROPHYSICAL CHARACTERIZATION OF CHICHALI SHALE

As discussed in earlier chapters, the Chichali Formation being a prominent Shale unit of the Kohat sub-basin can be a potential unconventional reservoir. To assess its potential for unconventional reservoirs an adequate characterization of the Chichali Formation is required. The prominent requirements for a formation to be a good unconventional reservoir are; low clay volume, Adequate kerogen content, enough effective porosity, minimum saturation of water, high young modulus and low Poisson's ratio (Kenomore et al., 2017).

The petrophysical analysis is needed to completely evaluate the Cretaceous Chichali Formation of the Kohat Sub-basin. Petrophysical analysis of good bore is assumed as a one-dimensional investigation of formation for hydrocarbon reserves (Khan & Khan, 2017). Two ways of measuring petrophysical properties are known i.e. core analysis and wireline logs. Petrophysical properties like porosity, permeability, saturation, and capillary pressures are computed from wireline logs and core analysis. Well, logs information when are aided by the analysis of core gives us a high degree of precision by correlation. Besides conventional reservoir analysis, geochemical properties of source rock like TOC, and mineralogy of Shales are also probed in petrophysical analysis. Good log analysis of these source rocks is are complex process and involves both routine conventional logs and unconventional logs to be interpreted.

The present chapter is focused on the evaluation of TOC for Chichali shale penetrated in Makori-01, Manzalai-02 and Maramzai-02 wells through open hole wireline logs

Two template has been utilized for portraying logs reading. One template referred to as input log template is used for portraying raw log curves. The second template referred as the output log template is used for the portraying of calculated attributes.

Input log template

This template shows the open hole wireline logs readings taken in well. The input log template includes 6 tracks of Correlation, Resistivity, Nphi-Rhob, PEF-DT, U-T-P and SGR.

i. 1st Track includes GR log on a scale of 0-150 API, Sp log on the scale of 0 to -100, Caliper log 0 to 16 Inches.
ii. 2nd Track includes Resistivity logs (MSFL, LLS, LLD) on scale from 0.2 to 2000 Ohm-m.
iii. 3rd Track of Density log on scale from 0.95 to 3 gm/cc, and Neutron log on a scale of -0.15 to 0.45 v/v.
iv. 4th track comprises Sonic log with a scale from 40 to 140 microsec/feet and PEF log on a scale of 0-10 Barns/electron.
v. Fifth track includes CGR and SGR curves.
vi. Sixth track includes Potassium on scale of 0 to 5%, Uranium and Thorium curves on a scale of 0-40 ppm. While last track includes ratios of Thorium-Potassium, Thorium-Uranium-Potassium, Uranium-Potassium.

Output log template

The output log shows all the attributes calculated for Chichali Formation utilizing the raw log curves. The output template includes nine tracks.

i. The first track of correlation shows us the reading of GR log (on a scale of 0-150 API).
ii. The second track shows us deep resistivity (on a scale of 0.01-100 ohm.m) and Sonic log. on a scale of (220-20 microsec/feet).
iii. The third track shows average and effective porosity on a scale of 0-0.3.
iv. The fourth track shows Shale porosity on a Scale of 0-0.3.
v. The fifth track shows the Saturation of water and hydrocarbon on a scale of 0-1.
vi. The sixth track shows the percentage of the matrix information depicting the main lithology.
vii. The seventh track shows the calculated total organic carbon on a scale of 0-4%.

viii. The eighth track shows the brittleness index on a scale of 0-1.

ix. While Ninth track shows the Shale flag marking the formation with Vshl greater than 60%.

5.1 Makori-01 well.

5.1.1 Well Description

The Makori-01 well bears coordinates of 71°13’ 26.730” **E**, 33°17’ 38.619” **N.** The well has been drilled up to the depth of 4399 meters. In Makori-01 well the Chichali Formation has been repeated three times depicting the fault structure in the subsurface. The Chichali Formation has been penetrated first at the depth of 3197-3288 m, the 2nd observation is at 3771-3823 m, and the 3rd observation is at 3863-3887 m. The raw log curves and their readings are given as

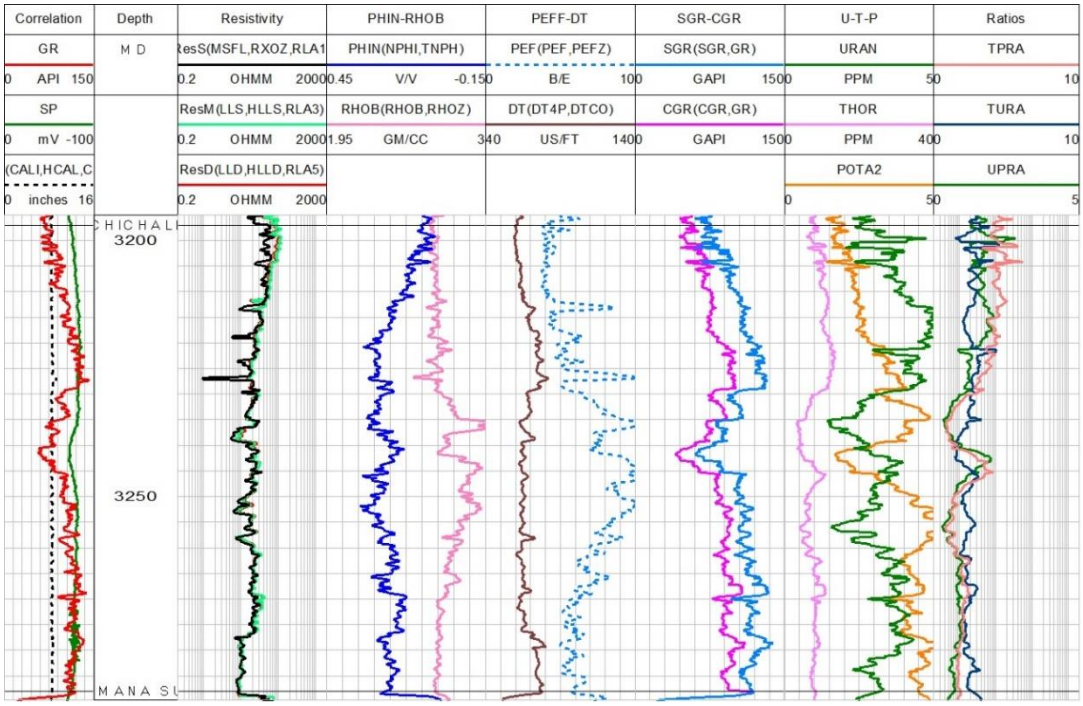

Figure 5.1 Open hole wireline logs for Chichali Shale in Makori-01 well.

5.1.2 Qualitative interpretation

The log responses (**Fig.** 5.1) show good borehole condition as the Caliper log shows consistent readings without fluctuations. The GR log shows whole Chihcali Formation can be partitioned into two Shale units. The first Shale unit referred to as zone-

1 ranges from 3209 to 3235 meters while the second Shale unit referred to as zone-2 ranges from 3245-3287 meters. Both zones are furthers investigated for their petrophysical attributes. The resistivity log shows high values at the top depicting the formation is inundated with hydrocarbon and is organic-rich. The density and PEF log shows abnormal high reading at various depths making it non-reliable and its utilization in our investigation could lead us to misinterpretation.

On other hand, Neutron and Sonic log shows us reliable readings. The SGR data shows that there is a reasonable presence of Uranium in formation and hence depicts the presence of organic richness.

5.1.3 Quantitaive Analysis

5.1.3.1 Zone-1 (3209 to 3235 meters)

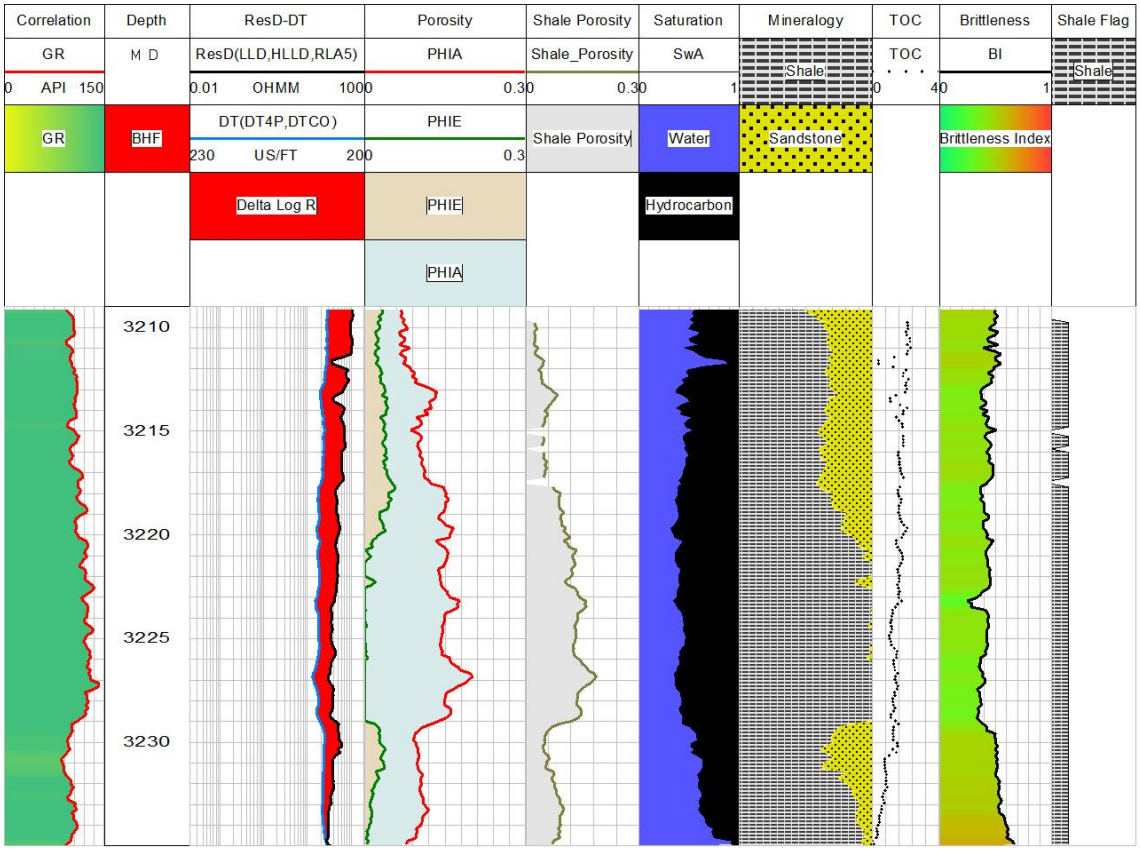

Figure 5.2 Calculated petrophysical attributes of Chichali Formation' zone-1 drilled in Makori-01 well.

The borehole condition shows no reasonable borehole rugosity, Mud cake and Bad hole flag. The Section is drilled with 8.5” of the drill bit and the maximum borehole rugosity recorded in the Chichali Formation is 0.5”.

The volume of Shale computation through CGR shows the average value of 80.6% where the minimum and maximum CGR encountered is 40 and 110 API respectively. Sonic porosity is considered more reliable in the present study and computed average porosity is 12.3% and Shale porosity is 6.34%. Lithology interpreted through three mineral model suggest Shale, and Sandstone mainly saturated with 48.3% of water. Organic richness analysis shows zone bears average value as 1.38% of TOC Mechanical properties assessment suggests brittleness index with an average value of 45%.

The Potassium-Thorium cross plot shows that the Chichali in Makori-01 well has a mineralogical composition of mixed-layer clay, Illite, Mica bearing and Glauconite.

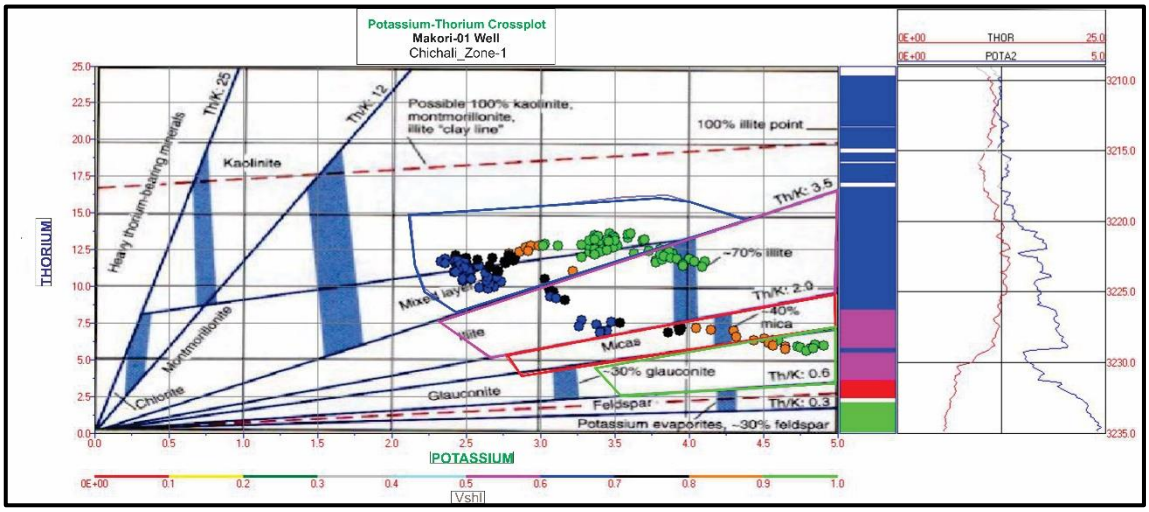

Figure 5.3 Potassium-Thorium crossplot depicting the Shale mineralogy of Chichali Formation’s zone-1 penetrated in Makori-01 well.

The mechanical property analysis shows a high young modulus and low Poisson ratio resulting in a good brittleness index with an average value of 45% in the first zone of the Chichali Shale unit. Additionally, the results are plotted on Grieser and Bray, 2007 Crossplots to assess the brittleness qualitatively. The results (**Fig.** 5.4 & 5.5) show the

Chichali Formation zone-2 encountered in Makori-01 well bears good brittleness with ranging in category from less brittle to brittle.

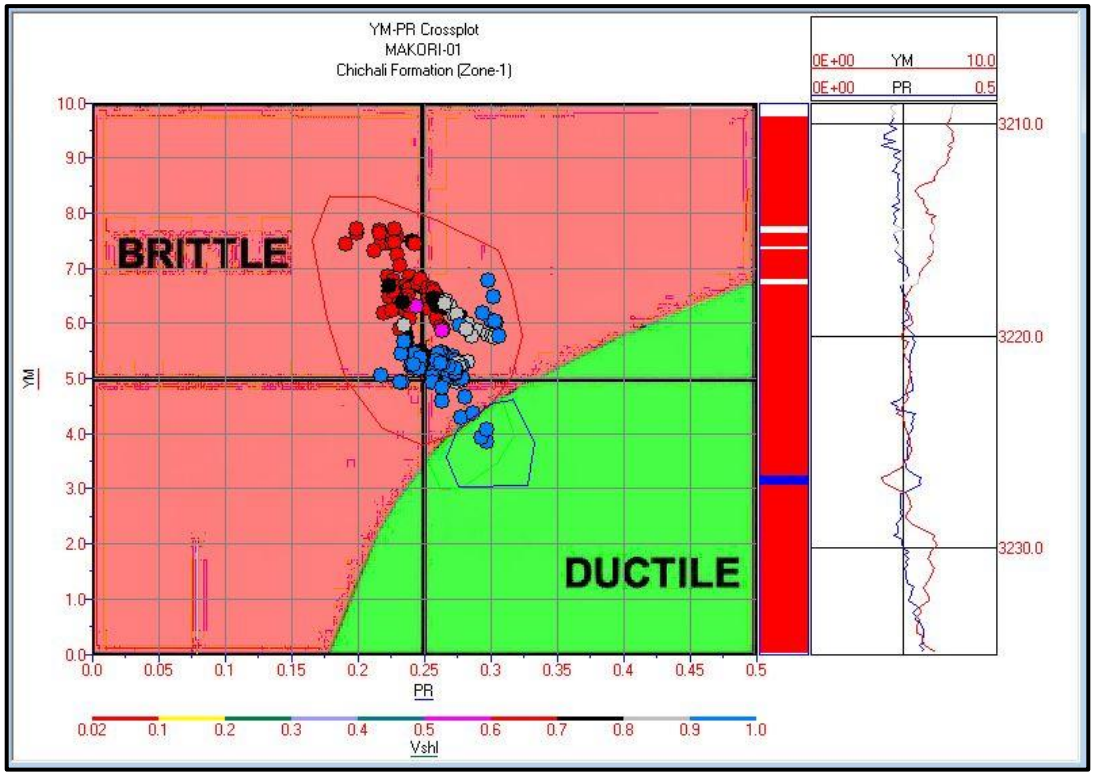

Figure 5.4 Young's Modulus (YM) - Poisson's Ratio (PR) Crossplot depicting Brittleness qualitatively of zone-1 drilled in Makori-01 well.

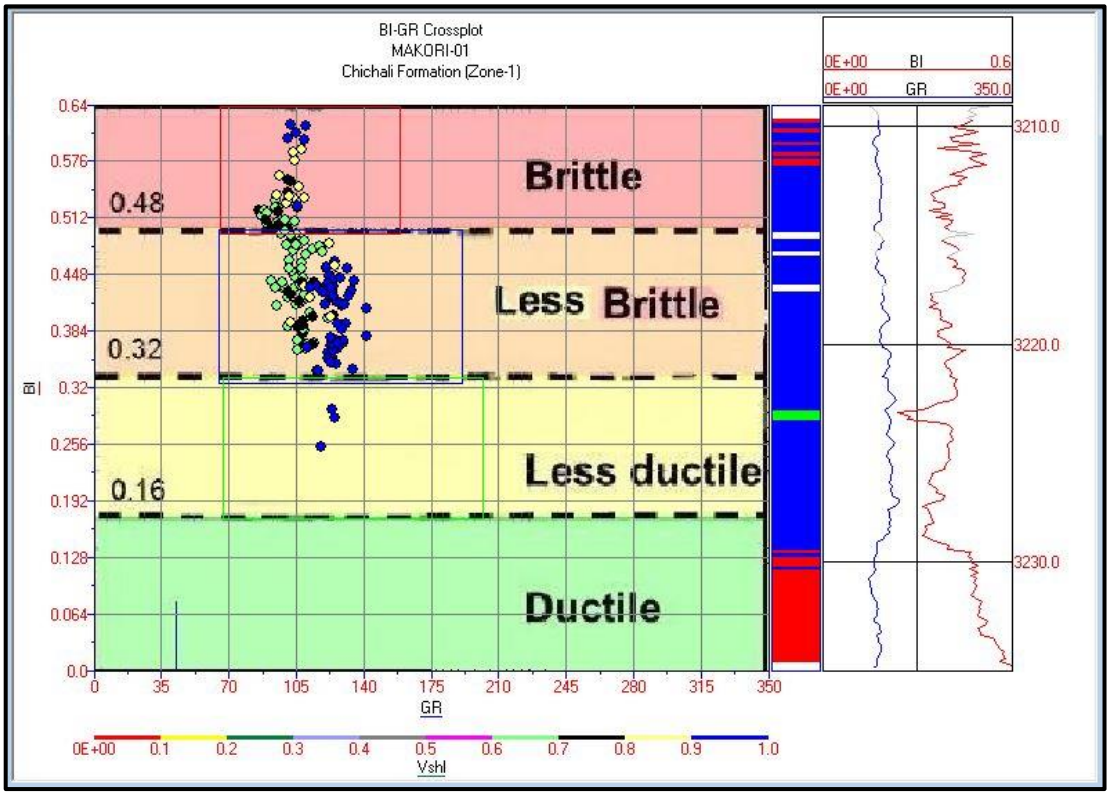

Figure 5.5 Brittleness index (%) vs Gamma ray (API) Crossplot depicting Brittleness qualitatively of Chichali Formation's Zone-1 drilled in Makori-01 well.

5.1.3.2 Zone-2 (3245-3287 meters)

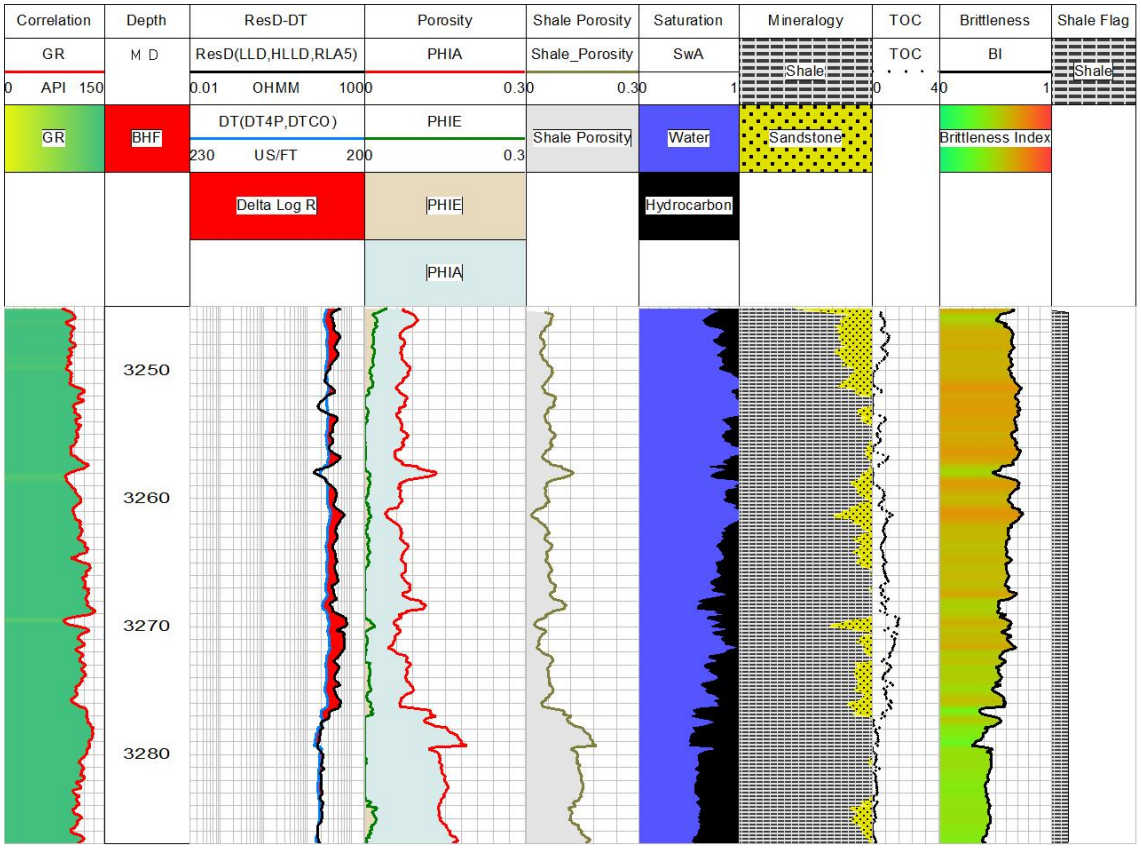

Figure 5.6 Calculated petrophysical attributes of Chichali Formation' zone-2 drilled in Makori-01 well.

Calculation utilizing CGR shows zone is characterized with 91% of volume Shale. Porosity through Sonic log computed average sonic porosity as 9.1% whereas, Shale Porosity as 7.9%. Saturation computation analyzed the zone as a water-bearing zone with an average of 77.3%. Matrix lithology interpretation shows Shale with the influx of Sandstone. TOC analysis shows the reduced TOC content with an average TOC value of 0.52%. Comparing to zone-1, zone-2 has shown a reasonable brittleness index with an average value of 57.73%

Shale mineralogy assessment through Potassium-Thorium crossplot shows the zone-2 of Chihcali Formation is mainly comprised of Illite Clay, Mica bearing clay, and Glauconite bearing Shale.

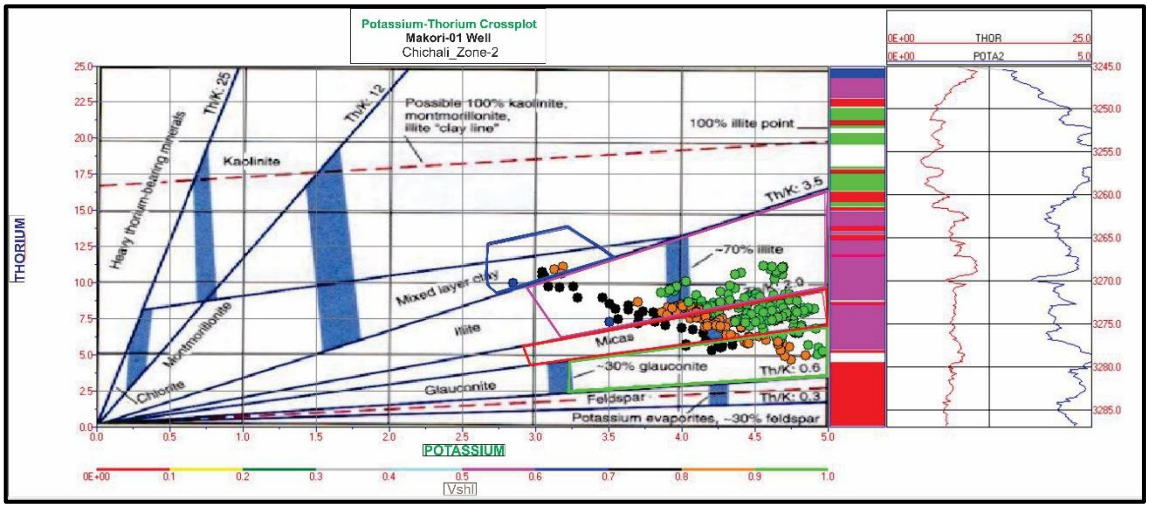

Figure 5.7 Potassium-Thorium Crossplot depicting Shale mineralogy for zone-2 of Chichali Formation penetrated in Makori-01 well.

Additionally, the mechanical assessment results are plotted on Grieser and Bray, (2007) Cross plots to assess the brittleness qualitatively. The results show the Chichali Formation encountered in Makori-01 well bears good brittleness.

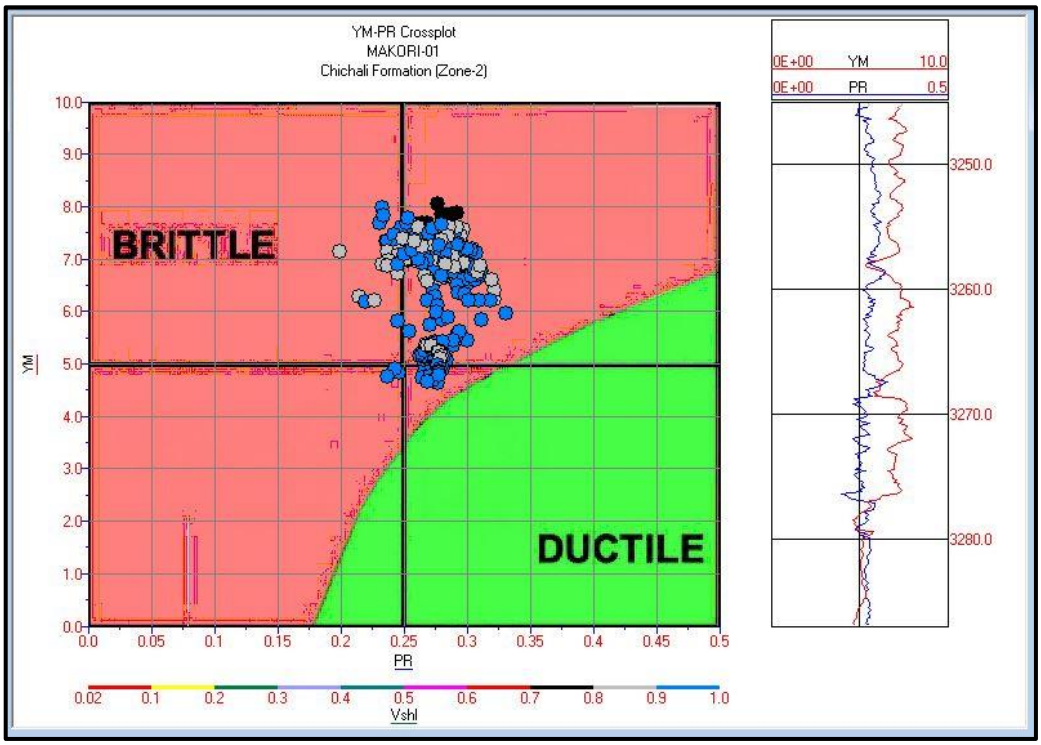

Figure 5.8 Young's Modulus (YM) - Poisson's Ratio (PR) Crossplot depicting Brittleness qualitatively of Chichali Formation's zone-2 drilled in Makori-01 well.

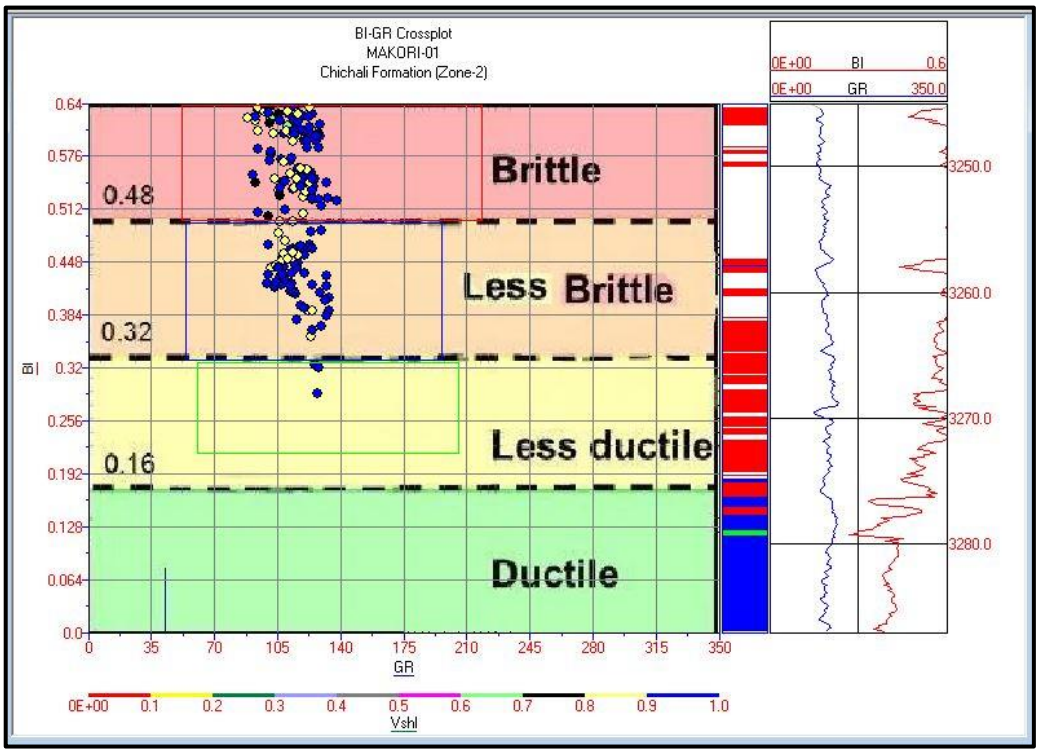

Figure 5.9 Brittleness index (%) vs Gamma-ray (API) Crossplot depicting Brittleness qualitatively of Chichali Formation's zone-2 drilled in Makori-01 well.

5.2 Manzalai-02 Well

5.2.1 Well Description

The Manzalai-02 well bears coordinates of 71°06' 56.42" **E**, 33°25' 58.61" **N.** The well has been drilled up to the depth of 4249 meters. The zone of interest in Manzalai-02 well for our current investigation is Chichali Formation. The Manzalai-02 penetrated the Chichali Formation at a depth from 3627 to 3762 meters. The response of open-hole wireline logs are given as;

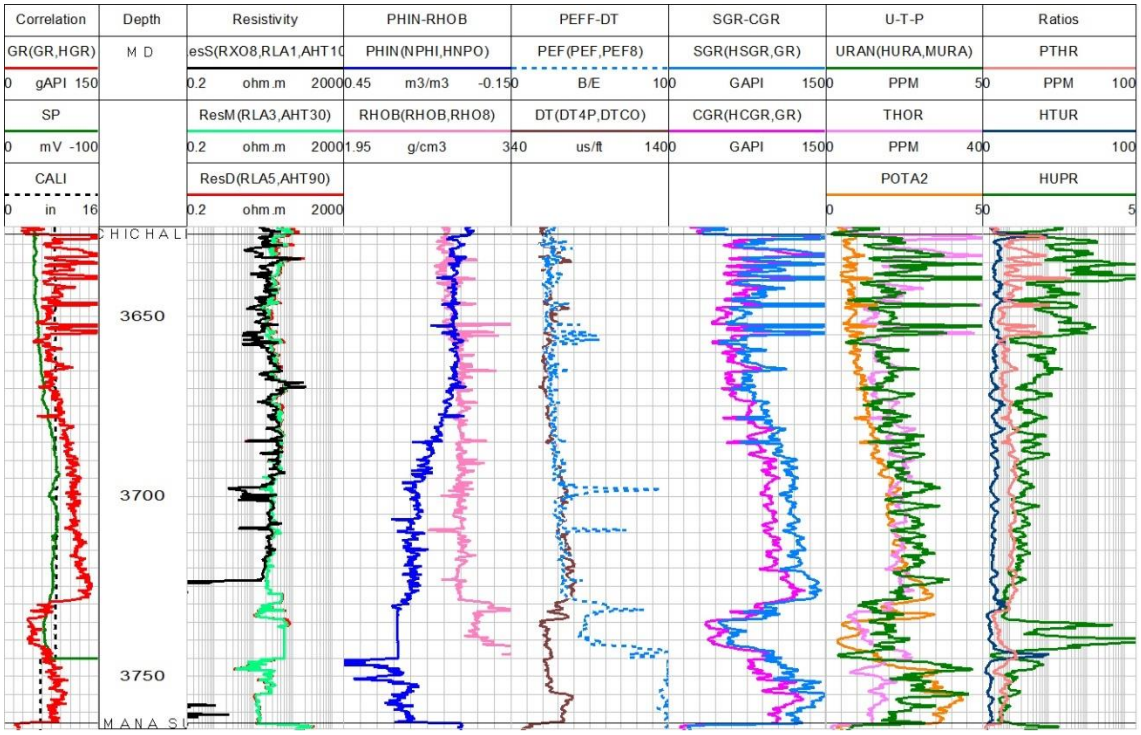

Figure 5.10 Image showing all available log run in Chichali Formation pentrated in Manzalai-02 well.

5.2.2 Qualitative Interpretation

The well log responses (**Fig.** 5.10) show good borehole condition as the caliper log shows no variation. GR reading shows Formation can be partitioned into two Shale units ranging in depth from 3688-3730 meters referred to as zone 1, and 3748-3762 meters referred as zone-2. The resistivity log shows moderate readings showing that formation bears some hydrocarbons. The density log and PEF log shows normal readings at top of the formation while the bottom formation reads the anomalous high-density value of greater than 3 gm/cm^3 making the density log of no use in interpretation. The sonic log shows good reading and makes it reliable to be used for porosity computation. The SGR and CGR logs show a reasonable difference depicting the presence of Uranium content. The presence of Uranium shows Formation bears adequate organic richness.

5.2.3 Quantitative Analysis

5.2.3.1 Zone-1 (3688-3730 meters)

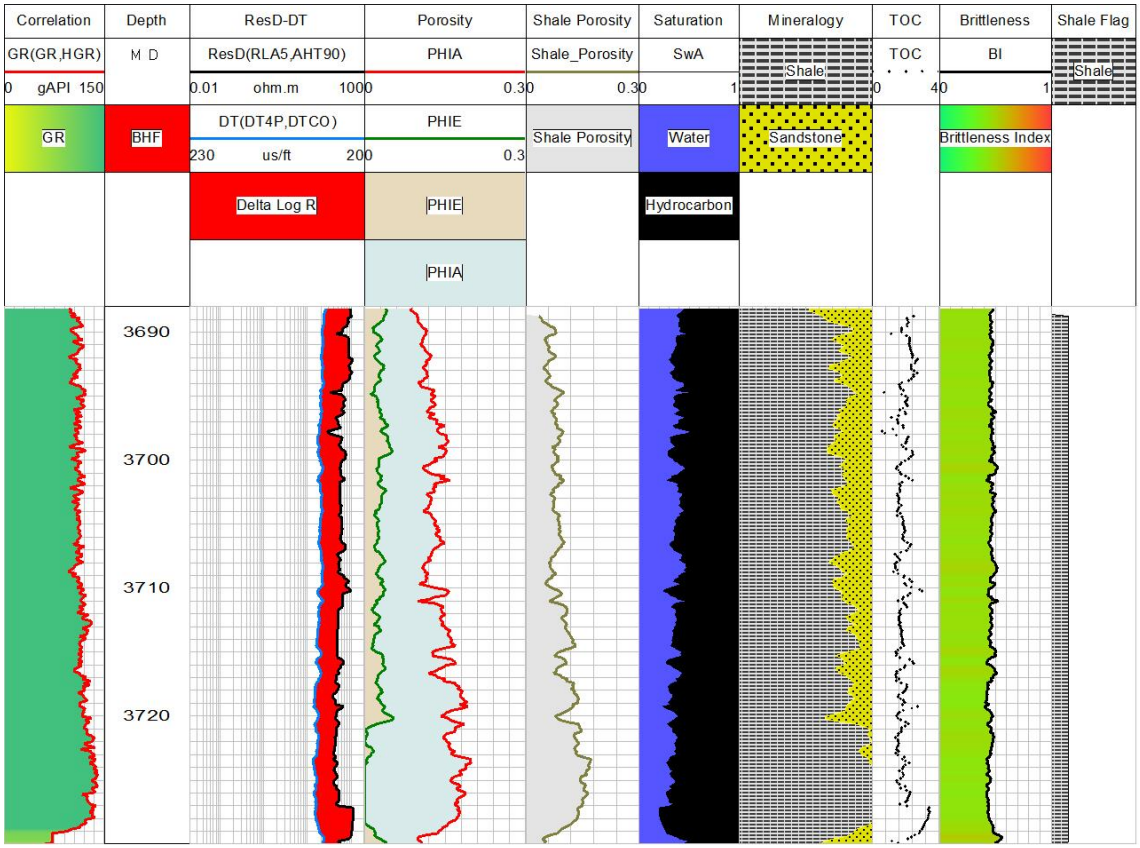

Figure 5.11 Calculated petrophysical attributes of Chichali Formation's zone-1 penetrated in Manzalai-02 well.

The caliper shows the section had been drilled initially with 8.5" at depth of 3745 meters, then the drill bit was changed to 6". The overall borehole condition shows no mud cake and washouts.

The zone possesses an average volume of Shale as 81.58%. Porosity computation shows zone bears average Sonic porosity as 14.3% and average Shale porosity value as 9.6%. Three mineral models revealed matrix lithology as Shale with minor Sandstone saturated with water of 35.7%. TOC assessment suggests zone is characterized with an average TOC value of 1.91%. The mechanical assessment shows a brittleness index with an average value of 46.4%.

The Potassium-Thorium crossplot shows the Shale of zone-1 to be mainly mixed-layer clay, and Kaolinite.

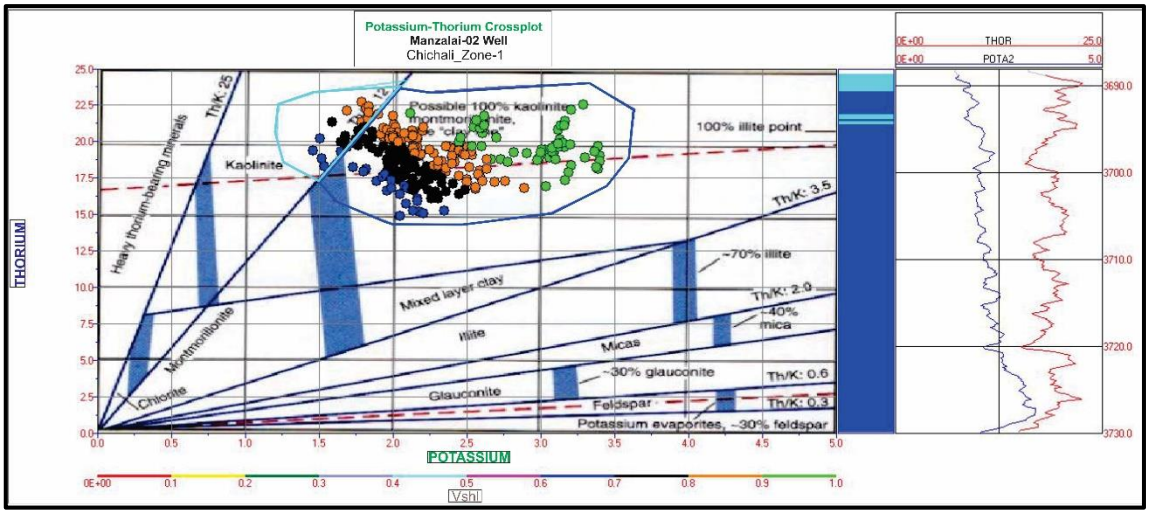

Figure 5.12 Potassium-Thorium crossplot depicting the Shale mineralogy of Chichali Formation's zone-1 penetrated in Manzalai-02 well.

Grieser and Bray (2007) crossplot shows zone is characterized by the mechanical property of brittle behaviour.

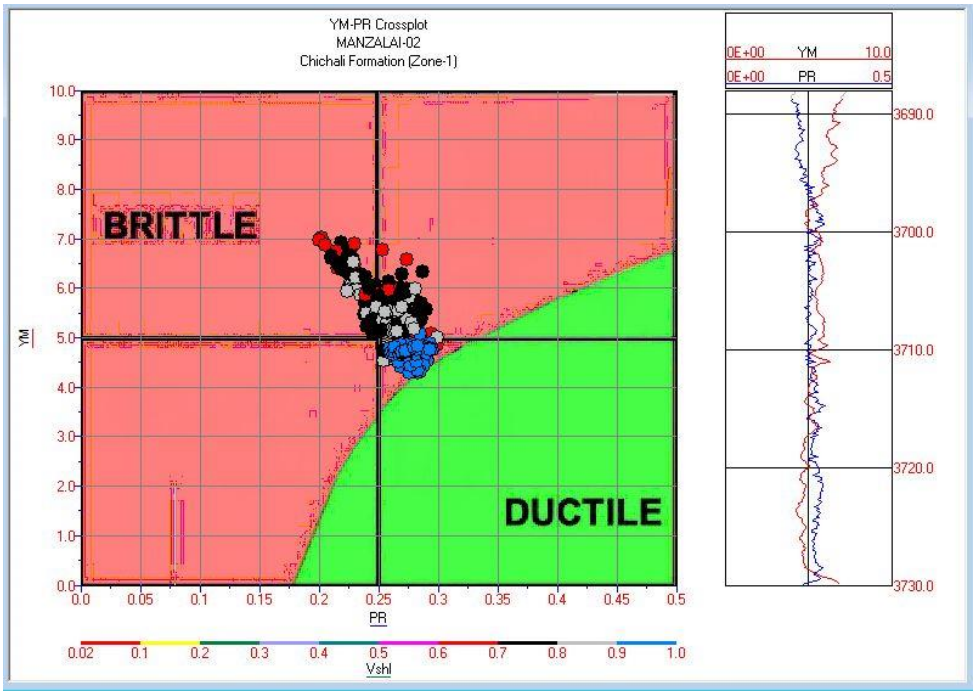

Figure 5.13 Young's Modulus (YM) - Poisson's Ratio (PR) Crossplot depicting Brittleness qualitatively of Chichali Formation's zone-1 drilled in Manzlai-02 well.

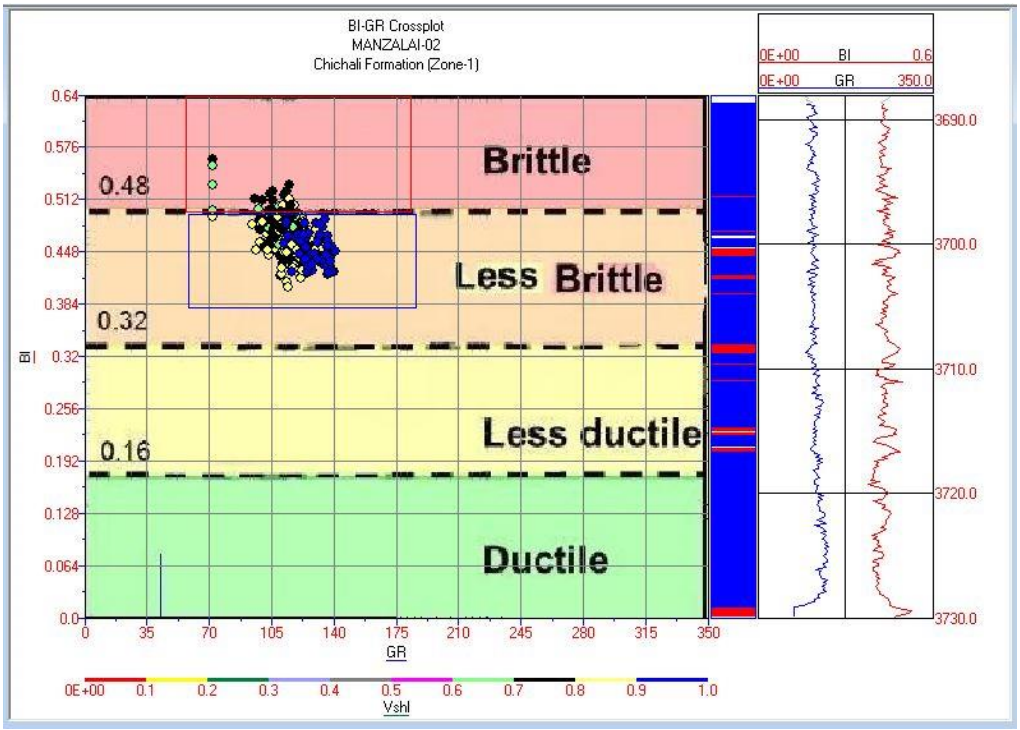

Figure 5.14 Brittleness Index vs Gamma Ray (GR) Crossplot depicting Brittleness qualitatively of Chichali Formation's zone-1 drilled in Manzlai-02 well.

5.2.3.2 Zone 2 (3748-3762 meters)

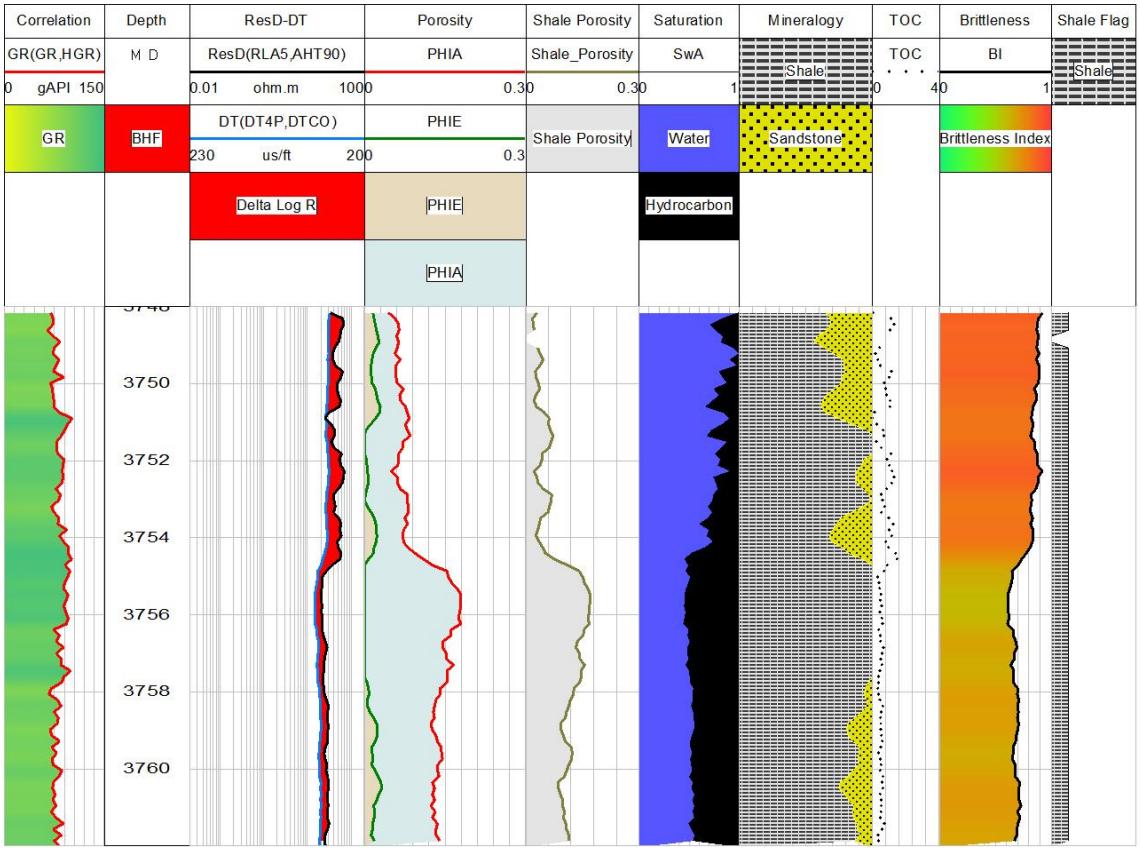

Figure 5.15 Calculated petrophysical attributes of zone-2 penetrated in Manzalai-02 well.

The zone is characterized by a high volume of Shale with an average value of 85.95%. The porosity calculation shows the average Sonic Porosity as 10.92% and the average Shale porosity as 8.71%. Lithology interpretation through three mineral models suggests Shale and Sandstone bearing zone. The zone bears average water saturation of 64.5%. Whereas, zone-2 has shown a reasonable reduction in total organic carbon content. The average value of TOC is computed as 0.63%.

Mineralogy assessment through Potassium-Thorium crossplot shows Shale to be mainly mixed layer, Illite and mica bearing Shale. Mechanical behaviour assessment suggests zone bears good elastic properties by delivering high Poisson's ratio, low Young modulus value and brittleness index with an average of 76.25%.

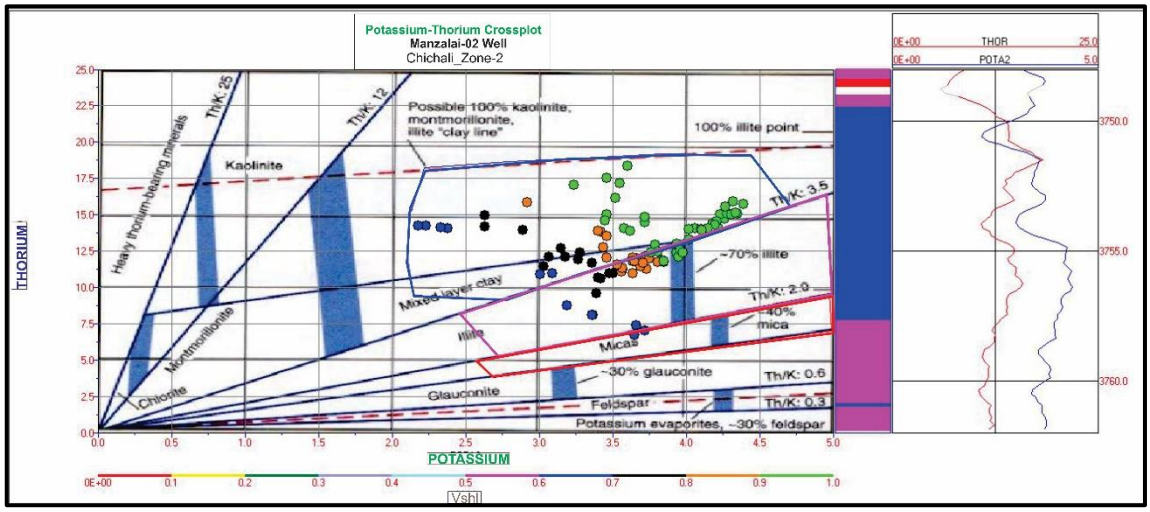

Figure 5.16 Potassium-Thorium crossplot depicting the Shale mineralogy of Chichali Formation's zone2 penetrated in Manzalai-02 well.

Moreover, the qualitative assessment of mechanical behaviour through Grieser and Bray, 2007 crossplot also verify the quantitative results calculated in the above method and shows zone-2 as good brittleness bearing zone.

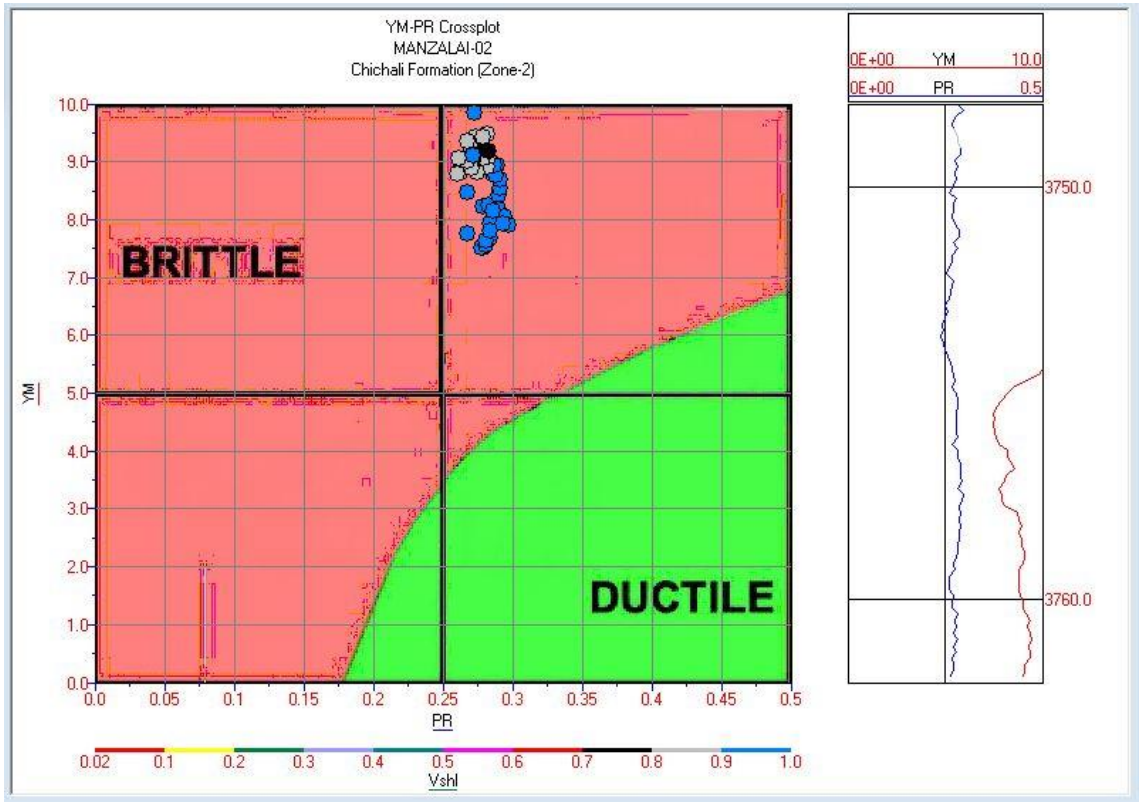

Figure 5.17 Young's Modulus (YM) - Poisson's Ratio (PR) Crossplot depicting Brittleness qualitatively of Chichali Formation'zone-2 drilled in Manzalai-02 well.

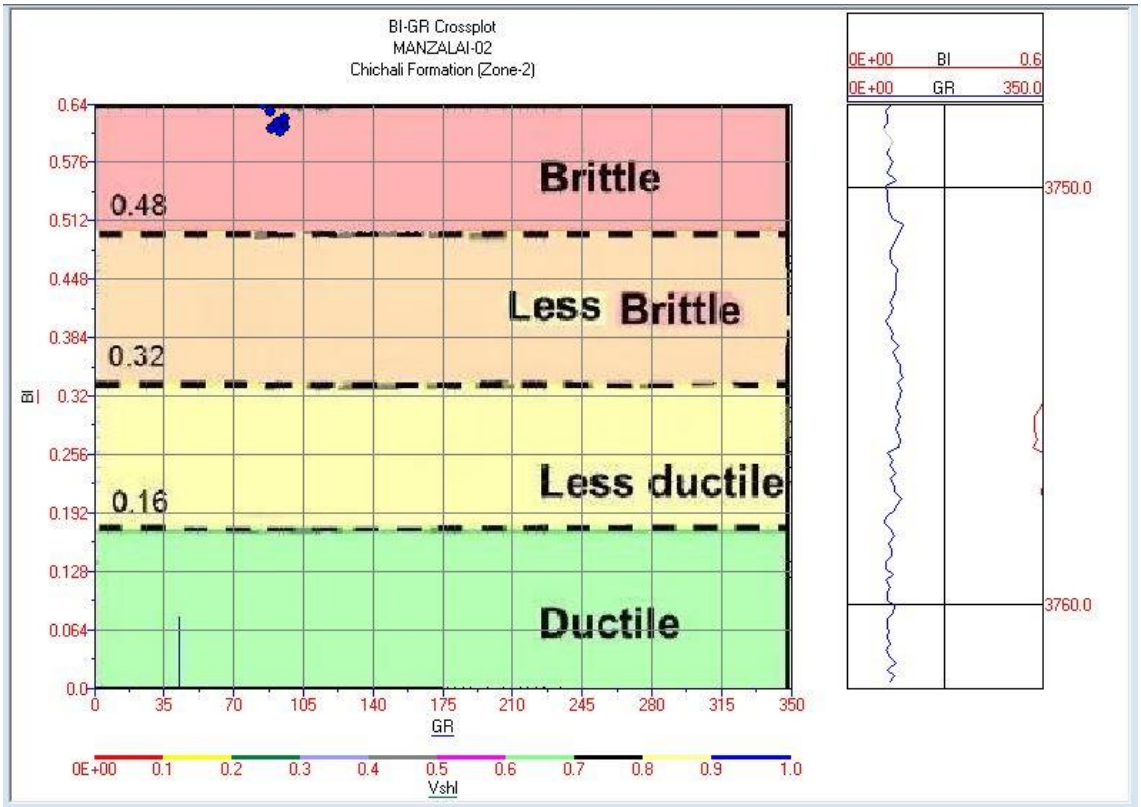

Figure 5.18 Brittleness index (%) vs Gamma-ray (API) Crossplot depicting Brittleness qualitatively of Chichali Formation's zone-2 drilled in Manzalai-02 well.

5.3 Maramzai-02 well

5.3.1 Well Description

The Maramzai-02 well bears coordinates of 70°59’ 17.00” **E**, 33°16’ 29.87” **N.** The well has been drilled up to the depth of 3499 meters. The formation of interest for our current analysis is Chichali Formation. Maramzai-02 well has penetrated the Chichali Formation at depth of 2917 meters and the bottom is at 3008 meters.

. The LAS file of Maramzai-02 well contained complete open hole wireline logs that are needed for analysis of Chichali Shale for their source rock potential analysis.

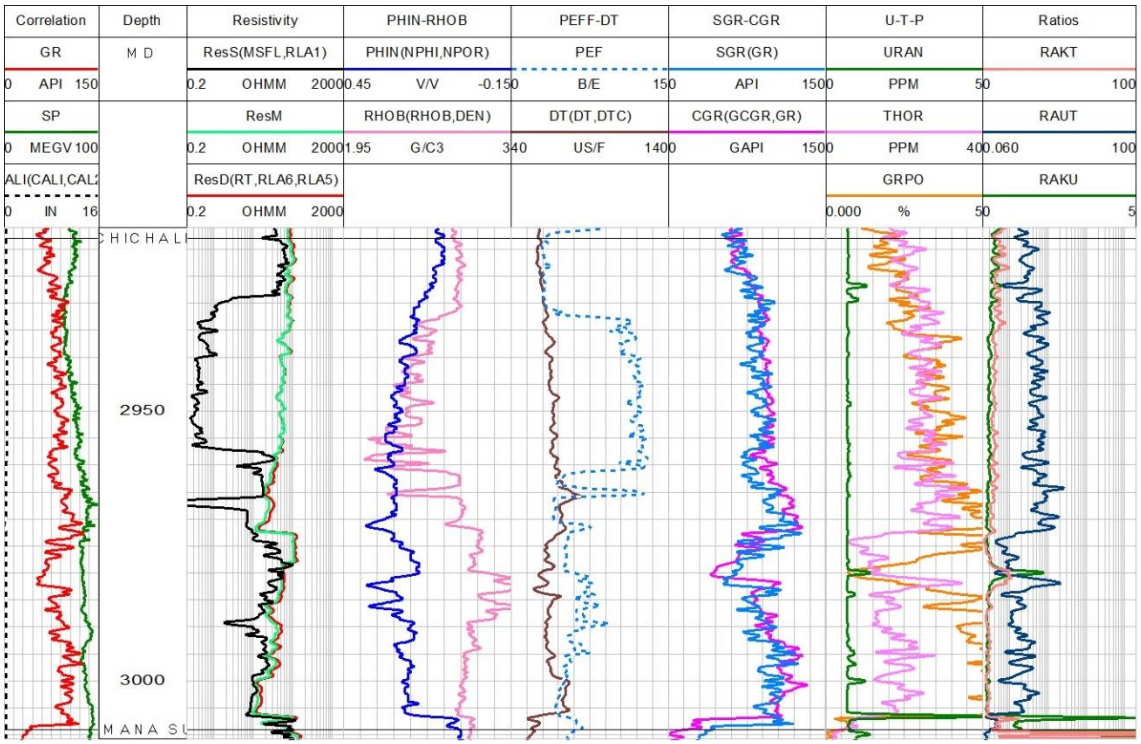

Figure 5.19 Image showing available open hole wireline logs in LAS file of Maramzai-02 well for Chichai Formation.

5.3.2 Qualitative Interpretation

The Chichali Formation in Maramzai-02 well (**Fig.** 5.19) shows no reliable reading of Caliper log to interpret about borehole condition. The gamma-ray log shows high reading showing formation bears a high volume of Shale. Low resistivity of Formation suggests it bears adequate water saturation. Density and PEF log shows high

reading at the bottom which can mislead us in interpretation. The sonic log shows reliable reading and is used for porosity interpretation. SGR and CGR logs show little difference depicting less abundance of Uranium content and low organic richness of Formation.

5.3.3 Quantitative Analysis

5.3.3.1 Zone-1 (2918 to 2977 meters)

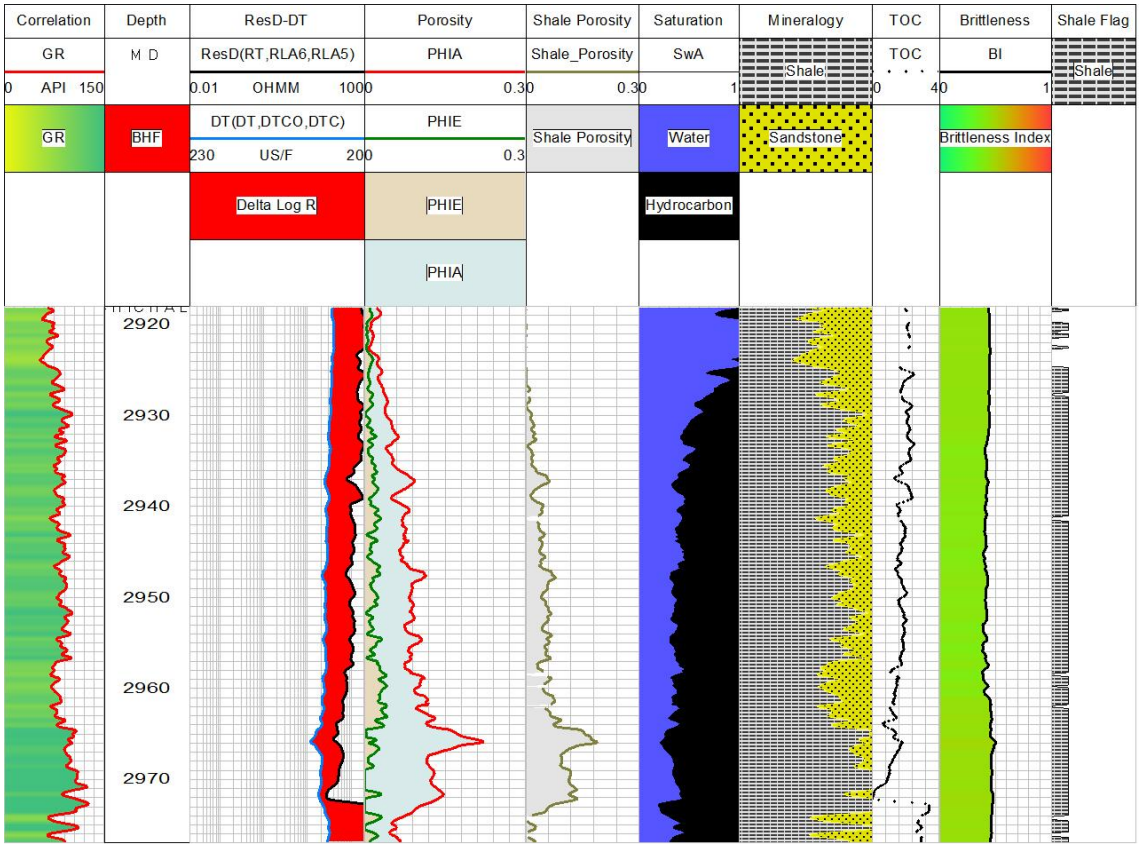

Figure 5.20 Calculaed petrophysical attributess for Chichali Formation's zone-1 in Maramzai-02 well.

Computation of volume of Shale through GR reveals zone bears average volume of Shale as 76%. The porosity analysis shows average porosity of 7.8% and a Shale porosity with an average value of 5.1%. Lithology assessment shows zone bears Shale, and Sandstone as a matrix with average water saturation of 47.2%. Organic richness assessment calculated the average total organic carbon as 1.7%. Mechanical property analysis shows formation bears a brittleness index of 43.6%.

The principal mineralogical composition interpreted from the Potassium-Thorium crossplot shows a zone comprised of mixed-layer clay and Illite.

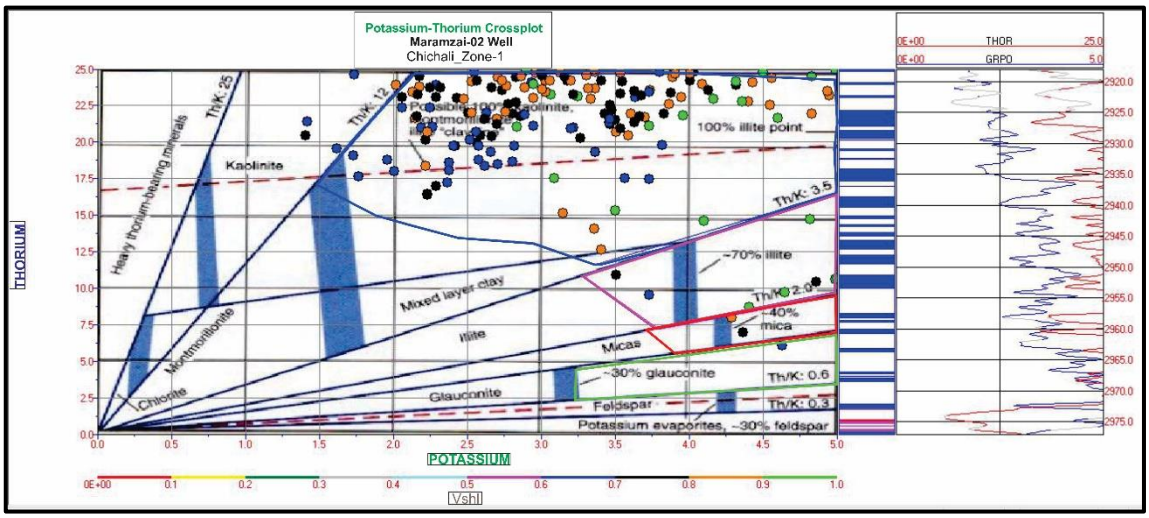

Figure 5.21 Potassium-Thorium crossplot depicting the Shale mineralogy of Chichali Formation's zone-1 penetrated in Maramzai-02 well.

To qualitatively assess the mechanical behaviour of zone the Grieser and Bray, 2007 crossplots shows the zone-1 bears less brittle to brittle properties.

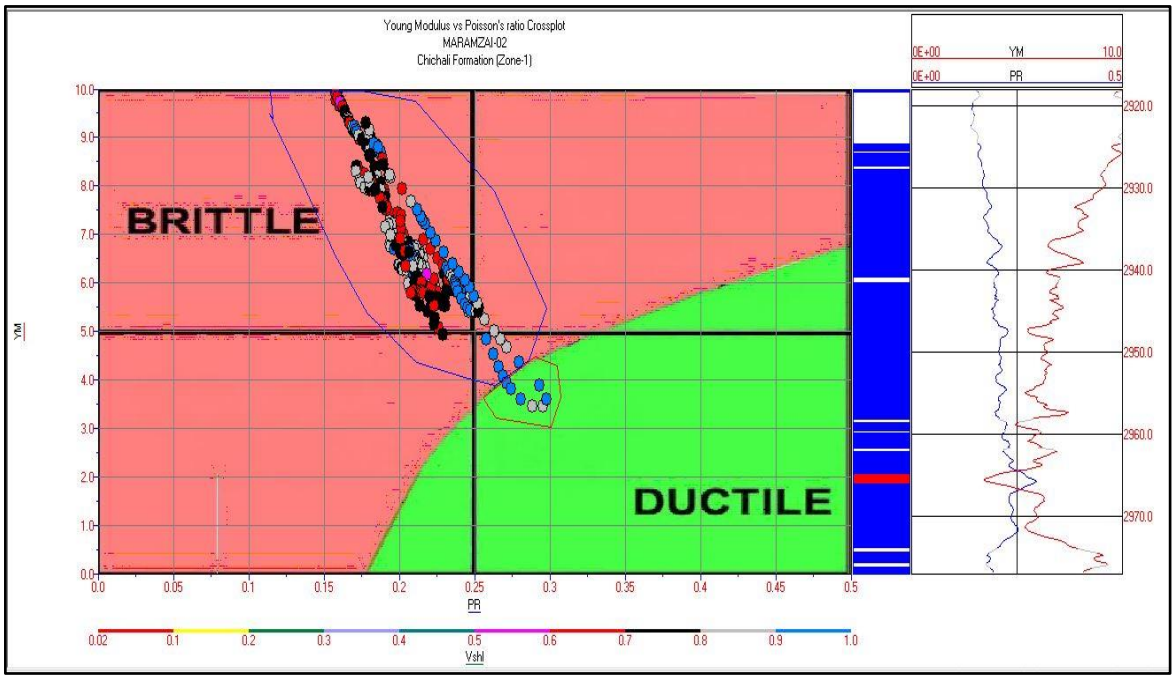

Figure 5.22 Young's Modulus (YM) - Poisson's Ratio (PR) Crossplot depicting Brittleness qualitatively of Chichali Formation's zone-1 drilled in Maramzai-02 well.

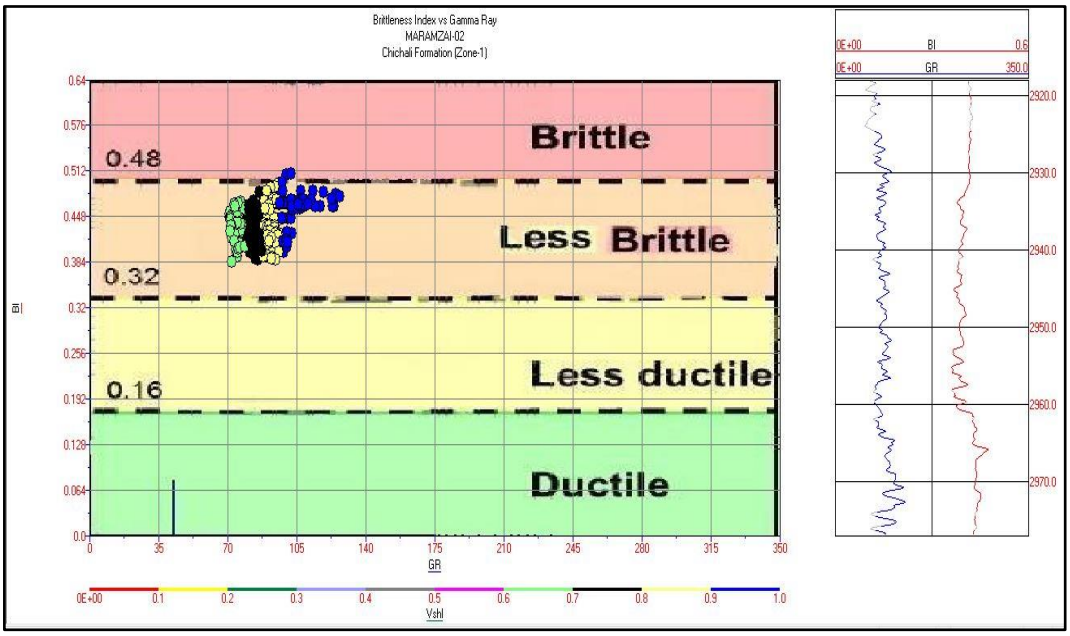

Figure 5.23 Brittleness Index vs Gamma Ray (GR) Crossplot depicting Brittleness qualitatively of Chichali Formation's zone-1 drilled in Maramzai-02 well.

5.3.3.2 Zone-2 (2982 to 3008 meters)

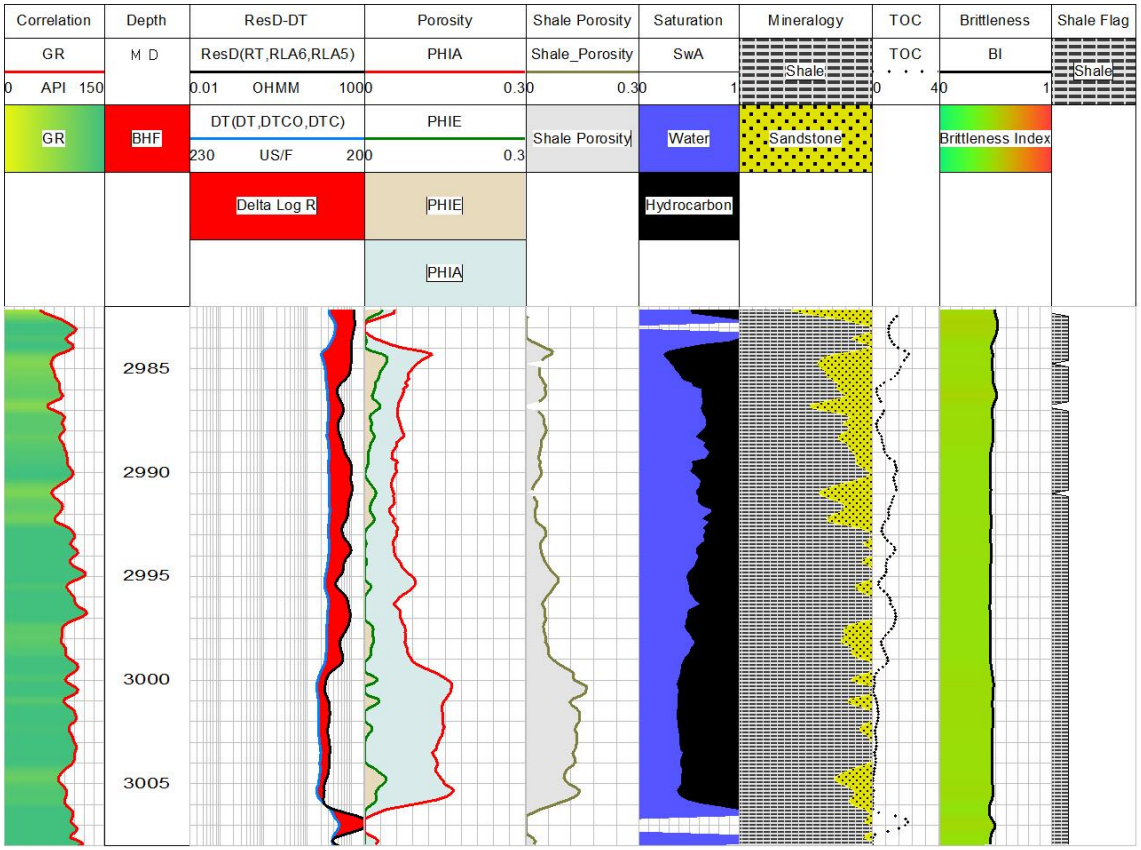

Figure 5.24 Calculated petrophysical attributes for Chichali Formation's zone-2 in Maramzai-02 well.

This zone shows the average volume of Shale about 86.1% through calculation from GR. The average porosity computed from the Sonic log appears as 8.1%. while average Shale porosity of 6.4%. Matrix lithology is interpreted through three mineral models as Shale with Sandstone, which is saturated with 55.5% of water. Organic richness computation suggests average total organic carbon of 0.73%. Mechanical assessment analysis shows it possesses an average brittleness index of 47%.

The Potassium-Thorium crossplot depicted that the mineralogy of Shale is mainly mixed-layer clay with the minor influx of Illite clay and Montmorillonite.

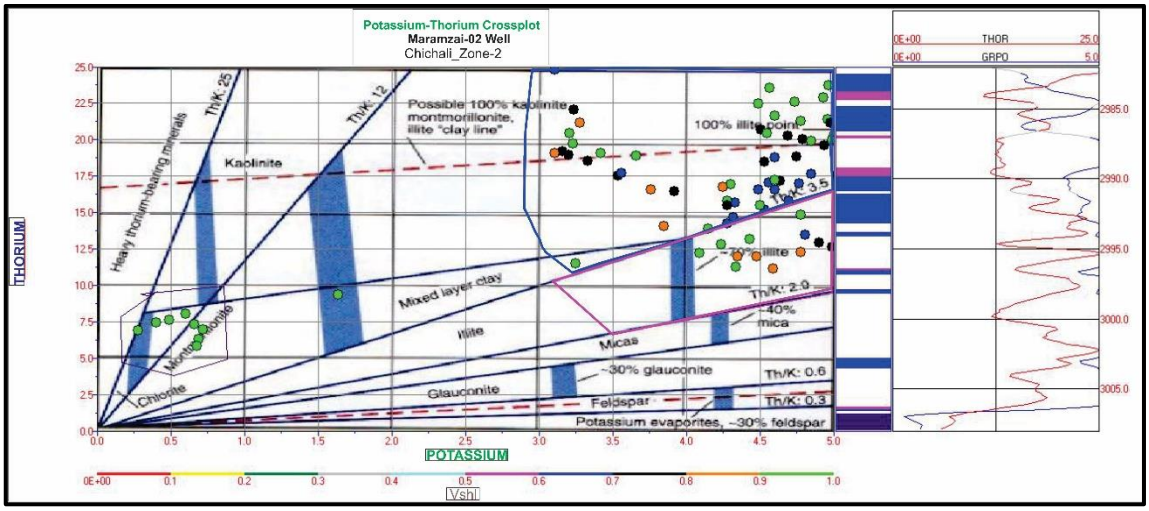

Figure 5.25 Potassium-Thorium crossplot depicting the Shale mineralogy of Chichali Formation's zone-2 penetrated in Maramzai-02 well.

Additionally, the zone has been probed through qualitative analysis to assess its grade of brittleness through utilization of Grieser and Bray, (2007) crossplot which shows the zone bears brittle behaviour.

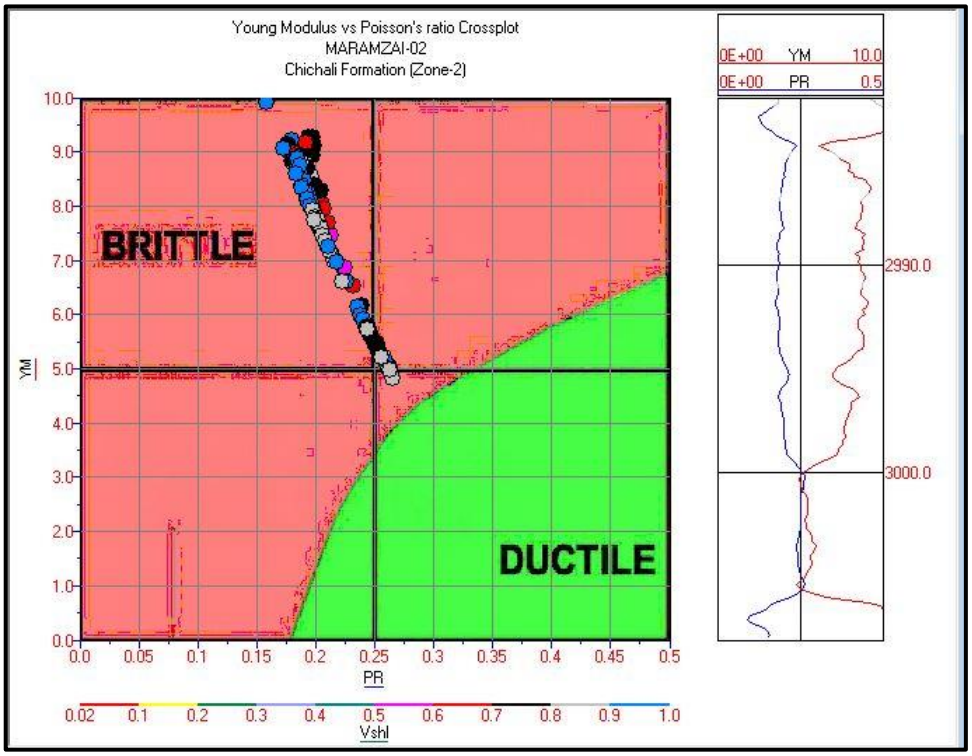

Figure 5.26 Young's Modulus (YM) - Poisson's Ratio (PR) Crossplot of zone-2.

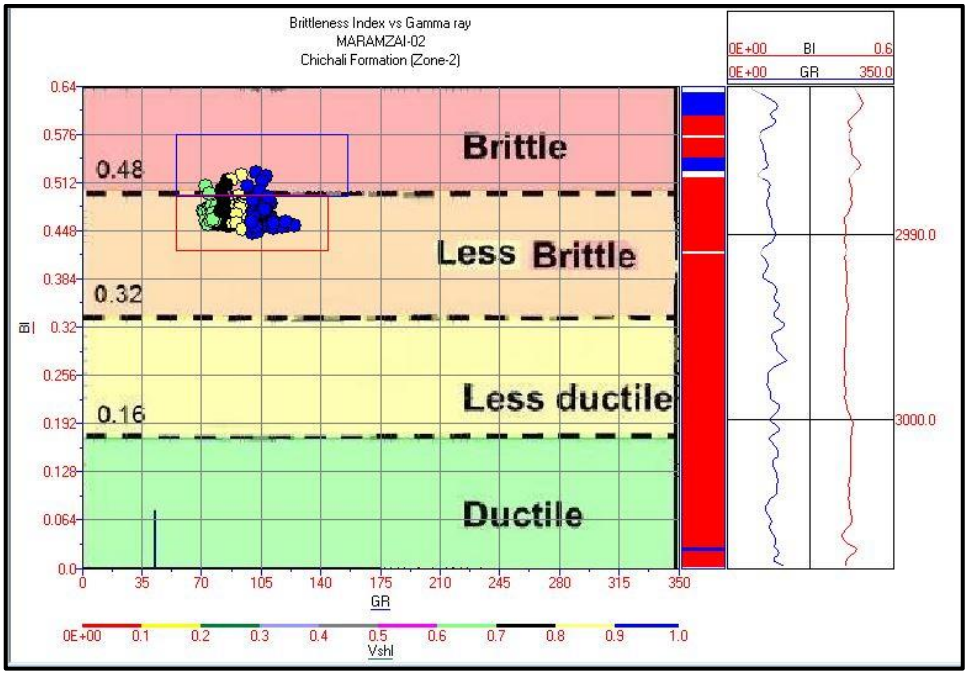

Figure 5.27 Brittleness index (%) vs Gamma ray (API) Crossplot of zone-2

CHAPTER 6

CONVENTIONAL PETROPHYSICAL CHARACTERIZATION OF SAMANA SUK LIMESTONE

The Samana Suk Formation of the Jurassic age is considered a tight reservoir because of its low permeability and porosity. All three wells of Makori-01, Maramzai-02 and Manzalai-02 have encountered Samana Suk Formation. The same methodology discussed in Chapter 4 will be applied to calculate the reservoir parameters Samana Suk Formation. The main parameters of reservoir crucial to be measured in the petrophysical analysis are Volume of Shale, Porosities, Hydrocarbon saturation and Permeability. This chapter is focused on the reservoir characterization of the Samana Suk Formation based on well logs responses from the aforementioned wells.

Two templates have been used to portray the wireline log responses and calculated attributes. One template referred to as input log template is used for portraying raw log curves. The second template referred to as the output log template is used for the portraying of calculated attributes.

Input log template

This template (**Fig.** 6.1) shows the open hole wireline logs readings taken in well. The input log template includes four tracks of Correlation, Resistivity, Nphi-Rhob and PEF-DT.

i. 1st Track includes GR log on a scale of 0 to 150 API, Sp log on a scale of 0 to 100, Caliper log 0 to 16 Inches.
ii. 2nd Track includes Resistivity logs (MSFL, LLS, LLD) on a scale from 0.2 to 2000 Ohm-m.
iii. 3rd Track of Density log on a scale from 0.95 to 3 gm/cc, and Neutron log on scale of -0.15 to 0.45 v/v
iv. 4th track comprises a Sonic log with scale from 40 to 140 microsec/feet and PEF log on scale of 0-10 Barns/electron .

Output log template

The output log shows all the attributes calculated for Samana Suk Formation utilizing the raw log curves. The output template includes seven tracks.

i. 1st tracks of correlation show us the reading of the GR log (on a scale of 0-150 API).
ii. Second shows resistivity logs (on a scale of 0.01-100 ohm.m).
iii. The third track shows average and effective porosity on a scale of 0-0.3.
iv. The fourth track shows the Saturation of water and hydrocarbon on a scale of 0-1.
v. The fifth track shows the matrix percentage of lithology.
vi. The sixth track shows the permeability on a scale of 0.01 to 10.
vii. The seventh track shows the reservoir, net reservoir and net pay flag, while the last track shows a tight reservoir flag.

6.1 Makori-01 well

6.1.1 Well Description

The Samana Suk Formation has been penetrated by Makori-01 well at the depth of 3288-3355, 3823-3862, and 3887-3960 meters depicting Fault structure in the subsurface. The present study investigated the main first section of the Samana Suk Formation drilled at depth of 3288-3355 meters.

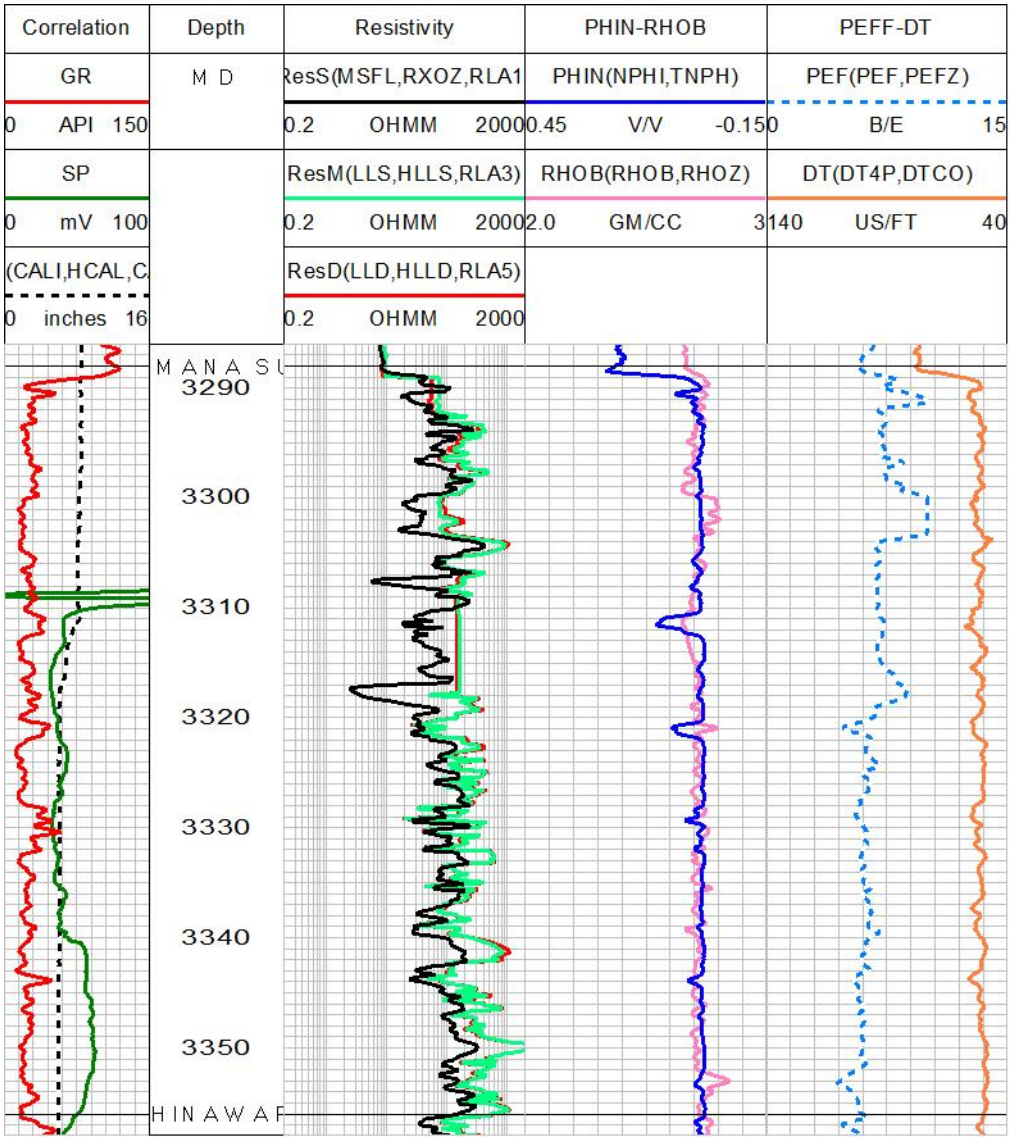

Figure 6.1 Image showing complete log suits available for Samana Suk Formation drilled in Makori-01 well.

6.1.2 Qualitative Interpretation

Caliper log shows good borehole condition as there is no variation in reading is observed. The bit size is changed at depth of 3312 due to which caliper log has changed its reading from 8 to 6 inches. Resistivity log shows a variable reading of extreme high and low depicting formation possesses change in fluid content. The density log shows a high reading of greater than 2.71 gm/cm^3 making it non-reliable for interpretation. The sonic log gives us good reading. PEF log shows normal reading at top of the formation while anomalous reading at bottom of the formation.

6.1.3 Quantitative Analysis

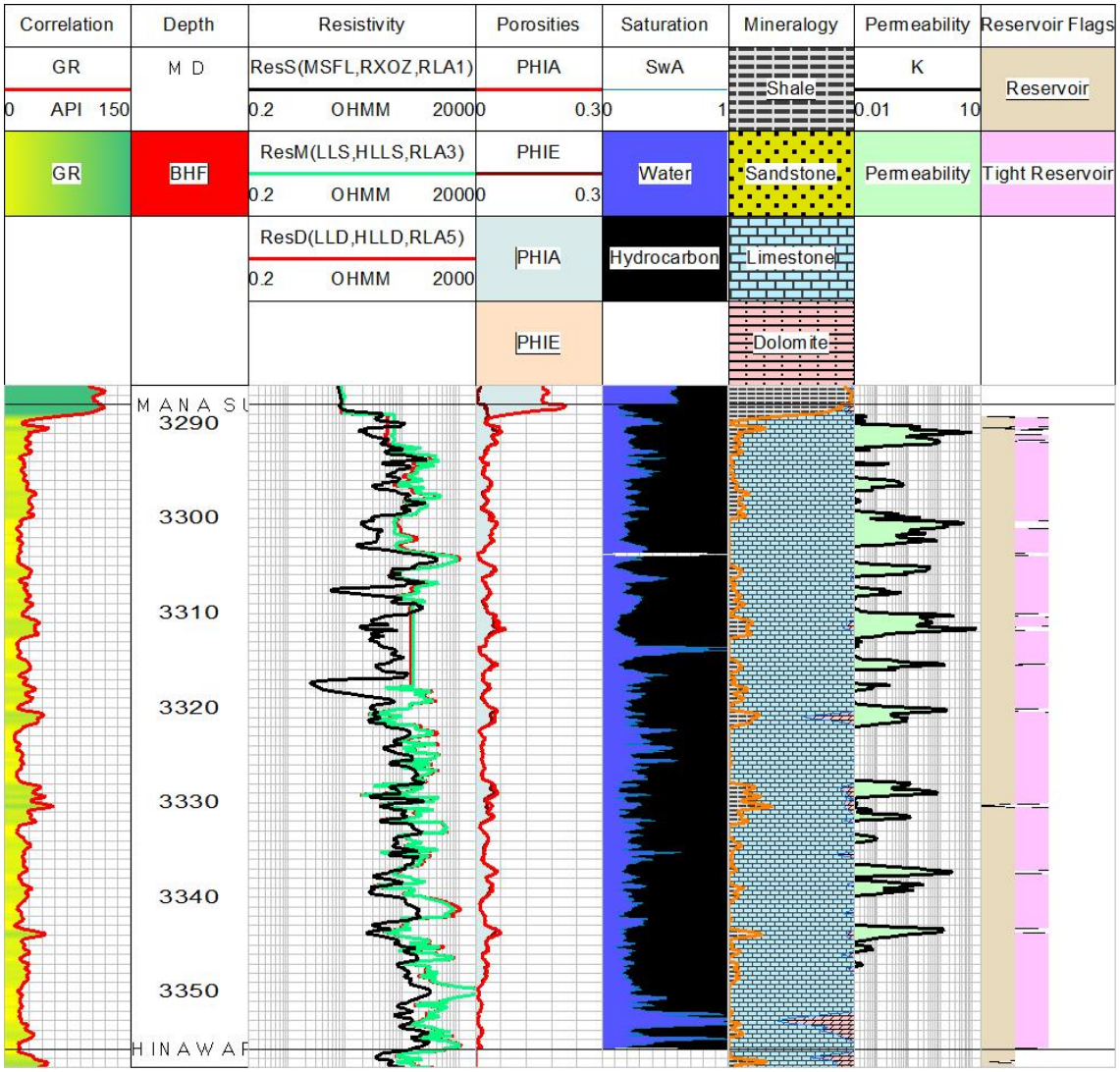

Figure 6.2 Image shows the interpreted logs and calculated petrophysical attributes in Samana Suk Formation drilled in Makori-01 well.

The borehole condition indicated by the caliper log is interpreted shows to be good as no mud cake and washout is observed. Samana Suk shows a low CGR reading with an average value of 20 API suggesting a clean reservoir with average value volume of Shale computed as 4.9%.

The porosity assessment shows average Sonic porosity and effective porosity of 2.9%. Due to the low volume of Shale formation bears the same average and effective porosity. The Archie equation has been used to calculate the saturation of water. The results show formation has been characterized with average water saturation of 27.02%,

and the Formation is inundated with Hydrocarbon. The average hydrocarbon saturation is computed as about 72.98%.

Permeability analysis suggests Samana Suk Formation in the present study also has been characterized with low permeability of less than 0.1 mD. Although, at certain depth points with thickness less than 3 meters the formation has shown permeability with a value greater than 0.1 mD.

As the Formation is characterized by low porosity and low permeability hence, Samana Suk limestone comprises of no adequate thick zone which can be marked as a good zone for the production of hydrocarbon resources. The cut-offs set for marking the reservoir zone is Vshl < 30%, and for tight reservoir is permeability < 1mD..

Additionally, Samana Suk has been probed through different crossplots i.e DT-PHIN, RHOB-DT, and RHOB-PHIN to assess its porosity and matrix lithology. All three crossplots shows Samana Suk is mainly composed of a Calcite matrix with Dolomite at some depths.

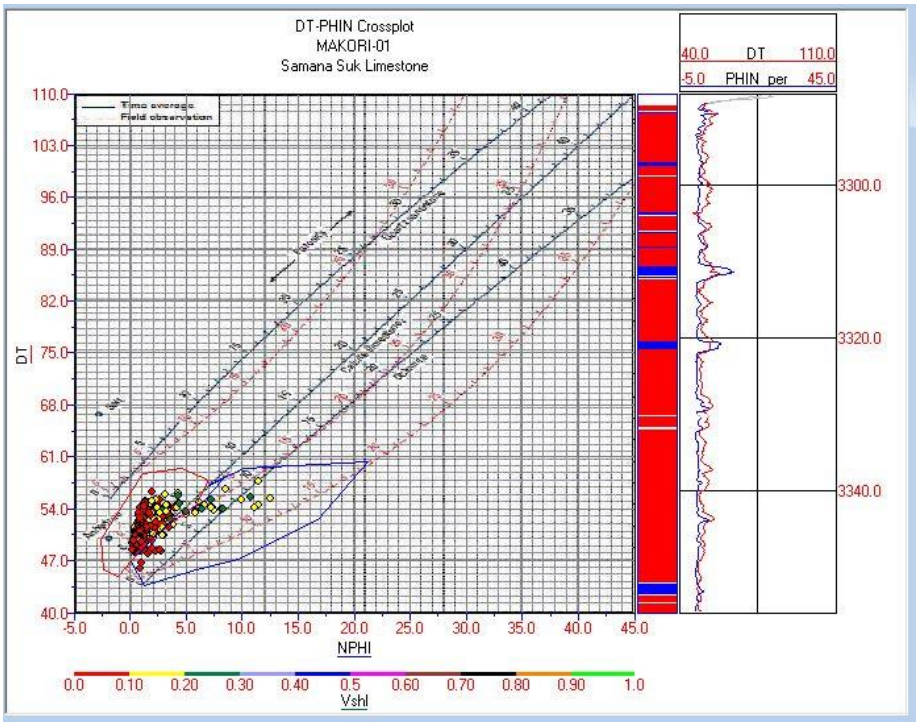

Figure 6.3 DT-PHIN crossplot showing the porosity ranges and matrix mineralogy of Samana Suk Formation.

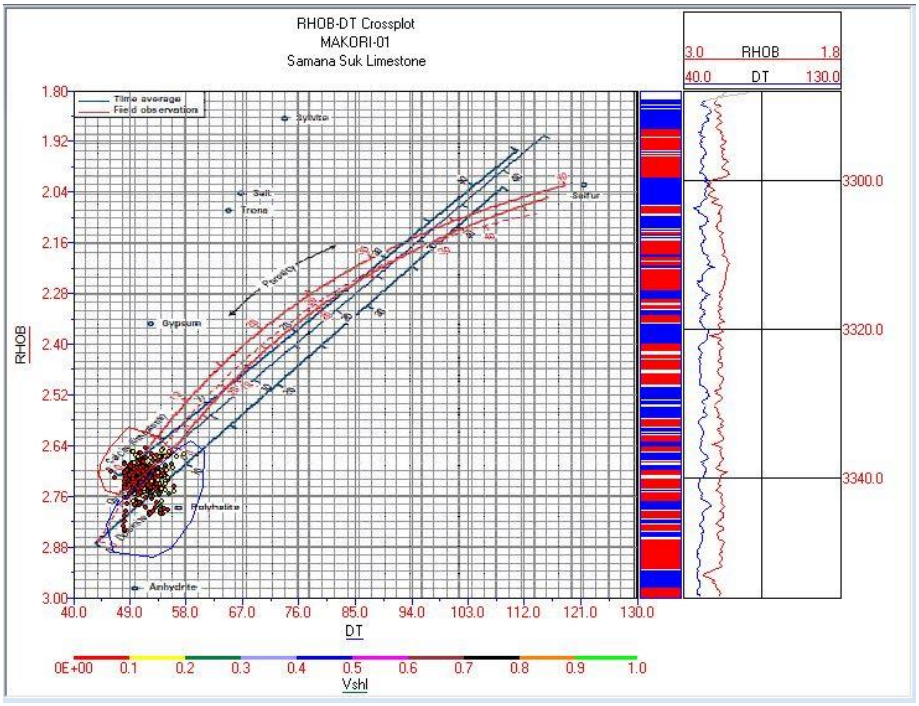

Figure 6.4 RHOB-DT crossplot showing the porosity ranges and matrix mineralogy of Samana Suk Formation.

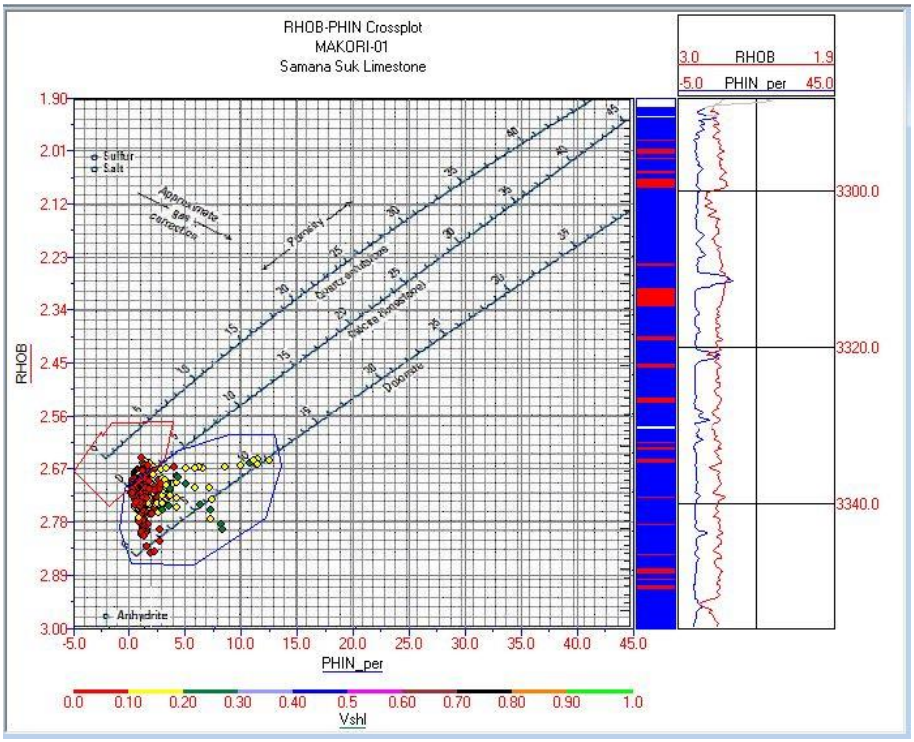

Figure 6.5 RHOB-PHIN crossplot showing the porosity ranges and matrix mineralogy of Samana Suk Formation.

Both qualitative and quantitative analysis of Samana Suk Formation shows the formation bears average porosity around 3 % with matrix mainly of Calcite mineralogy. Although at few depth points it has shown matrix mineralogy as Dolomite.

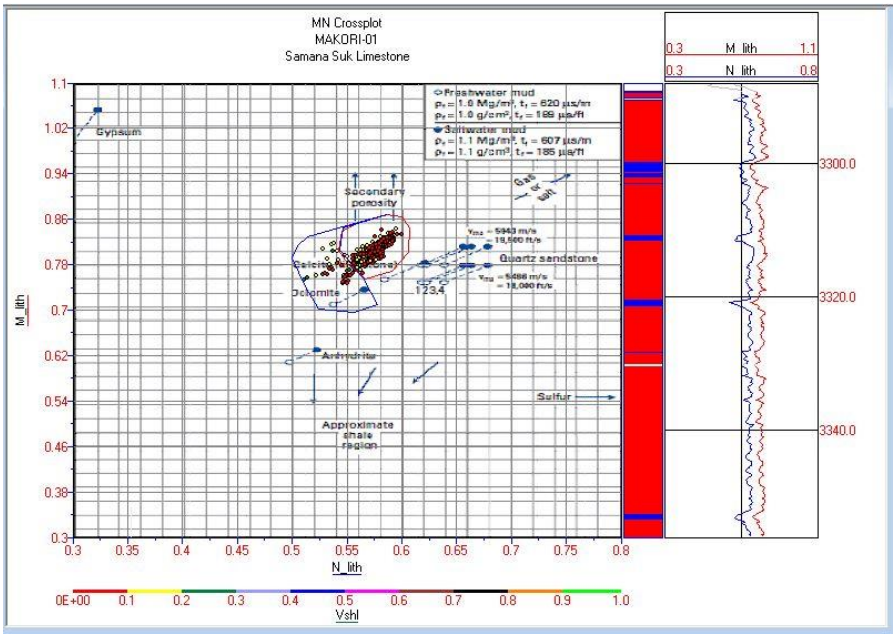

Figure 6.6 M-N Crossplot showing matrix lithology of Samana Suk Formation drilled in Makori-01 well.

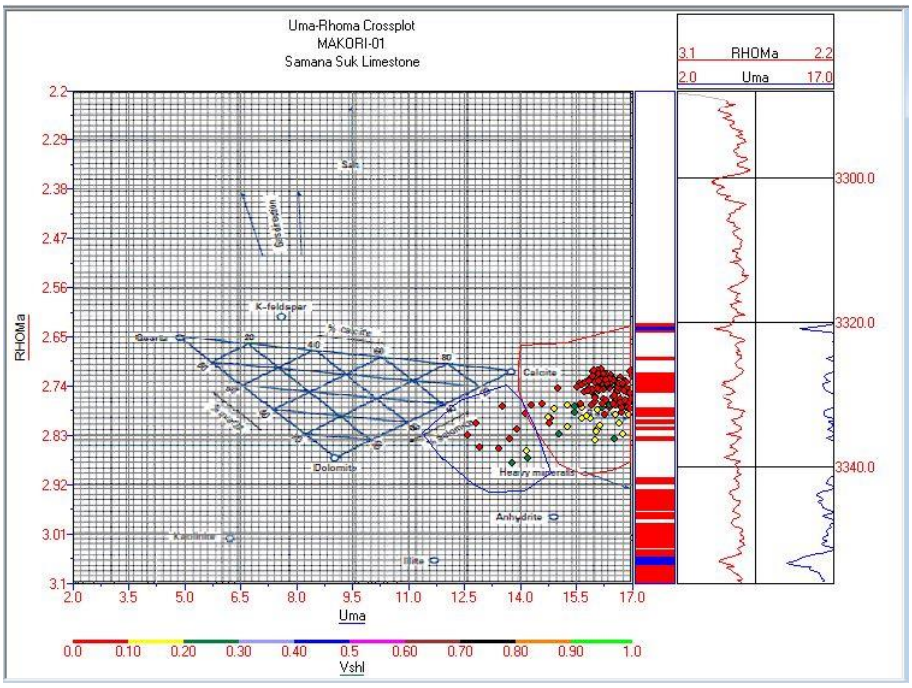

Figure 6.7 Uma-Rhoma Crossplot drawn for assessing matrix lithology of Samana Suk Formation drilled in Makori-01 well.

6.2 Manzalai-02 well

6.2.1 Well Description

In Manzalai-02 well Samana Suk Formation is drilled at depth of 3763 and the bottom of Samana Suk lies at depth of 3920 meters. The complete log suit is utilized for analysis of the Samana Suk Formation in the Manzalai well.

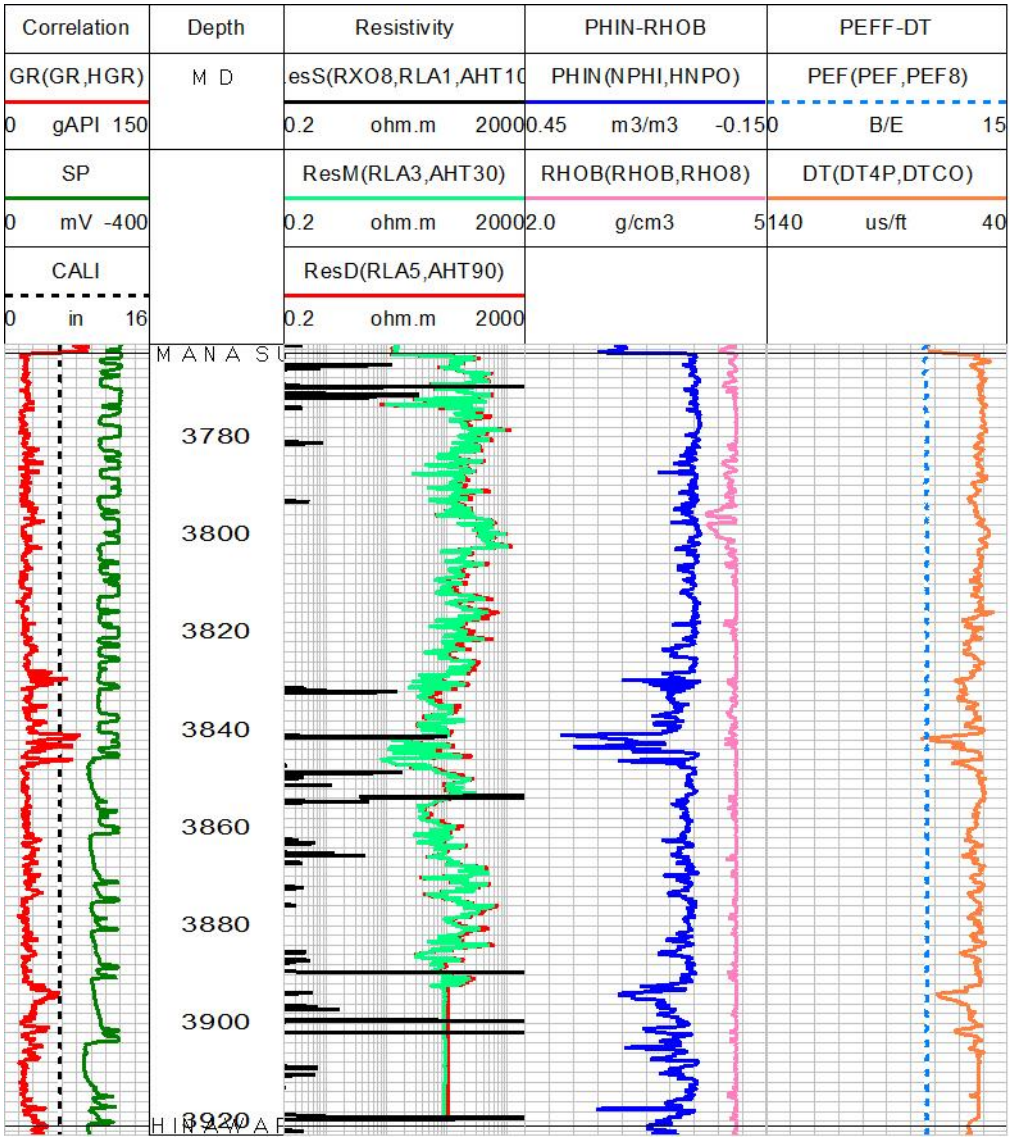

Figure 6.8 Image showing all available logs run in Samana Suk Formation drilled in Manzalai-02 well.

6.2.2 Qualitative Interpretation

Consistent caliper log reading indicates no washouts and mud cakes in the borehole. Gamma-ray shows low reading making Samana Suk Formation a clean reservoir with a minimum volume of Shale. The Density and PEF log shows anomalous high value up to 4 gm/cm^3 due to which it was not utilized for analysis. The resistivity log shows formation bears high deep resistivity giving a good sign of hydrocarbon saturation. The sonic log shows reliable and sound reading due to which it can be used for porosity analysis.

6.2.3 Quantitative Analysis

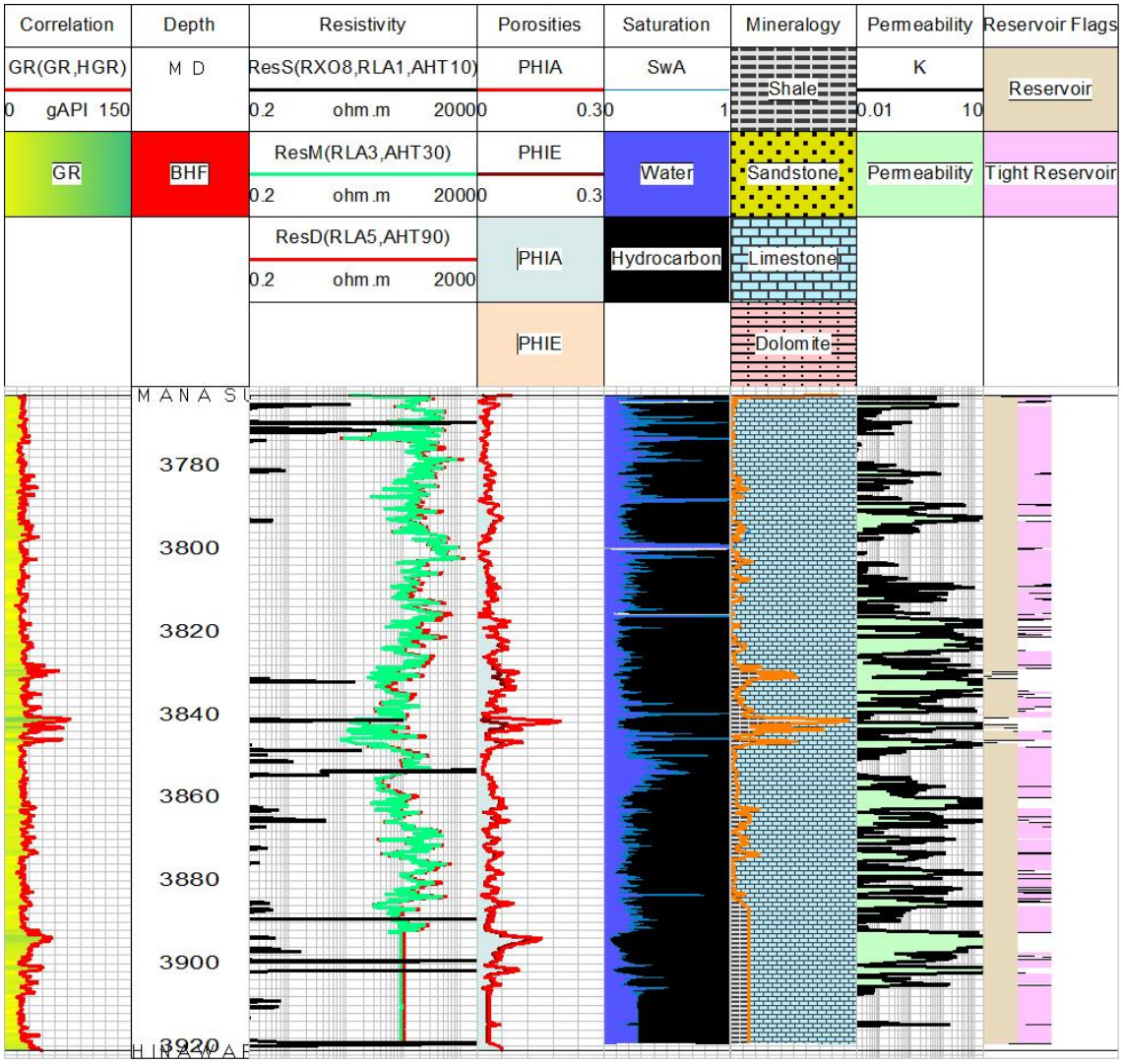

Figure 6.9 Image shows the interpreted logs and calculated petrophysical attributes of Samana Suk Formation drilled in Manzalai-02 well.

No washouts and mudcake is observed and borehole shows sound conditions interpreted from Caliper log. The calculation of volume of Shale shows average percentage around 9.02%. Porosity computation revealed average Sonic porosity as 3.9% and effective porosity as 3.4%. The numerical estimation of water saturation shows formation bears very low saturation of water. The average value of water saturation is computed as 23.6% and saturation of Hydrocarbon as 76.4%. The formation shows good permeability readings at some peaks while low permeability is observed for overall section and is characterized with permeability less than 0.1 mD.

The porosity and matrix lithology is also assessed qualitatively through crossplots. The DT-PHIN crossplot only could be utilized to assess porosity and matrix qualitatively. The result shows Formation bears the main matrix as mainly Calcite with average porosity around 3%.

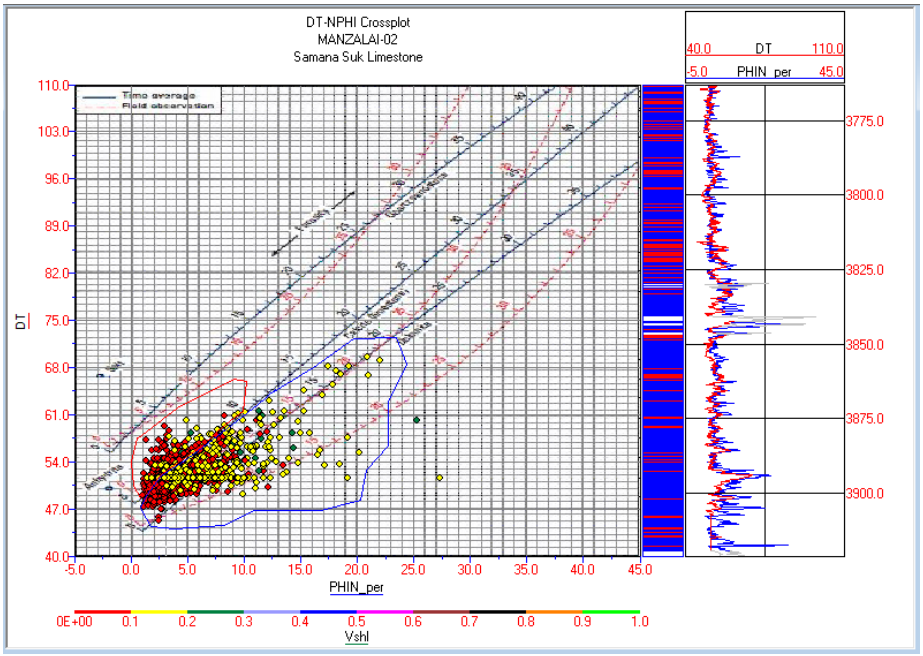

Figure 6.10 DT-PHIN crossplot furnished for Samana Suk Formation drilled in Manzalai-02 well.

6.3 Maramzai-02 well

6.3.1 Well Description

The Maramzai-02 well contained the Chichali Formation ranging from a depth of 3009-3119 meters. The input open hole wireline logs responses are given below;

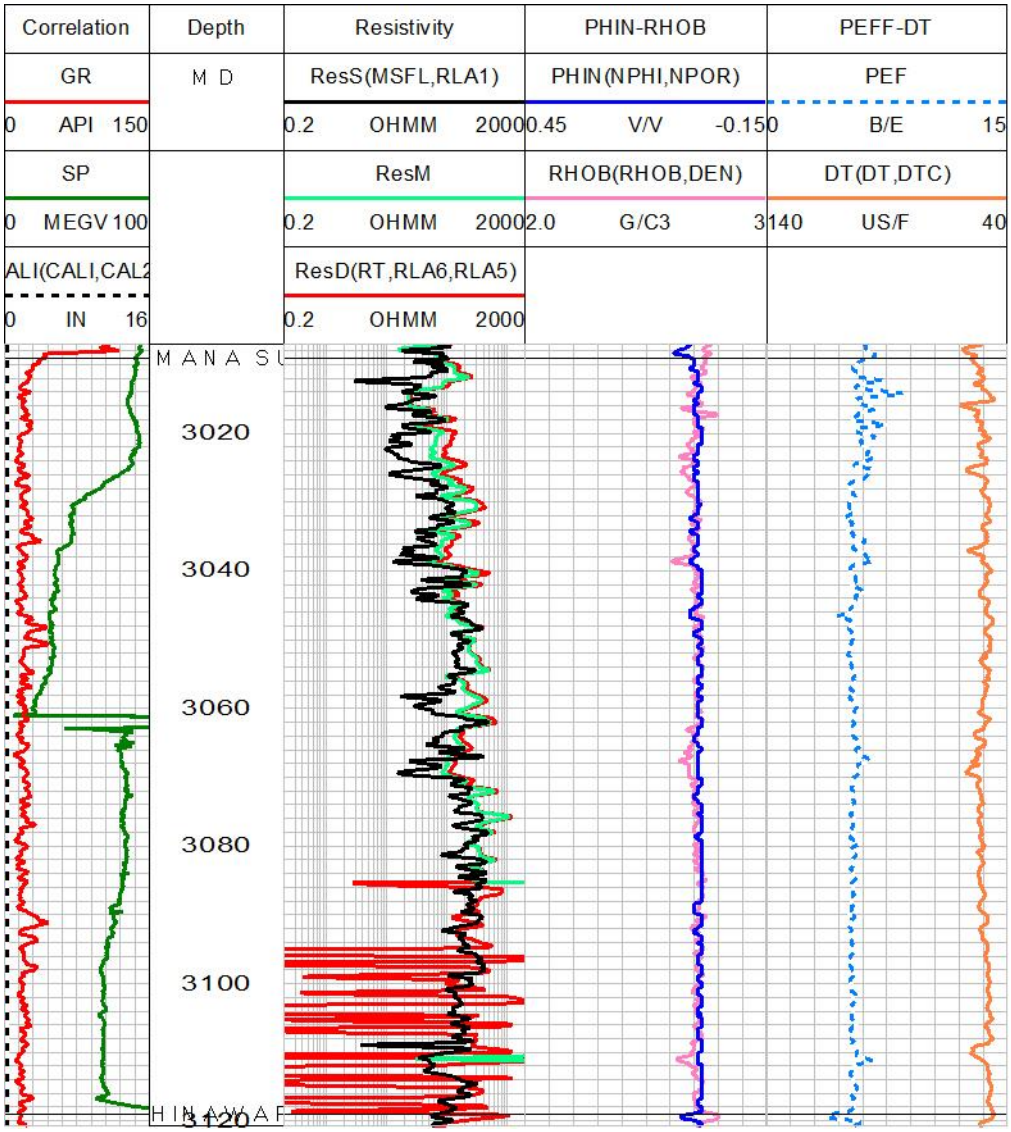

Figure 6.11 logs available for analysis of Samana Suk Formtion drilled in Maramzai-02 well.

6.3.2 Qualitative interpretation

The caliper log indicates anomalous low values indicating erroneous response hence, could not be used for any interpretation. Deep resistivity shows some missing values over a certain depth. The resistivity log shows high variation over short depths marking that zone bears different fluids. The low Sonic transit time shows formation is a tight reservoir with low porosity and permeability. The Density log shows high readings indicating formation as high density bearing with low porosity.

6.3.3 Quantitative Analysis

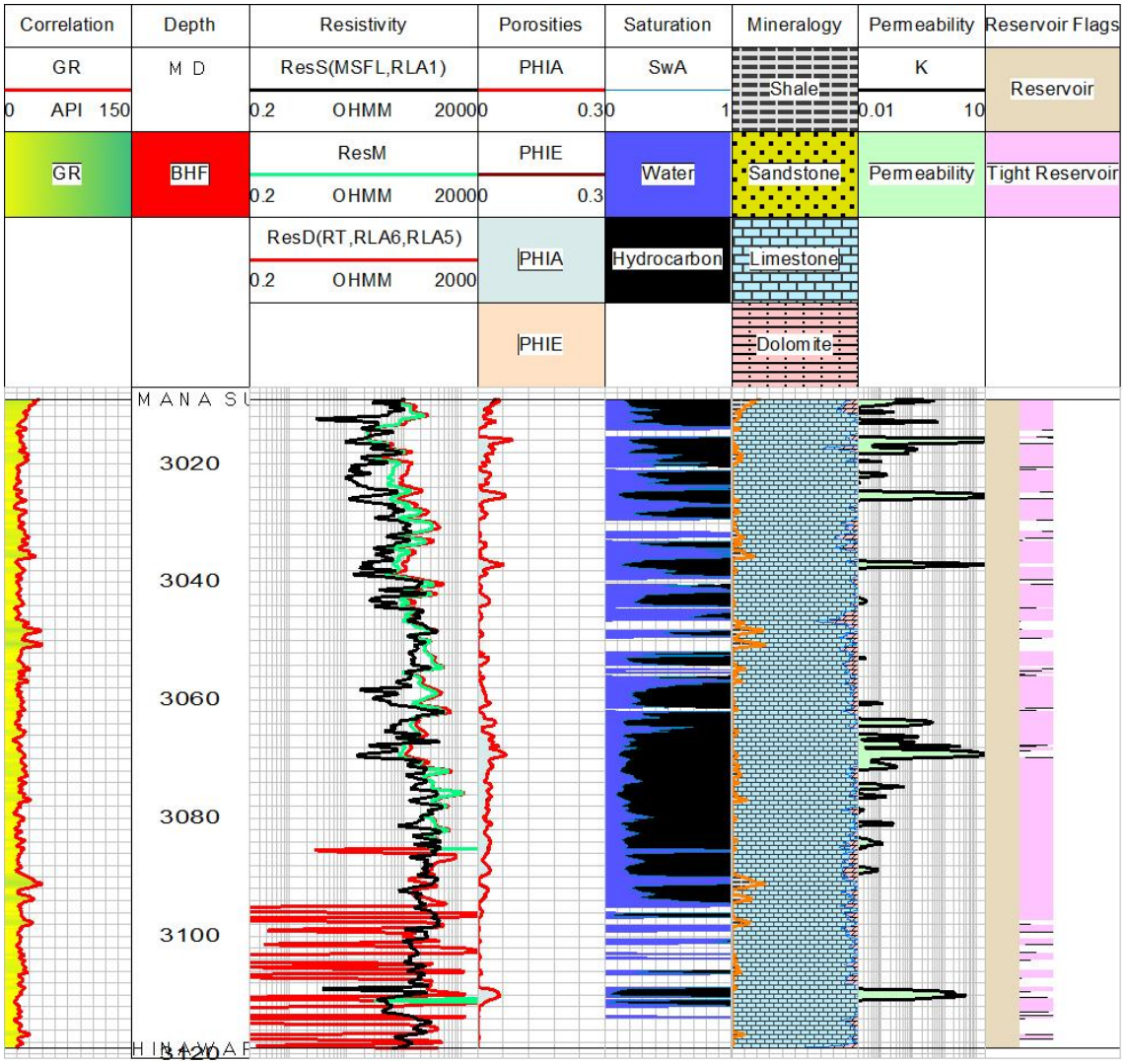

Figure 6.12 Image showing the interpreted logs and calculated petrophysical attributes for Samana Suk Formation drilled in Maramzai-02 well.

Analysis indicates Formation bears average volume of Shale as 3.8% whereas, maximum reading encountered is 43 API. Upon calculation of Sonic porosity, the reservoir shows average porosity of 1.58% and 1.55% of effective porosity. Analysis shows Formation holds high saturation of water, and inadequate saturation of hydrocarbons to be a good hydrocarbon-bearing reservoir. The average value of water saturation is computed as 44.06%, and Hydrocarbon saturation as 55.94%. The lithology analysis shows Samana Suk Limestone mainly bears a matrix of Calcite with some Dolomites at certain points.

Permeability estimation shows the formation has characteristics of the tight reservoir by holding extreme low permeability with an average of 0.87 mD marking it as a tight reservoir.

Besides the quantitative analysis of Porosity from the algorithm, DT-PHIN, RHOB-DT and RHOB-PHIN crossplot is also used to analyse and cross-check the porosity and matrix lithology of the Samana Suk Formation.

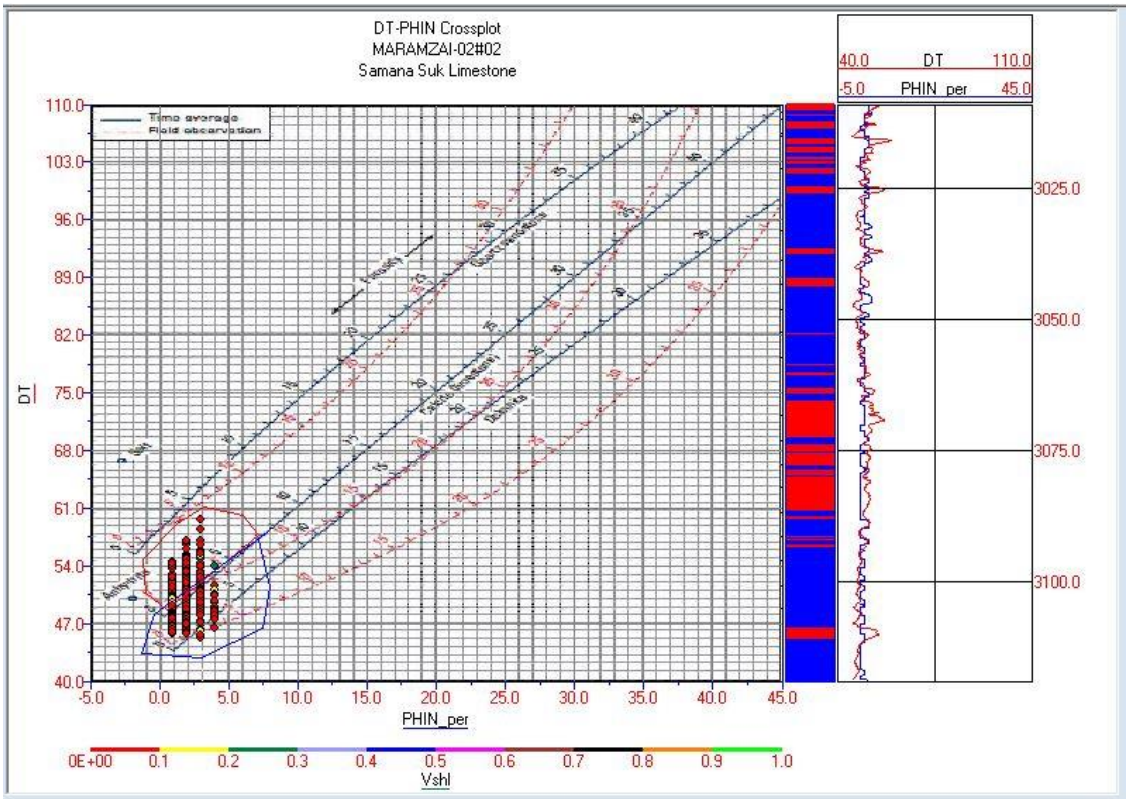

Figure 6.13 DT-PHIN crossplot furnished for Samana Suk Formation drilled in Maramzai-02 well.

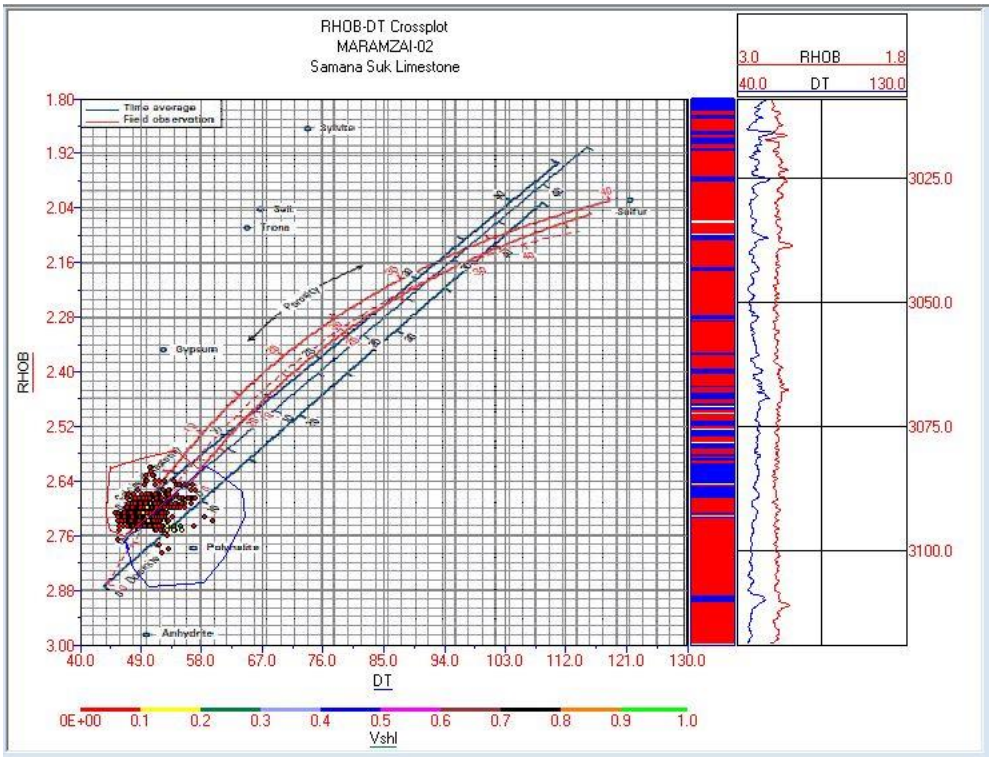

Figure 6.14 RHOB-DT crossplot furnished for Samana Suk Formation drilled in Maramzai-02 well.

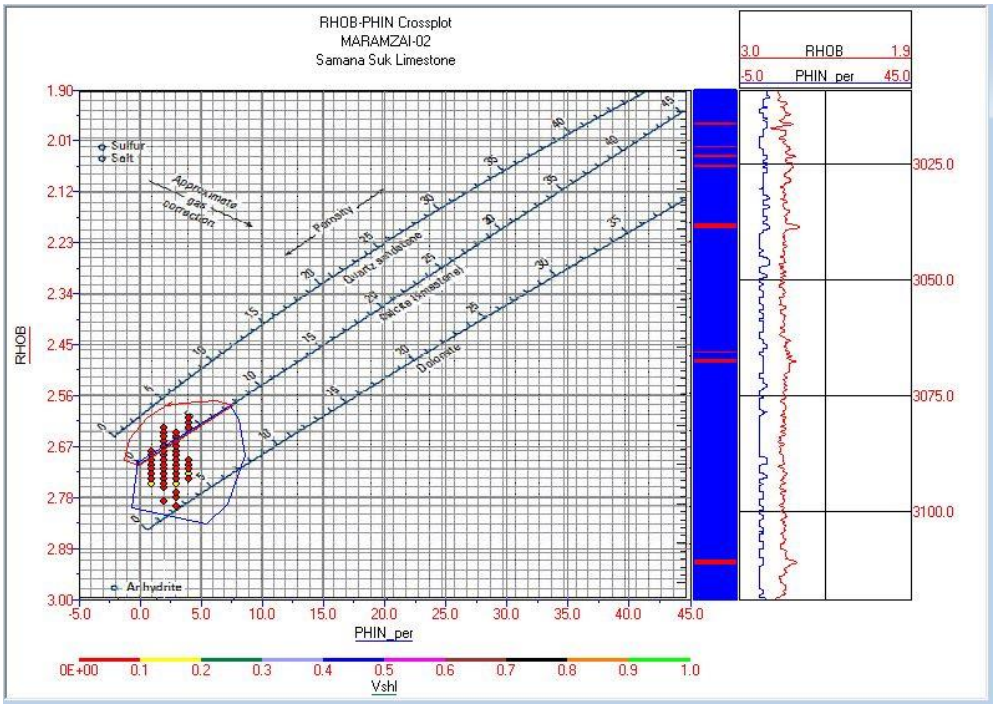

Figure 6.15 RHOB-PHIN crossplot furnished for Samana Suk Formation drilled in Maramzai-02 well.

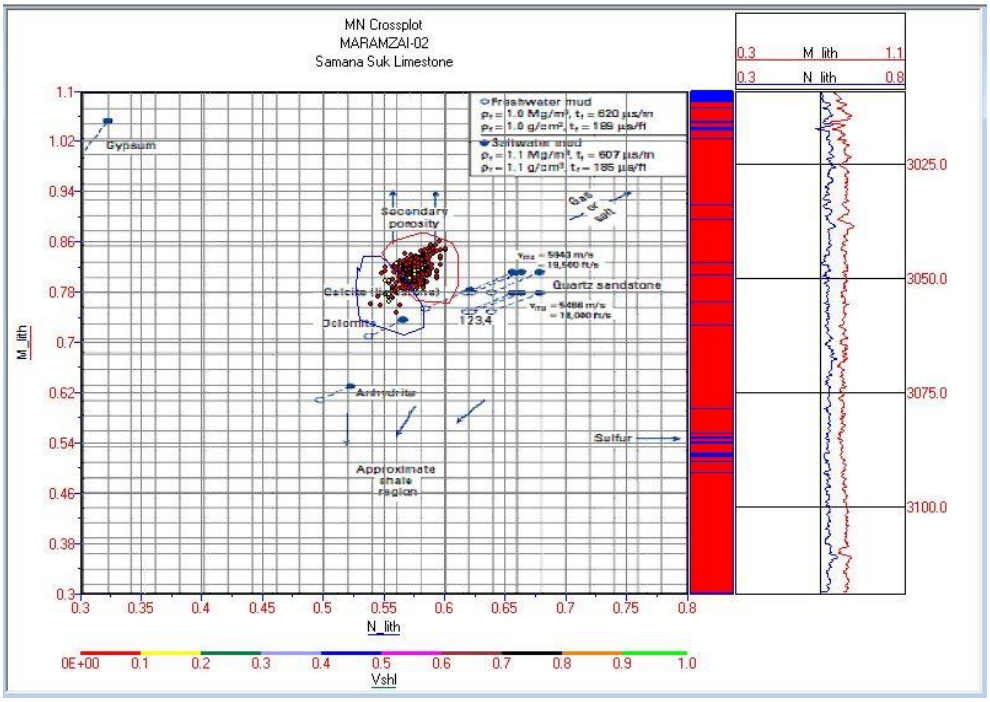

Figure 6.16 Uma-Rhoma crossplot drawn for assessing matrix lithology of Samana Suk Formation drilled in Maramzai-02 well.

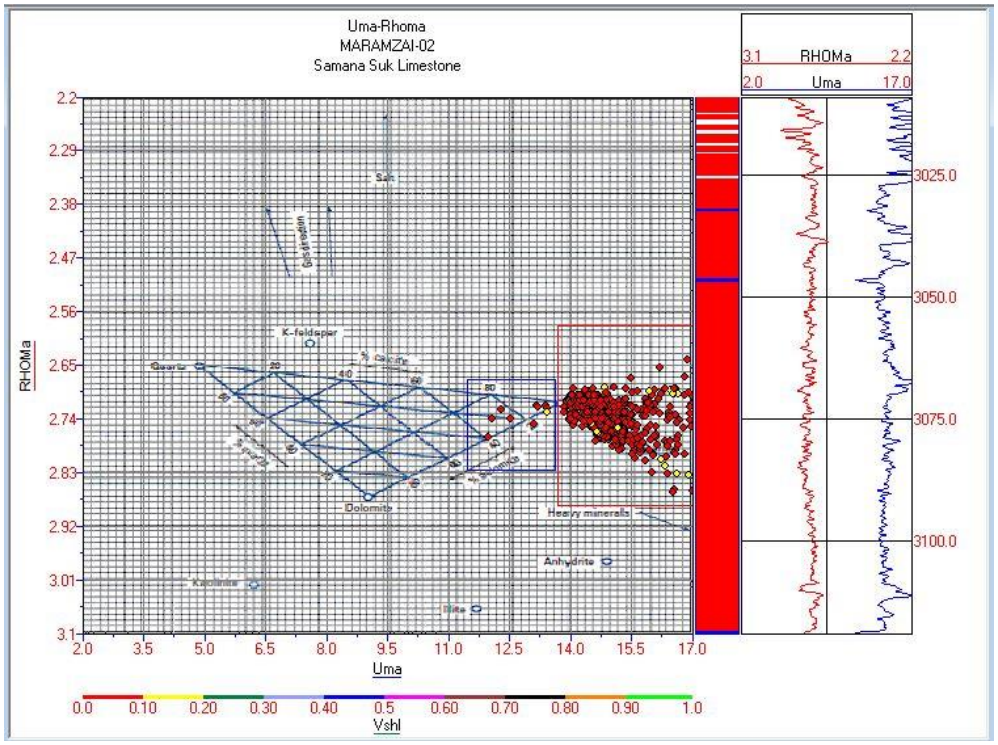

Figure 6.17 Uma-Rhoma Crossplot drawn for assessing matrix lithology of Samana Suk Formation drilled in Maramzai-02 well.

CHAPTER 7
STRATIGRAPHIC CORRELATION AND ATTRIBUTE MAPPING

7.1 Stratigraphic Correlation

Stratigraphic correlation has been constructed among all three wells for both Chihcali and Samana Suk Formation. The correlation is constructed (**Fig**. 7.2)utilizing the Gamma-ray in the first track on a scale of 0 to 150 API and Sonic log in the second track on a scale of 140 to 40 microseconds/feet. The signatures show a positive correlation among these formations in all three wells.

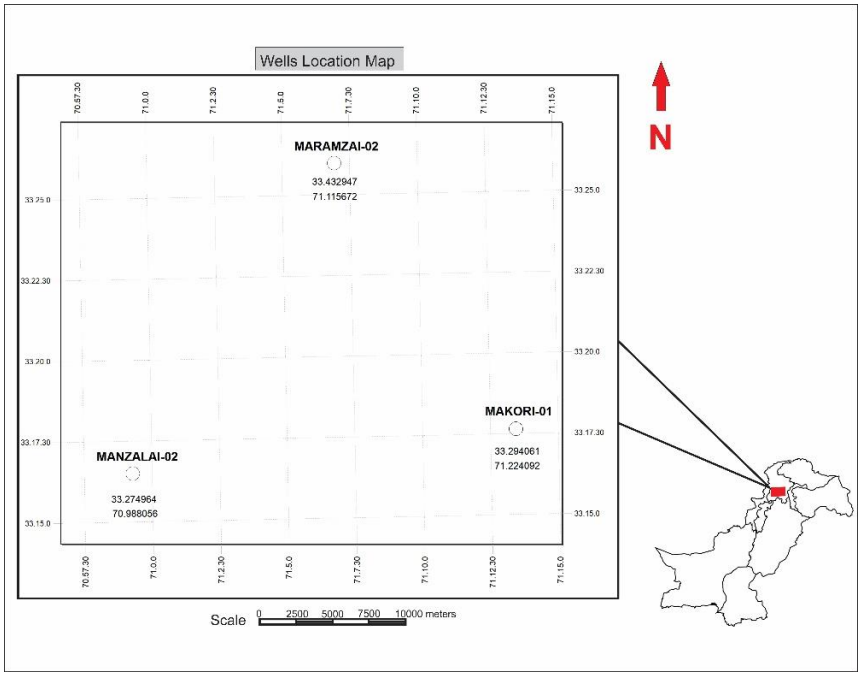

Figure 7.1 Base map showing the location of of wells.

Correlation (**Fig.** 7.2) shows Formation truncates towards Eastern direction as Manzalai-02 well in West shows high thickness of Formation while, Maramzai in NE and Makori in East shows reduction in thickness and marks the direction of Chichali Formation truncation.

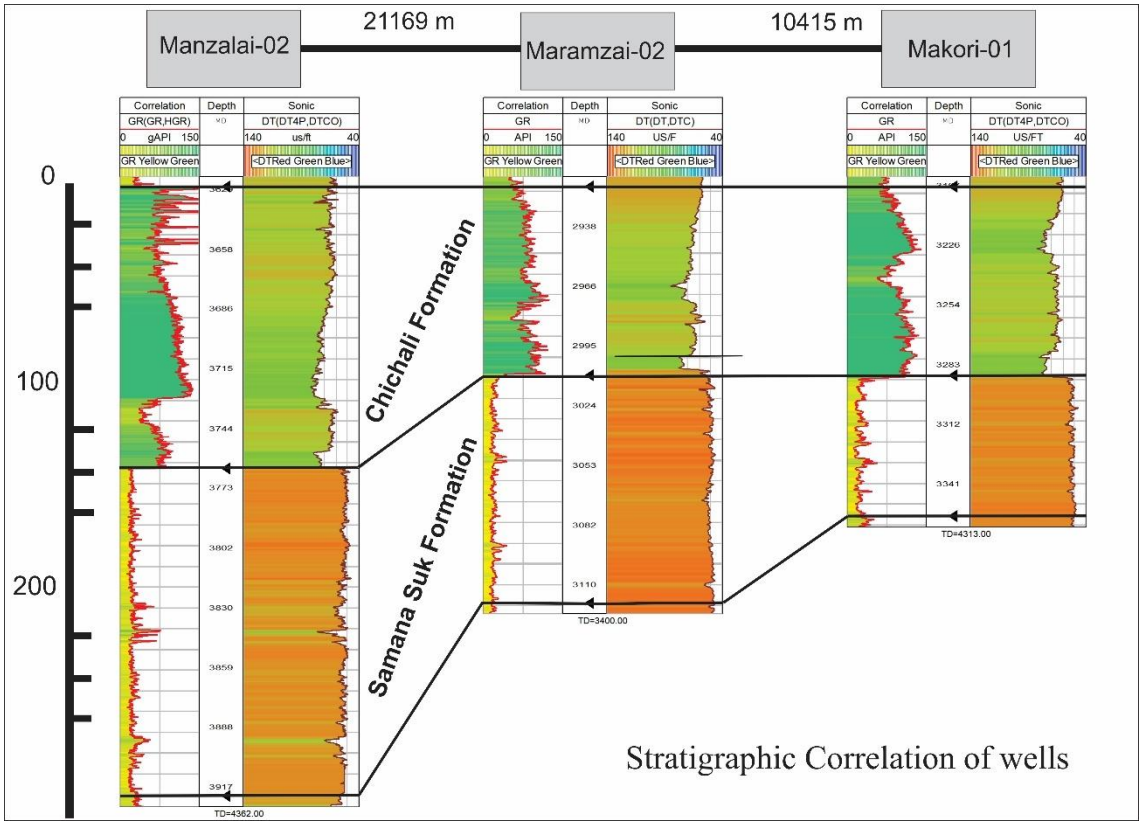

Figure 7.2 Stratigraphic correlation constructed among wells of Manzalai-02, Maramzai-02 and Makori-01 well.

The Chichali Formation shows a high Gamma-ray response at top of the formation which gradually decreases toward the bottom and again increases at lower depths in all three wells. Based on these responses, the Chichali Formation depicts the partition of Shale sequence in two zones which are positively marked in all three wells. Similarly, the response is also constructed for Sonic log. Chichali Formation shows high Sonic transit time at Shale sequence at top and bottom. while low transit time marks a non-Shale sequence in all three wells at of Chichali Formation.

Contrary to Chichali, Samana Suk Formation shows low GR readings and low Sonic transit time in all three wells. A very good correlation is constructed for Samana Suk Formation in all three wells. Both logs show consistent readings and suggest single lithology of Formation. The correlation shows Formation bears high thickness in Southern well of Manzalai-02 while, thickness decreases towards NE wells of Maramzai-

02 and Makori-01 well. High Sonic transit time suggests Formation bears characteristics of the tight reservoir in all three wells

7.2 Mapping Of petrophysical attribute

The petrophysical attributes of both formations have been mapped to construct the trend of attributes. Mapping makes us easy to interpret the trend of an attribute in any direction. The unconventional attributes mapped are; the volume of Shale, Average porosity, Shale porosity and total organic carbon. While conventional attributes mapped are; Volume of Shale, Average porosity, Effective porosity, and Saturation of water.

7.2.1 Chichali Formation

Both zones are mapped separately to interpret the trend of attributes.

7.2.1.1 Zone-1

The mapping shows the volume of Shale increases in a Southward direction for the Chichali Formation. The Maramzai-02 well in the north shows the lowest volume of Shale, while Manzalai-02 in the South shows the highest clay content.

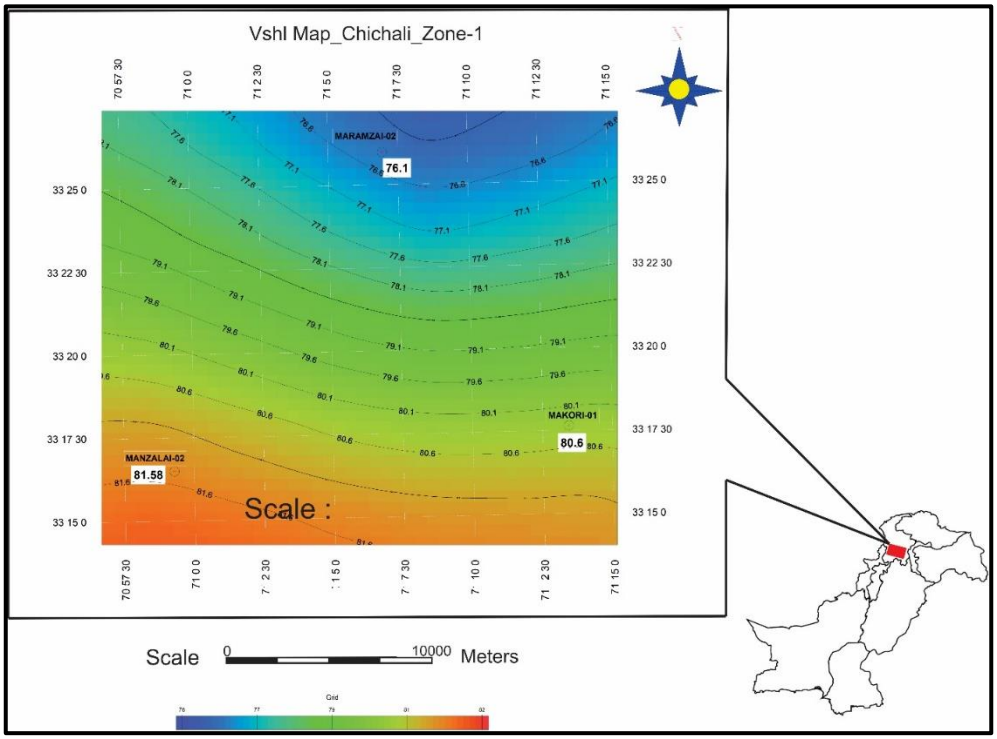

Figure 7.3 Volume of Shale map constructed for zone-1.

Likewise, Visual average porosity also shows the same trend with increasing porosity in the Southward direction.

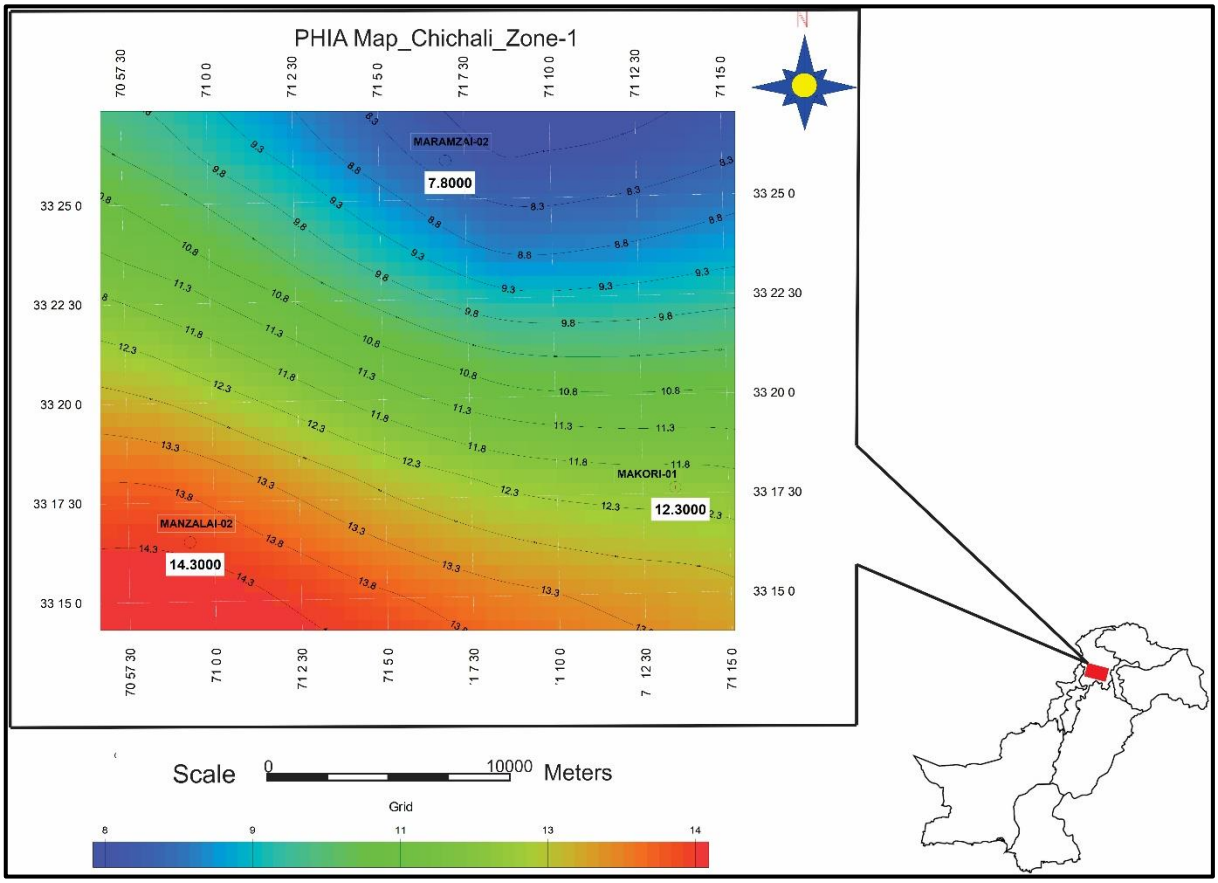

Figure 7.4 Average porosity map constructed for zone-1.

Map shows Shale porosity increases from Maramzai-02 well in North towards Manzalai-02 well in South. The Makori-01 in middle shows intermediate Shale porosity.

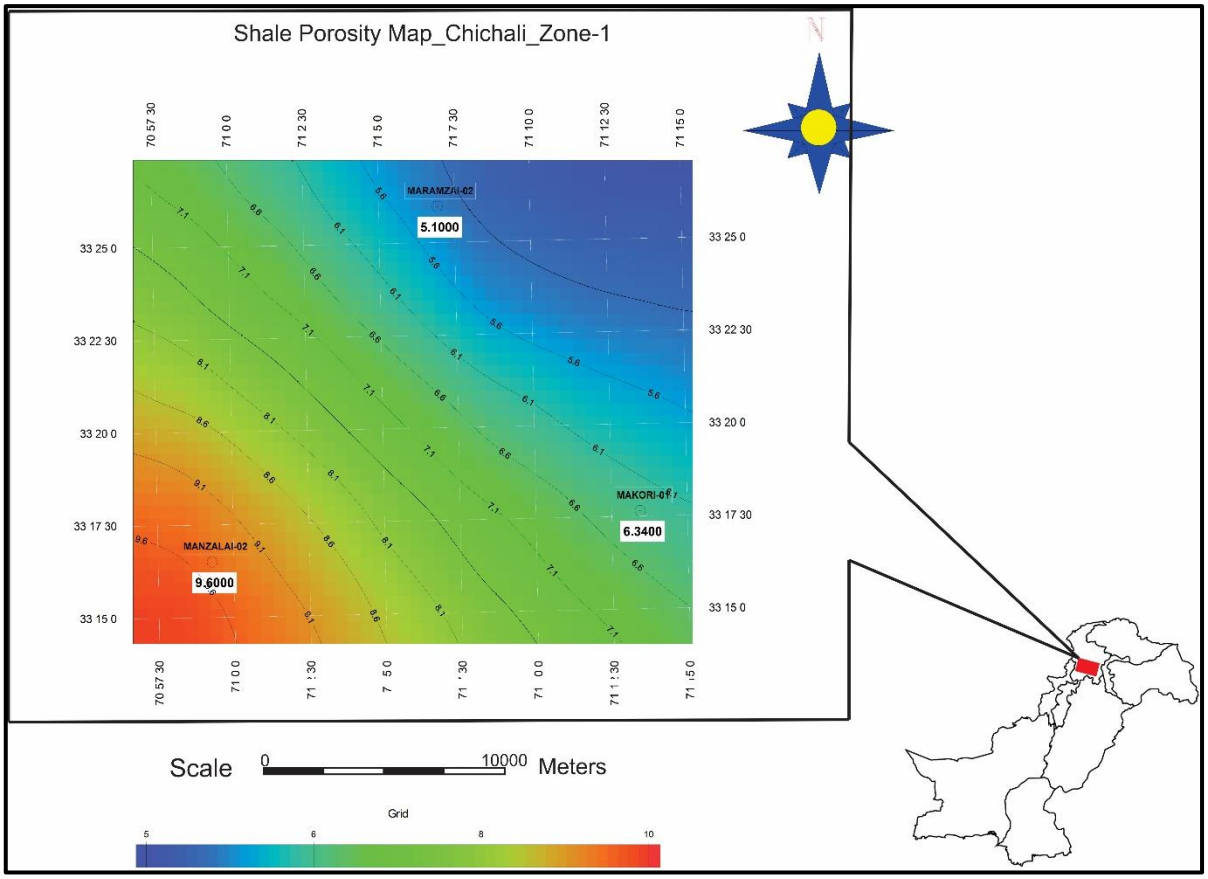

Figure 7.5 Shale porosity map constructed for zone-1.

The TOC increases in the SW direction while decreases in the SE direction. The Maramzai-02 well in Noth shows intermediate TOC while Manzalai in SE shows high while Makori-01 in SW shows the lowest value.

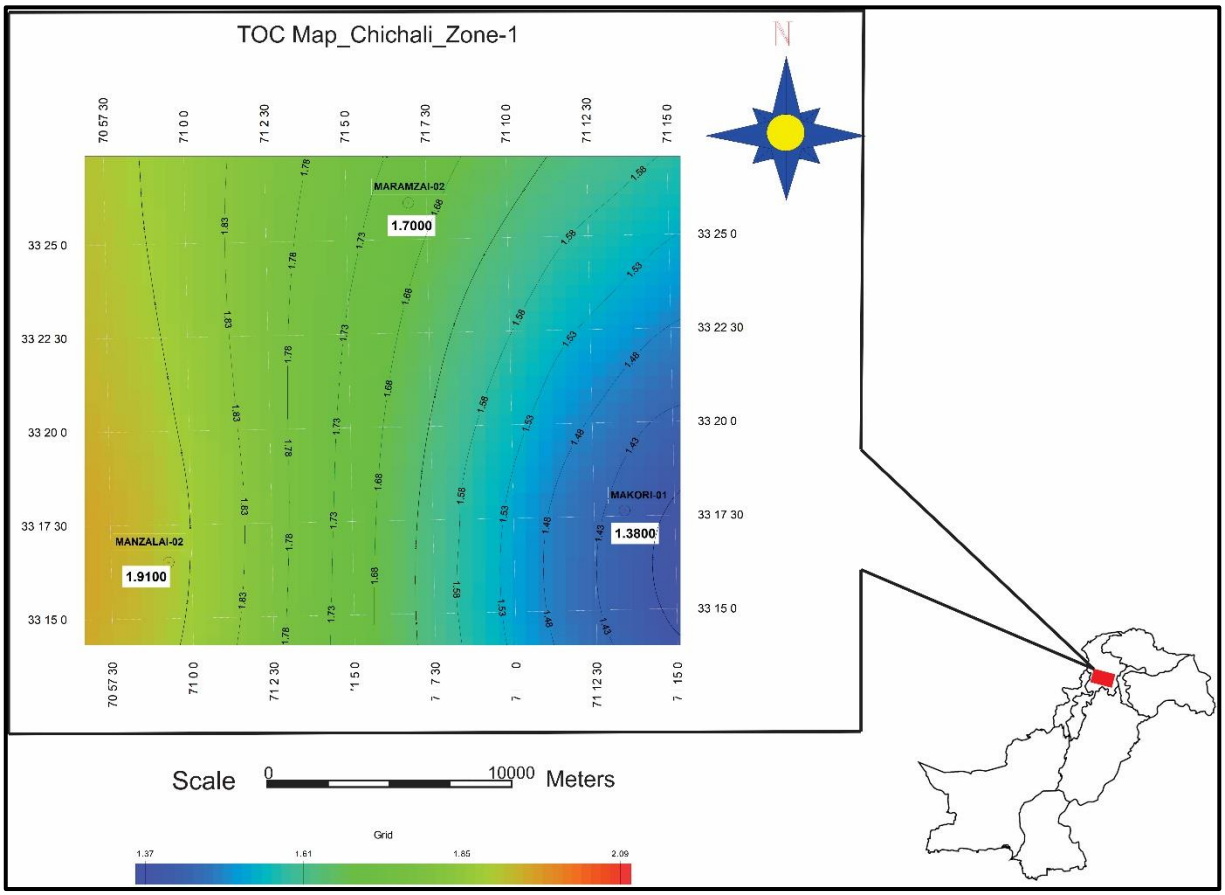

Figure 7.6 Total organic carbon richness map constructed for zone-1.

7.2.1.2 Zone-2

The volume of Shale map for zone-2 shows clay content increases from NW towards SE. Maramzai-02 and Manzalai-02 well show the low volume of Shale while Makori-01 show high clay content.

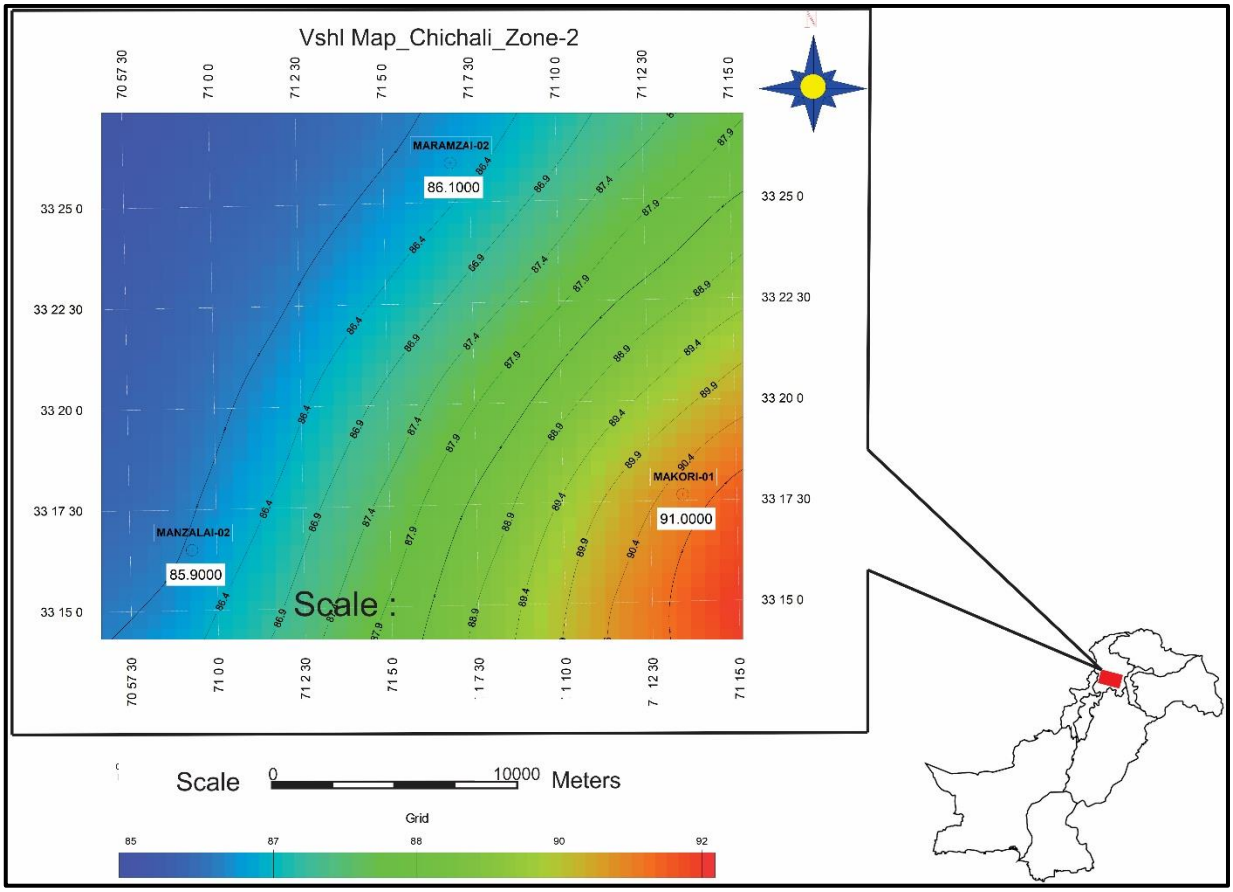

Figure 7.7 Volume of Shale map constructed for zone-2.

Average porosity and Shale porosity shows the same trend. Maps show porosity content increase from Manzalai-02 well in SW towards Maramzai-02 in NE.

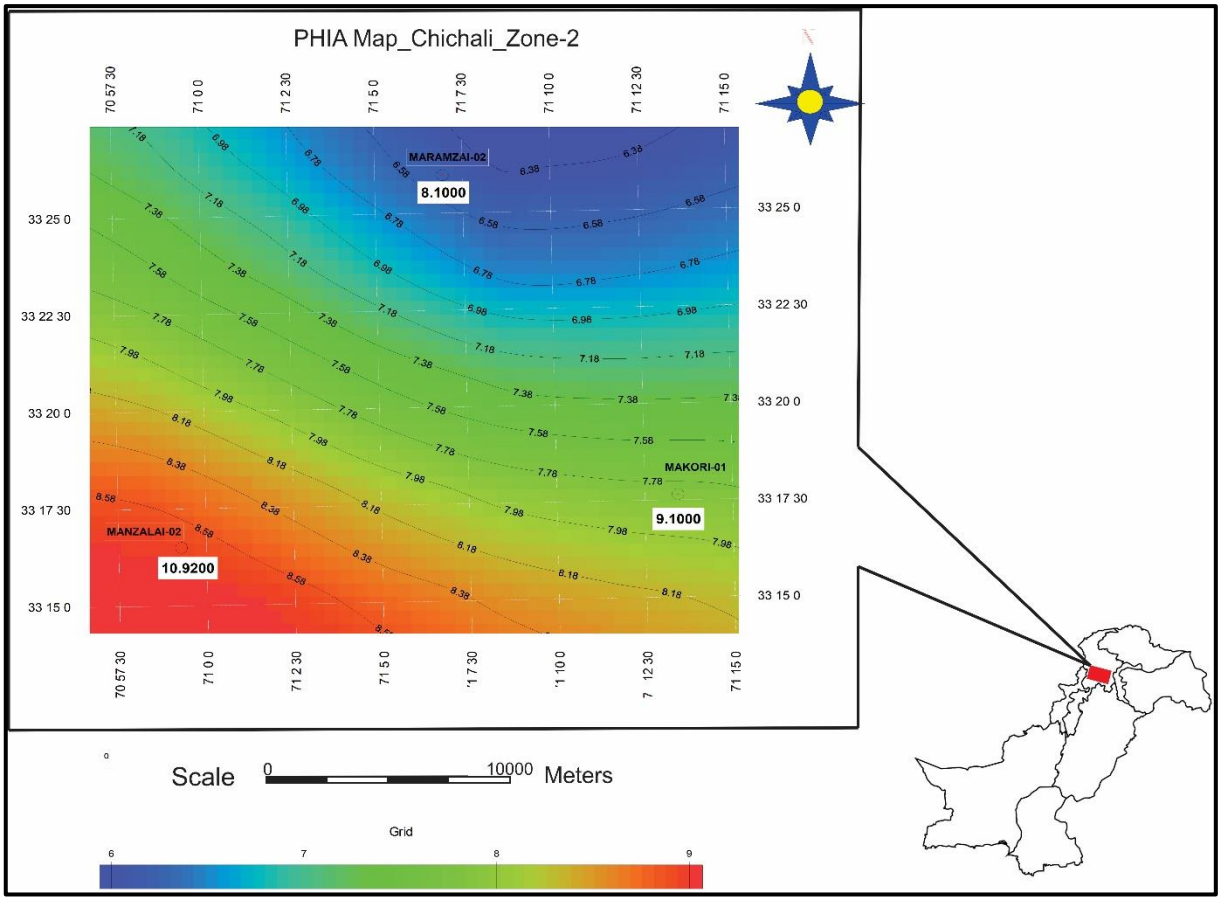

Figure 7.8 Average porosity map constructed for zone-2.

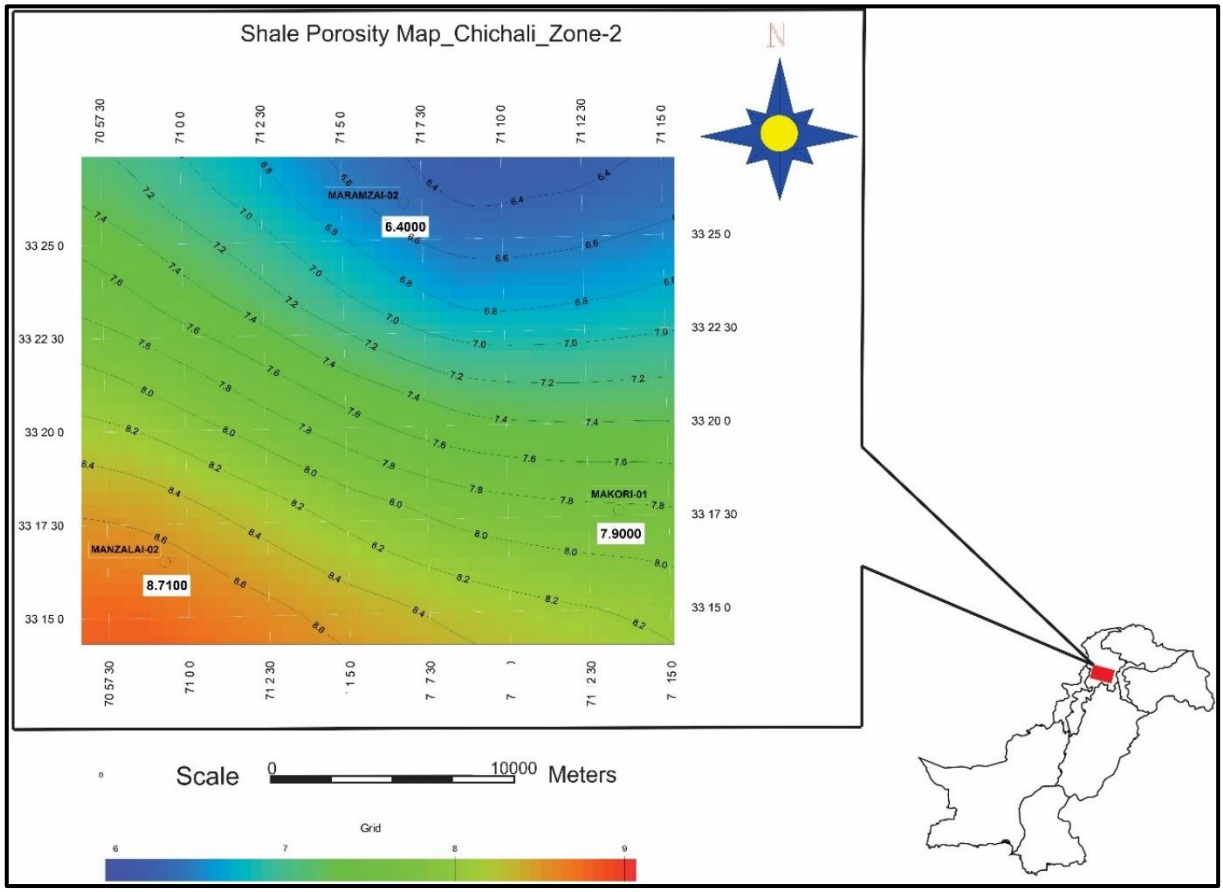

Figure 7.9 Shale porosity map constructed for zone-2.

TOC map shows that organic richness increases from SW towards NE. The Maramzai-02 well in the North shows high TOC while Makori-01 in SW shows low TOC.

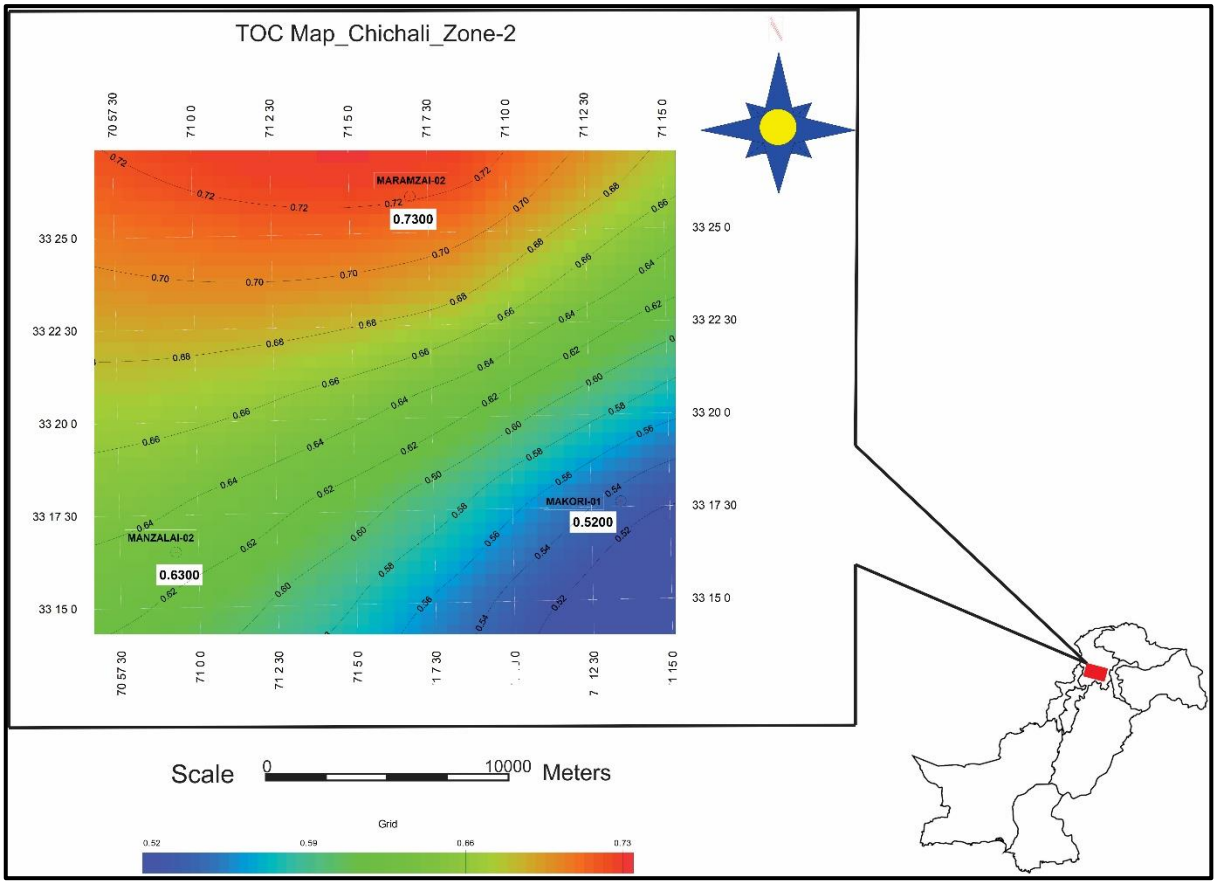

Figure 7.10 Total organic carbon richness map constructed for zone-2.

7.2.2 Samana Suk Formation

The mapping shows Samana Suk in SW is characterized by a high volume of Shale than in NE. Hence the Maramzai-02 well shows the lowest volume of Shale while Maznalai-02 shows the highest clay content.

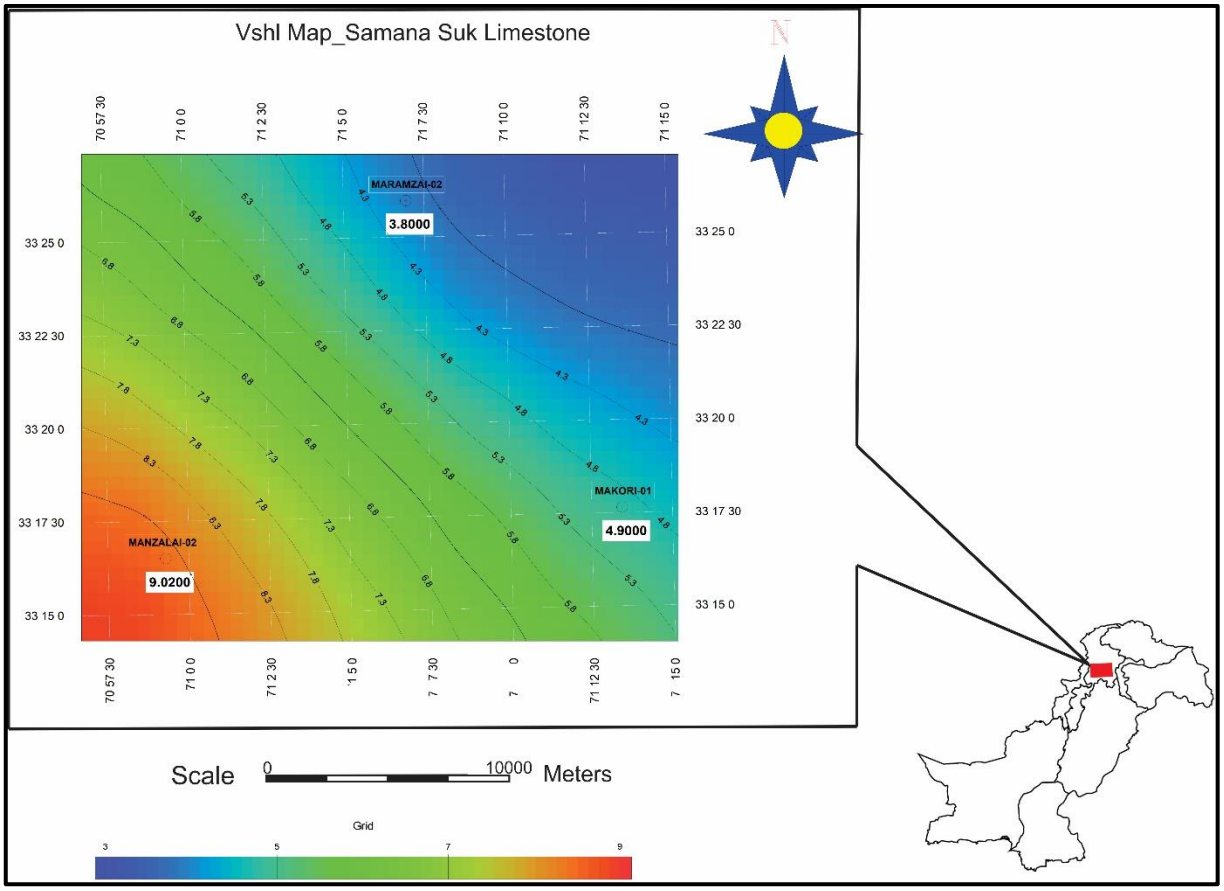

Figure 7.11 Volume of Shale map constructed for Samana Suk Formation.

The average porosity and effective porosity shows the same trend as of volume of Shale. The average and effective porosities increase from Maramzai-02 in NE towards Manzalai-02 in SW.

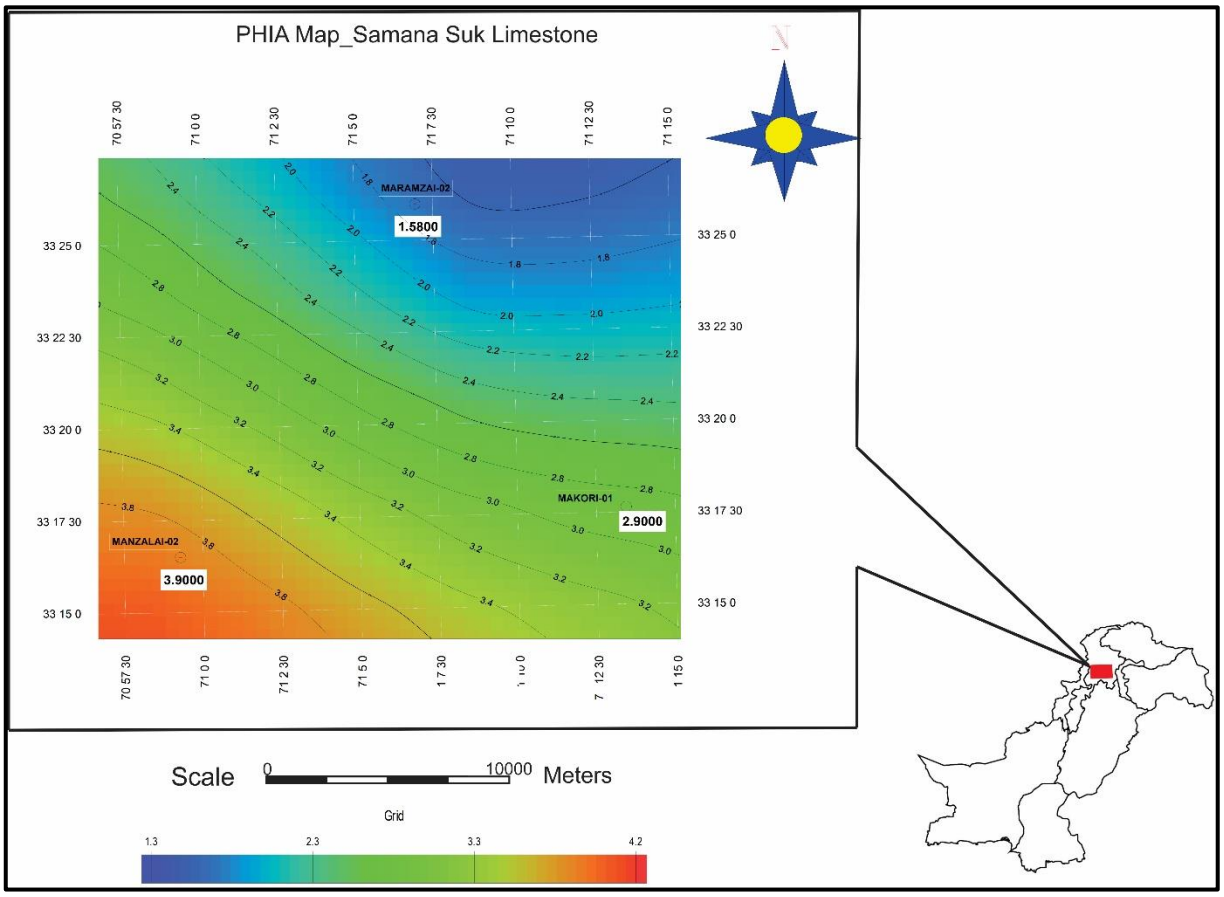

Figure 7.12 Average porosity map constructed for Samana Suk Formation.

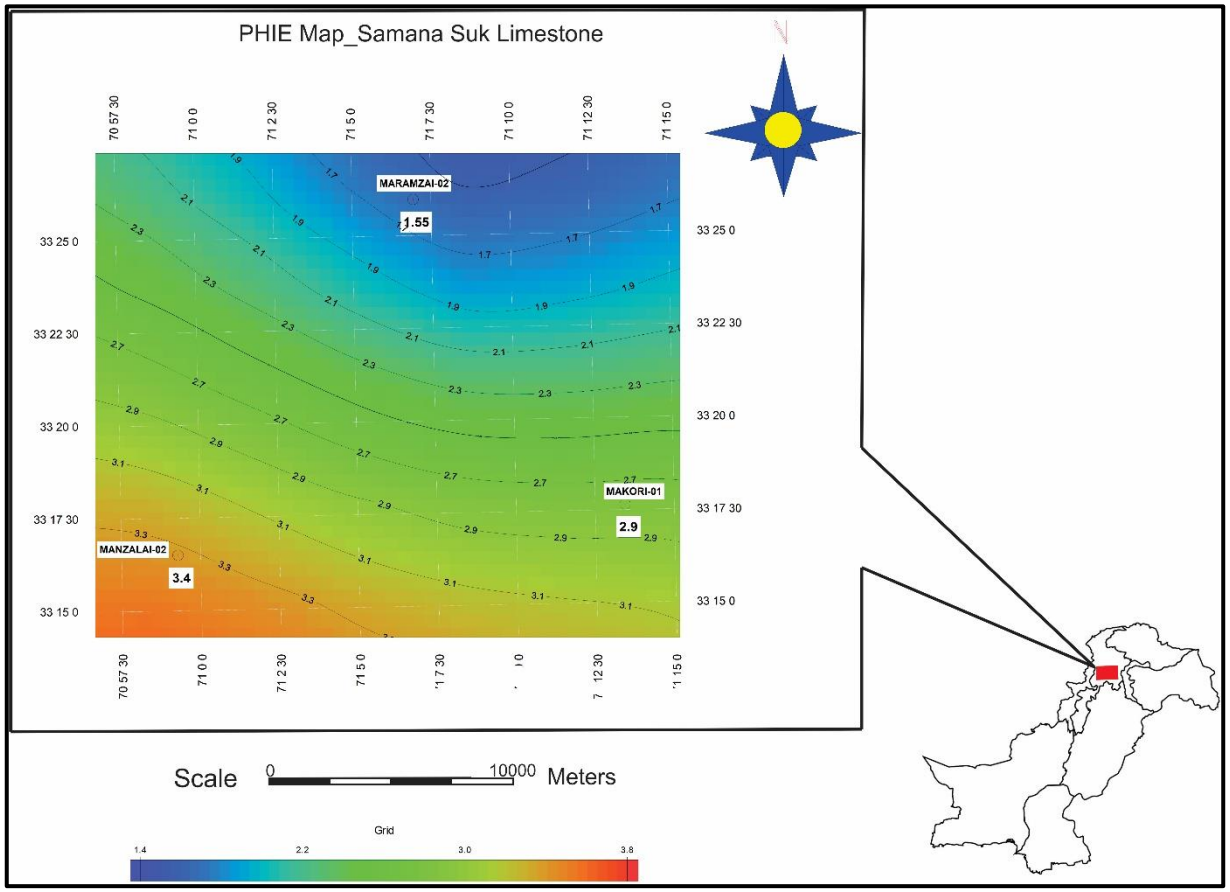

Figure 7.13 Effective porosity map constructed for Samana Suk Formation.

While, Saturation of water shows opposite trend as of other attribute's trend. The water content of the Samana Suk Formation increases from SW direction towards NE direction. Hence, the Maramzai-02 well in the North shows high water content, Makori in between shows intermediate, while Manzalai-02 in South shows the lowest water content.

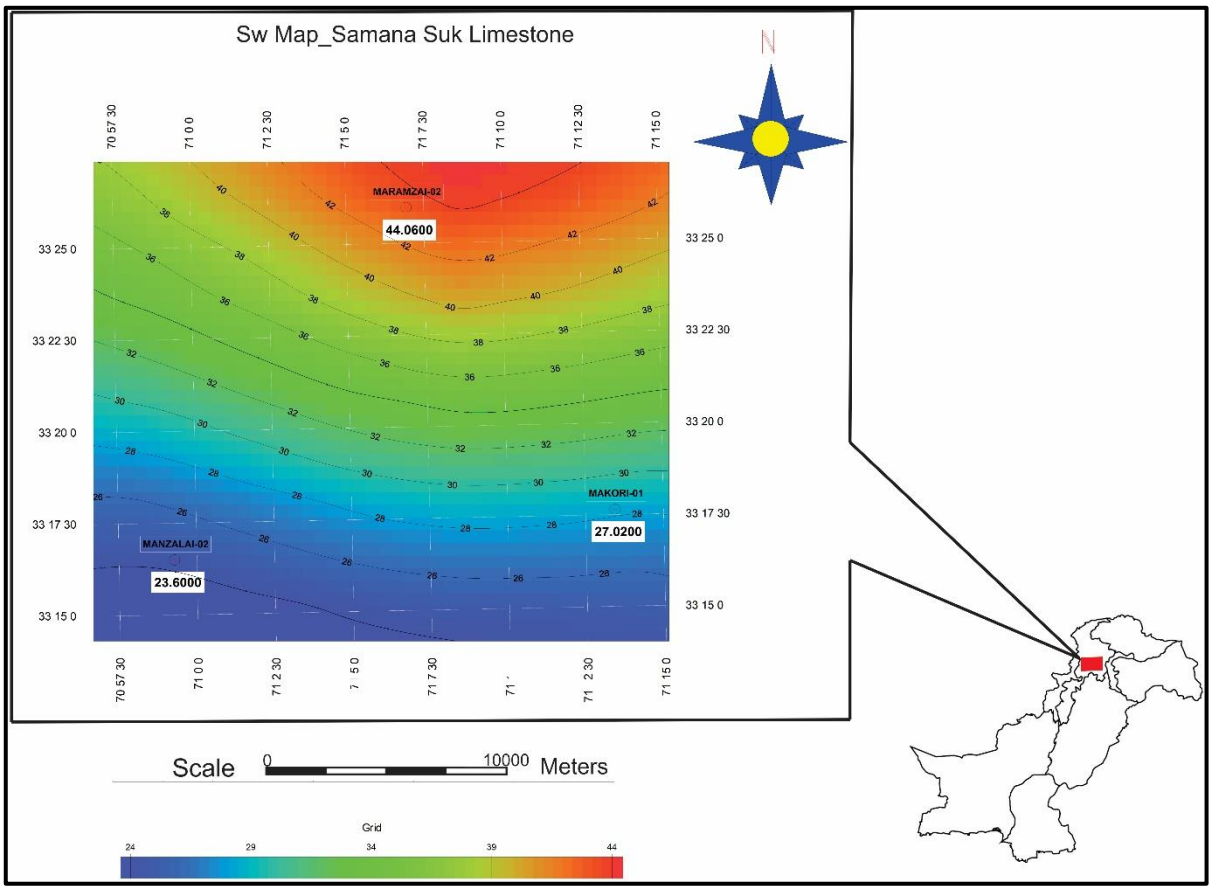

Figure 7.14 Saturation of water map constructed for Samana Suk Formation

CHAPTER 8

RESULTS

As present investigations has been carried out, the following results have been revealed regarding Chihcali and Samana Suk Formation's hydrocarbon Potential.

i. Investigation reveals that both Chichali and Samana Suk Formation truncates towards the North direction. Both Formation's high thickness is encountered in Manzalai-02 well in South while lowest thickness is in of Maramzai-02 well in North.
ii. In all three wells, two zones of Shale are marked in Chichali Formation demarcated by a thin non-Shale unit.
iii. The first zone is demarcated at depth of 3209-3235 meters, 3688-3730 meters, 2918-2977 meters, in Makori-01, Manzalai-02 and Maramzai-02 well respectively.
iv. The second zone is demarcated at depth of 3245-3287 meters, 3748-3762 meters, 2982-3008 meters in Makori-01, Manzalai-02 and Maramzai-02 well respectively.
v. In Manzalai-02 well, zone-1 shows 81.58%, 14.3%, 9.6%, and 1.91% of Vshl, PHIA, Shale porosity and TOC respectively. The first zone of the Chichali Formation in Makori-01 well is characterized with 80.6%, 12.3%, 6.34%, and 1.38% of Vshl, PHIA, Shale Porosity, and TOC respectively. While, in Maramzai-02 well, zone-1 illustrates 76.1%, 7.8%, 5.1%, and 1.7% of Vshl, PHIA, Shale Porosity, and TOC respectively.
vi. The zone-2 on other hand in Manzalai-02, shows 85.9%, 10.92%, 8.71%, and 0.63% and In Makori-01, 91%, 9.1%, 7.9%, and 0.52% of Vshl, PHIA, Shale Porosity, and TOC respectively. While in Maramzai-02 well, zone-2 encounters 86.1% Vshl, 8.1% PHIA, 6.4% Shale Porosity, and 0.73% of TOC.
vii. The mineralogical assessment shows both zones in all wells comprises mainly of mixed layers of clay with the influx of Illite, Glauconite and Mica bearing Shale.

viii. The Source rock analysis shows, Zone-1 of the Chichali Formation in all three well is categorised as a good source rock, while zone-2 is a fair source rock on basis of organic richness. The porosity content also favours zone-1 of the Chichlai Formation as good porosity bearing than zone-2.

ix. Brittleness analysis shows both zones in each well shows good mechanical properties with category of less brittle to brittle making Chichali Formation as good brittleness possessing Formation.

x. Lithology analysis shows, Chichali Formation contains a matrix of Shale as dominating while, Sandston and Limestone in minor proportion.

xi. The Samana Suk Formation in Manzalai-02 shows good results comparing to other wells as it revealed 9.2% Vshl, 3.9% PHIA, 3.4% PHIE and 34.7% of water saturation. In Makori-01 it comprises 4.9% Vshl, 2.9% PHIA, 2.9% PHIE, and 46.1% of Sw. While, in Maramzai-02 Samana Suk Limestone is characterized with 3.8%, 1.58%, 1.55%, and 57.5% of Vshl, PHIA, PHIE and Sw respectively.

xii. Porosity computation shows Samana Suk Limestone bears poor porosity with a range of 0-5%. Permeability analysis in all three wells shows permeability of Samana Suk Limestone as less than 1 mD categorising it as a tight reservoir.

xiii. Lithology interpretation shows Samana Suk Limestone bears matrix of Calcite with the minor influx of Dolomite.

Table 8.1: Summarised computed petrophysical attributes of Chichali and Samana Suk Formations in Makori-01, Manzalai-02 and Maramzai-02 wells.

FORMATION	ZONE	WELL	Vshl	PHIA	SHALE POROSITY/ PHIE	Sw	TOC	B.I	MINERALOGY	REMARKS
CHICHALI	ZONE-1	MAKORI	80.3	12.6	6.34	48.3	1.38	45	MXD, ILLITE, MICA, GLCNT,	Good Source Rock
		MANZALAI	81.5	14.3	9.6	35.7	1.91	46.4	MXD, KAOLINITE	Good Source Rock
		MARAMZAI	76.1	7.8	5.1	47.2	1.7	43.6	MXD	Good Source Rock
	ZONE-2	MAKORI	91	9.1	7.9	77.3	0.52	57.7	ILLITE, MICA,MXD	Fair Source Rock
		MANZALAI	75.9	10.92	8.71	64.5	0.63	76.2	MXD, ILLITE,MICA	Fair Source Rock
		MARAMZAI	86.1	8.1	6.4	55.5	0.73	47	MXD, ILLITE	Fair Source Rock
SAMANA SUK	N/A	MAKORI	4.9	2.9	2.9	27.0	N/A	N/A	L.ST, DLMT	Tight Reservoir
		MANZALAI	9.02	3.9	3.4	23.6	N/A	N/A	L.ST, DLMT	Tight Reservoir
		MARAMZAI	3.8	1.58	1.55	44.0	N/A	N/A	L.ST, DLMT	Tight Reservoir

8.1 Conclusions

i. Both formations truncates toward East.
ii. In all three wells, two zones of Shale are marked in Chichali Formation demarcated by a thin non-Shale unit.
iii. Zone-1 bears good TOC content and can be categorised as good source rock, while zone-2 bears low TOC comparatively and is categorised as Fair Source rock.
iv. The mineralogical assessment shows both zones in all wells comprises mainly of mixed layers of clay with the influx of Illite, Glauconite and Mica bearing Shale.
v. Lithology analysis shows, Chichali Formation contains a matrix of Shale as dominating while, Sandstone in minor proportion.
vi. Samana Suk Formation bears good hydrocarbon saturation with low porosity and permeability and categorized as tight reservoir.
vii. Lithology interpretation shows Samana Suk Limestone bears matrix of Calcite with the minor influx of Dolomite.

8.2 Recommendations

Chichali Shale seems to be a promising unconventional candidate. Chichali Shale in Makori-01, Manzalai-02 and Maramzai-02 needs additional assessment, as a present available dataset for this study was insufficient. Thorough mineralogical, geochemical and geomechanical examinations are suggested for the unconventional Chichlai shale prospects. It is highly recommended to:

i. Obtain maximum quantity of cores or drill cutting in Chichali Shales to accomplish comprehensive laboratory analysis including;
    a) Rock-Eval Pyrolysis for Total Organic Carbon.
    b) Rock-Eval Tmax for Rock Genetic Potential.
    c) X-Ray Diffraction (XRD) for identification of Shale Mineralogy.
    d) Mercury Injection Capillary Pressure (MICP) for Porosity and Matrix Permeability distributions.
ii. Evaluate Chichali Formation through Pulsed Neutron Mineralogy log to compute clay minerals proportion, i,e., Glauconite, Illite etc.
iii. Assess Chichali Formation through Nuclear magnetic resonance (NMR) log to calculate effective porosity, permeability and clay bound water.
iv. Accomplish 3D Basin Modeling to estimate the gas initially in place (GIIP) and recognize the sweet spots

REFERENCES

Ahmad, S., Wadood, B., Khan, S., Ahmed, S., Ali, F., & Saboor, A. (2020). *Integrating the palynostratigraphy, petrography, X-ray diffraction and scanning electron microscopy data for evaluating hydrocarbon reservoir potential of Jurassic rocks in the Kala Chitta Range, Northwest Pakistan*. Journal of Petroleum Exploration Production Technology, 1-13.

Amjad, M. R., Hameed, M. S., Mujtaba, M., & Munir, M. N. (2017). *Petrophysical and Geochemical Analysis of Chichali Formation for the Source Rock Evaluation: A Case Study of Chanda-01 Well, Upper Indus Basin, Pakistan*. International Journal of Economic Environmental Geology, 32-39.

Arif, M., Mulk, A., Mehmood, M., & Shah, S. (1999). *Petrography and mechanical properties of the Mansehra granite, Hazara, Pakistan*. Geological Bulletin, University of Peshawar, 32, 41-49.

Asquith, G. B., Krygowski, D., & Gibson, C. R. (2004). *Basic well log analysis (Vol. 16)*. American Association of Petroleum Geologists Tulsa.

Bohacs, K., & Miskell-Gerhardt, K. (1998). *Well-log expression of lake strata; controls of lake-basin type and provenance, contrasts with marine strata*. Paper presented at the AAPG Annual Meeting Expanded Abstracts, Tulsa, Oklahoma A.

Cheema, A. H. (2010). *Microfacies, Diagenesis and Depositional Environments of Samana Suk Formation (Middle Jurassic) Carbonates exposed in South East Hazara and Samana Range*. University of the Punjab.

Charles R. Meissner Jr., J.M. Master, M.A. Rashid, and Muzaffar Hussain (1974). *Stratigraphy of the Kohat quadrangle, Pakistan.* United States Geological Survey.

Crain, E. (1986). The log Analysis Handbook. Tulsa, Oklahoma: Penn-Well Publishing Company, , USA.

Danilchik, W. (1961). *The iron formation of the Surghar and western Salt Range, Mianwali District, West Pakistan*. US Geol Surv Prof Pap, 424, 228-231.

EIA. (2013). *Technically recoverable shale oil and shale gas resources: an assessment of 137 shale formations in 41 countries outside the UnitedStates*.

Hayat, M., ur Rahman, M., Khan, N. A., & Ali, F. (2019). *Sedimentology, Sequence Stratigraphy and Reservoir Characterization of Samana Suk Formation Exposed in Namal Gorge Section, Salt Range, Mianwali, Punjab, Pakistan*. International Journal of Economic and Environmental Geology, 4-15.

Hussain, H., & Zhang, S. (2018). *Structural Evolution of the Kohat Fold and Thrust Belt in the Shakardarra Area (South Eastern Kohat, Pakistan)*. Geosciences, 8(9), 311.

Hussain, H. S., Fayaz, M., Haneef, M., Hanif, M., & Gul, B. (2012). *Microfacies and diagenetic fabrics of Samana Suk Formation at Harnoi section, Abbottabad, Khyber Pakhtunkhwa*. Journal of Himalayan Earth Sciences, 45(2), 51.

Hyne, N. J. (2012). *Nontechnical guide to petroleum geology, exploration, drilling, and production*: PennWell Books.

Iqbal, M. A., & Shah, S. I. (1980). *A guide to the stratigraphy of Pakistan*.

Jamil, A., Waheed, A., & Sheikh, R. A. (2012). *Pakistan's major petroleum plays-An Overview of Dwindling Reserves*.

Johnson, B., Powell, C. M., & Veevers. (1976). *Spreading history of the eastern Indian Ocean and Greater India's northward flight from Antarctica and Australia*. Geological Society of America Bulletin, 87(11), 1560-1566.

Joseph A. DiPietro, Kevin R. Pogue (2004). *Tectonostratigraphic subdivisions of the Himalaya: A view from the west*. Tectonics, Vol. 23 (5).

Jurčić, H., Čogelja, Z., & Maretić, S. (2012). *Petrophysical Parameters Evaluation in Unconventional Reservoirs by Well Logging and Mud Logging Data Interactive Correlation Method*. Paper presented at the SPE/EAGE European Unconventional Resources Conference & Exhibition-From Potential to Production.

Kadri, I. (1995). *Petroleum Geology of Pakistan*: Pakistan Petroleum Limited Karachi. In: Pakistan.

Kemal, (1991). *Geology and new trends for petroleum exploration in Pakistan. New directions strategies for accelerating petroleum exploration production in Pakistan*. Ministry of Petroleum Natural Resources, Pakistan, 16-57.

Kenomore, M., Hassan, M., Dhakal, H., Shah, (2017). *Total organic carbon evaluation of the Bowland Shale Formation in the Upper Bowland of the Widmerpool Gulf*.

Khan, Asad, Ahmed, R., Raza, H. A., & Kemal, A. (1986). *Geology of petroleum in Kohat-Potwar depression, Pakistan*. AAPG bulletin, 70(4), 396-414.

Khan, M. Khan & M. Ali, (2017). *Gamma ray-based facies modelling of lower Goru formation: A case study in Hakeem Daho Well Lower Indus Basin Pakistan*. Bahria University Research Journal of Earth Sciences Vol. 2.

Kumar, T., & Shandilya, A. (2013). *Tight reservoirs: An overview in Indian context*. Paper presented at the 10th Biennial International Conference and Exposition.

Lobo, C., Molina, A., Faraco, A., Mendez, J., Delgadillo, J., & Rincon, G. (2017). *Methodology for Petrophysical and Geomechanical Analysis of Shale Plays. Case Study: La Luna and Capacho Formations, Maracaibo Basin*. SPE Latin America and Caribbean Petroleum Engineering Conference.

McKenzie, D.P. & Sclater, (1973). *The Evolution on the Indian Ocean.* Adrift an Continents Aground. Scientific American Continents.

Michael H. , Antony H. , and Dominic H., (2012), A Petrophysical Model for Shale Reservoirs to Distinguish Macro-Porosity, Micro-Porosity, and TOC. AAPG Search and Discovery Article (40916)

Michael P. Coward, David C. Rex, M. Asif Khan, Brian F. Widley, Roger D. Broughton, Ian W. Luff, Michael G. Petterson and Carol J. Pudsey (1986). *Collision tectonics in the NW Himalayas*. Geological Society, London, Special Publications 19(1), 203-219.

Middlemiss, C. S. (1896). *The geology of Hazara and the Black Mountain* (Vol. 26). Geological Survey of India.

Ministry of Petroleum and Natural Resources, (2011). *Tight gas exploration and production policy.* Pakistan: The Gazette of Pakistan.

Mukerji, T., & Dvorkin, J. (2009). *The Rock Physics Handbook 2ed*: Cambridge University Press.

Natasha, R. (2019). *Petrophysical evaluation and fluid substitution modeling for reservoir depiction of Jurassic Datta Formation in the Chanda oil field, Khyber Pakhtunkhwa, northwest Pakistan*. Journal of Petroleum Exploration Production Technology, 9(1), 159-176.

Nizami, A. R. (2019). *Faunal Assemblages of the Middle Jurassic Samana Suk Formation, Chichali Gorge Section, Surghar Range, Sub-Himalayas, Pakistan*. Punjab University Journal of Zoology, 34(1), 55-60.

Oldham, R. D. (1892). *Report on the geology of Thal Chotiali and part of the Mari Country:* Geological Survey of India.

Orlandi, M., Bartelucci, P., & Chelini, V. (2011). *Unconventional reservoir characterization methods using core and well logging data: shale gas and tight gas sand examples*. 10th Offshore Mediterranean Conference and Exhibition, Italy.

Paracha, W. (2004). *Kohat plateau with reference to Himalayan tectonic general study*. CSEG recorder.

Passey, Creaney, Kulla, Moretti, & Stroud. (1990). *A practical model for organic richness from porosity and resistivity logs*. AAPG bulletin, 74(12), 1777-1794.

Perez, R., (2013), *Brittleness Estimation from Seismic Measurements in Unconventional Reservoirs: Application to the Barnett Shale*: Ph.D. Dissertation, ConocoPhillips School of Geology and Geophysics: The University of Oklahoma.

Petroconsultants. (1996). *Petroleum exploration and production digital database*: Petroconsultants.

Petterson, M. G., & Windley, B. (1985). *Rb-Sr dating of the Kohistan arc-batholith in the Trans-Himalaya of north Pakistan, and tectonic implications*. Earth Planetary Science Letters, 74(1), 45-57.

Quirein, J. A., Gardner, J. S., & Watson, J. T. (1982). *Combined natural gamma ray spectral/litho-density measurements applied to complex lithologies*. SPE Annual Technical Conference and Exhibition.

Qureshi, Ghazi, Butt, Ahmad, & Masood, (2007). *Microfacies Analysis And The Environmental Pattern Of The Chichali Formation, Kala Chitta Range, Pakistan*. Geology Bulletin, University of Punjab.

Rahim, Corbella, & Navarro-Ciurana, (2020). *Diagenetic evolution and associated dolomitization events in the middle Jurassic Samana Suk Formation, Lesser Himalayan Hill Ranges, NW Pakistan*. Carbonates Evaporites, 35(4), 1-26.

Rehman, Ahmed, Hasan, Rehman, (2018). *Aggregate suitability studies of Middle Jurassic Samana Suk Formation exposed at Sheikh Budin Hill, Marwat Range, Pakistan*.

Rezaee, R. (2015). *Fundamentals of gas shale reservoirs*: John Wiley & Sons.

Rickman, Mullen, Petre, Grieser, & Kundert, (2008). *A practical use of shale petrophysics for stimulation design optimization: All shale plays are not clones of the Barnett Shale*. SPE annual technical conference and exhibition.

Rider, (1986). *The geological interpretation of well logs*.

Sameeni, Haneef, Rehman, & Lipps, (2009). *Paleogene biostratigraphy of Kohat area, northern Pakistan*. Geology Bulletin, University of Punjab 44, 27-42.

Schlumburger. (1997). *Schlumburger logs interpretation charts*.

Schmoker, & Hester, (1989). *Organic carbon in Bakken formation, United States portion of Williston basin.* AAPG Bulletin (1983) 67 (12): 2165–2174.

Searle, M. Asif Khan, J. E. Fraser, S. J. Gough, M. Qasim Jan, (1999). *The tectonic evolution of the Kohistan-Karakoram collision belt along the Karakoram Highway transect, north Pakistan*. Tectonics, 18(6), 929-949.

Searle, M. P. (1991). *Geology and tectonics of the Karakoram Mountains*. John Wiley & Sons Incorporated: Wiley 1st edition (September 27, 1991

Shah, I. (1977). *Stratigraphy of Pakistan:* Memoirs of the Geological Survey of Pakistan, v. 12.

Shah, S. (2003). *A comparative study of structural styles in the Kohat Plateau, NW Himalayas, NWFP, Pakistan*. National Centre of Excellence in Geology, University of Peshawar, Pakistan.

Slatt, R. (2011). *Important geological properties of unconventional resource shales*. Central European Journal of Geosciences., 3(4), 435-448.

Tixier, M. P. (1949). *Evaluation of Permeability from Resistivity Gradient on Electric Logs*. Tulsa Geological Society. Vol. 17. (68-73).

Treloar, Broughton, Williams, M.Coward, & Windley, (1989). *Deformation, metamorphism and imbrication of the Indian Plate, south of the Main Mantle Thrust, North Pakistan*. Journal of Metamorphic Geology. 7(1), 111-125.

Treloar & Izatt, (1993). *Tectonics of the Himalayan collision between the Indian plate and the Afghan block: A synthesis*. Geological Society, London, Special Publications, 74(1), 69-87.

Wadood, Ahmad, Awais, & Sheikh, (2018). *Hydrocarbons prospects in the Kohat-Potwar Sub-Basins: An overview of Petroleum Play*. 1st International Conference on Advances in Engineering and Technology (ICAET-2018), Quetta, Pakistan.

Wadood, Khan, S. Ahmad, Li, H., Liu, Y., , S., & Jiao, X. (2020). *Sequence Stratigraphic Framework of the Jurassic Samana Suk Carbonate Formation, North Pakistan*: *Implications for Reservoir Potential.* Arabian Journal of Science and Engineering, Springer.

Wandrey, C. J., Law, B., & Shah, H. A. (2004). *Patala-Nammal composite total petroleum system, Kohat-Potwar geologic province, Pakistan*: US Department of the Interior, US Geological Survey Reston.

Yeats, R. S., & Hussain, A. (1987). *Timing of structural events in the Himalayan foothills of northwestern Pakistan*. Geological Society of America Bulletin, 99(2), 161-176.

Zeb, S. F., Zafar, M., Jehandad, S., Khan, T., Siyar, S. M., & Qadir, A. (2020). *Integrated geochemical study of Chichali Formation from Kohat sub-basin, Khyber Pakhtunkhwa, Pakistan*. Journal of Petroleum Exploration Production Technology, 10(7), 2737-2752.

Zou, C. (2017). *Unconventional petroleum geology*: Elsevier.

Analysis of Hydrocarbon Resource Potential of Chichali and Samana Suk Formations, Kohat Sub-basin, Pakistan

by Ahmad Khan

Submission date: 02-Oct-2021 07:04PM (UTC+0500)
Submission ID: 1663282918
File name: Ahmad_Khan_01-262192-012_Thesis_for_plagiarism_evaluation.docx (18M)
Word count: 14764
Character count: 81788

Analysis of Hydrocarbon Resource Potential of Chichali and Samana Suk Formations, Kohat Sub-basin, Pakistan

ORIGINALITY REPORT

8%	3%	5%	3%
SIMILARITY INDEX	INTERNET SOURCES	PUBLICATIONS	STUDENT PAPERS

PRIMARY SOURCES

1	Submitted to Higher Education Commission Pakistan Student Paper	3%
2	pt.scribd.com Internet Source	1%
3	mafiadoc.com Internet Source	1%
4	Shah Faisal Zeb, Muhammad Zafar, Samina Jehandad, Tahseenullah Khan, Syed Mamoon Siyar, Anwar Qadir. "Integrated geochemical study of Chichali Formation from Kohat sub-basin, Khyber Pakhtunkhwa, Pakistan", Journal of Petroleum Exploration and Production Technology, 2020 Publication	<1%
5	csegrecorder.com Internet Source	<1%
6	Bilal Wadood, Suleman Khan, Hong Li, Yiqun Liu, Sajjad Ahmad, Xin Jiao. "Sequence	<1%